Extreme Weather Conditions
Novel Tie-Down System for
Ship to Shore Cranes

An Analysis into Wind Induced Loading Effects on a Ship-to-Shore (STS) Crane and Investigation into Design Optimisation

Brian Hand

Bachelor of Engineering

First Class Honours

Final Year Capstone Project

in conjunction with

LIEBHERR

Extreme Weather Conditions Novel Tie-Down System for Ship to Shore Cranes

Synopsis

Over ninety percent of world cargo is transported by sea. Ship-to-Shore(STS) cranes account for 300 million containers annually. Ports are expected to double/triple output by 2020, further driving a global trend towards larger STS cranes. Conservative wind-loading standards lead to high mass crane structures, tie-down and quay foundation issues. STS crane configuration and dynamic/unpredictable nature of wind flow poses major challenges to divergence from the standards-based approach. Extensive modelling and wind tunnel testing of airflow around critical sections, undertaken by the author, indicates an optimal analysis method. A novel prototype crane tie-down system is developed/tested. Significant material/operation/quay-infrastructure/energy-usage improvements are predicted.

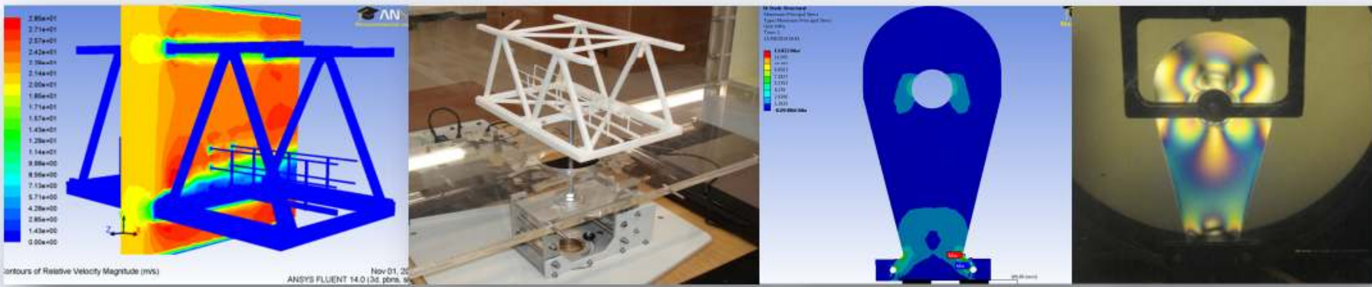

Analysis and Experimentation by B.Hand 2014

(See Video) https://www.youtube.com/watch?v=a3AHciPZrAE

"Give me a place to stand and,
with a lever long enough,
I will move the whole world"
(Archimedes)

Abstract

The maritime shipping industry dominates the transport of world cargo. Ship-to-Shore (STS) cranes play a crucial function in the provision of this safe and reliable means of transporting goods. The increasing transport demands of the maritime industry has dictated that STS container cranes are significantly increasing in size. The environmental and coastal locations of these cranes invariably leads to exposure to damaging meteorological effects of storms and other adverse weather phenomena.

Figure 1.1 Ship-to-Shore Cranes [1]

Currently traditional and highly conservative standards are utilised to quantify wind loading on these structures. The traditional standards based design approach leads to high mass crane structures and creates foundation problems in many harbour and quay structures - a problem exacerbated by the increasing trend towards larger STS cranes. The complex physical geometry of modern STS cranes combined with the dynamic and unpredictable nature of wind flow poses a major challenge to the designer / analyst wishing to diverge from the standards based approach. This analysis and validation challenge is undertaken by the author as a final year capstone project following work placement with Liebherr of Killarney, Co. Kerry, Ireland.

Extensive computational fluid dynamics (CFD) models are created and analyses conducted by the author to examine the airflow around critical modelled sections of a Liebherr STS crane. Physical scale model generation and wind tunnel testing is undertaken by the author to validate the determined CFD results. The CFD approach is indicated as an optimal analysis method - allowing the designer to accurately determine locations and magnitudes of high pressure and make informed design decisions based on these results. Significant operational and efficiency gains have been determined and are presented.

Design optimisation is conducted by the author on the crane tie-down system – this system significantly influenced by author CFD determined critical wind loading. A systematic design and prototype production approach is adopted to create and optimise a functional and dynamic design.

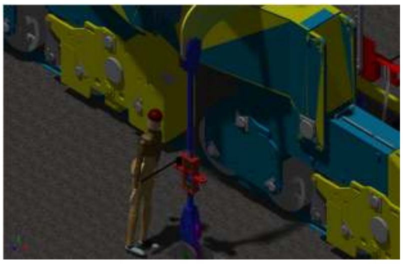

Figure 1.2 Tie Down System Design Optimisation
B. Hand 2014

Table of Contents


KAAN KALKAVAN

1 Nomenclature

Note - All units are presented in the following format unless otherwise stated:

1.1 Roman Symbols

Symbol	Name	SI Unit
E	*Young's Modulus*	GPa
F	*Force*	N
F_D	*Drag force*	N
F_L	*Lift force*	N
g	*Acceleration due to gravity*	m/s^2
G	*Shear Modulus*	GPa
I	*Turbulence intensity*	%
k	*Specific turbulent kinetic energy*	m^2/s^2
L	*Characteristic length*	m
M	*Mass*	Kg
P	*Power*	kW
p	*Pressure*	Pa
q	*Dynamic pressure*	Pa
v	*Velocity*	m/s
S_y	*Yield strength*	MPa
S_{ut}	*Ultimate tensile strength*	MPa
x	*Displacement*	mm
T	*Torque*	Nm

1.2 Dimensionless Roman Values

Symbol	Name
C_D	*Drag force coefficient*
C_L	*Lift force coefficient*
Fr	*Froude number*
Re	*Reynold's number*
St	*Strouhal number*

1.3 Greek Symbols

Symbol	Name	SI Unit
ε	*Kinetic energy dissipation rate*	m^2/s^3
ρ	*Density*	kg/m^3
μ	*Dynamic viscosity*	Pa.s
ω	*Frequency of eddy shedding*	Hz
τ	*Shear stress*	MPa
σ	*Normal stress*	MPa
σ'	*Von Mises stress*	MPa
ν	*Kinematic viscosity*	m^2/s

1.4 Dimensionless Greek Values

Symbol	Name
λ	*Scale factor*
ν	*Possion's ratio*
σ	*Standard deviation*

2 Introduction

This project was carried out in conjunction with the Liebherr Group - a worldwide leader in the design and manufacture of heavy machinery, particularly for the maritime industry. Since company inception in 1949, Liebherr's foremost attribute has been the design of functional superior cranes best suited to customer's needs. Liebherr Container Cranes, a sub-division of Liebherr Group, are the primary producer of maritime cranes for the company - specialising in the design and manufacture of Ship-to-Shore (STS) cranes.

Figure 2.1 Liebherr Plant, Killarney, Co Kerry, Ireland [1]

Due to the large and complex physical nature of the geometry of a STS container crane and the dynamic / unpredictable nature of wind flow, the accurate calculation of wind loads on a crane structure is very difficult, but if achieved would enable designers to accurately determine crane wheel loads and thus loads placed on the crane storm anchor system. Extensive state of the art computational fluid dynamics analysis, complemented by the use of wind tunnel testing, is conducted by the author on a critical section of the crane structure. Analyses of mesh size, mesh type, and turbulence model selection are undertaken to independently characterise developed mathematical model accuracy and grid independence. Key results from analysis and testing determine lower values for drag coefficients on these structures in comparison with those predicted by current standards based utilised methods.

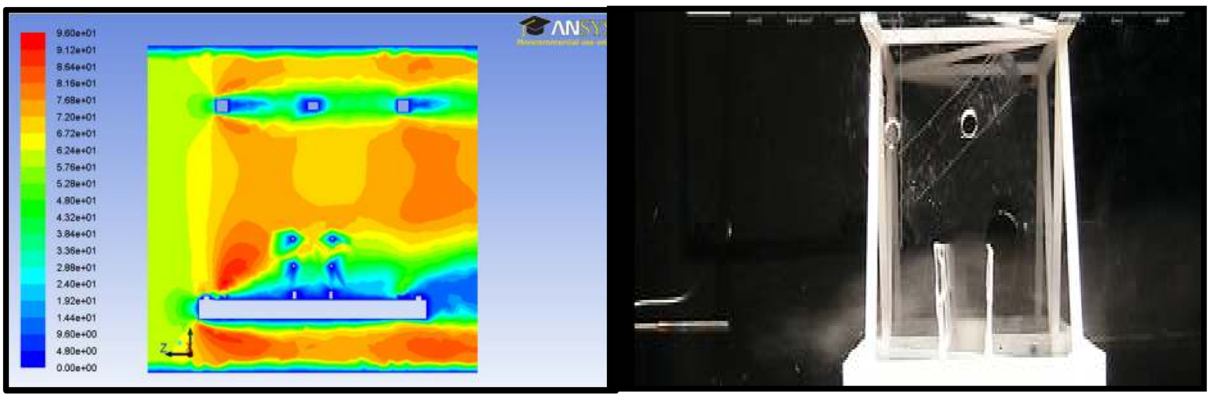

Figure 2.2 STS Crane Model Computational Fluid Dynamics Analysis and Wind Tunnel Validation / Smoke Visualisation - B. Hand 2014

3 Literature Research

3.1 Containerisation-The Concept

Containerisation is the global storage and transportation system, where containers carrying cargo can be easily, efficiently and systematically loaded onto containerships, freight-trains and vehicles, without handling the contents individually [2]. Before the inception of containerisation, international trade was a costly process where 25% of the price of goods was attributed to the insuring, transporting, loading, unloading and storing of cargo [3].

Figure 3.1 Shipping of Containerised Goods [4]

The whole shipping process was streamlined by American entrepreneur Malcolm McLean's Sea-land-Service in the 1950s, which developed an intermodal structure using standardised containers that foresaw the savings in time, labour and costs if the cargo containment part of a truck trailer could be simply lifted on and off the truck chassis and moved directly by ship [5]

Figure 3.2 McLean's Sea-Land Service [6]

Major growth in container volumes has occurred worldwide in the last fifty years, with particular accelerated expansion since the mid-1990s - See Figure 3.3 [7]. A UN study [8] estimates annual growth rate for global container trade volumes from 2005 to 2015 to be 7.6 % .

	1965	1970
Port labour productivity, tonnes per hour	1.7	30.0
Average ship size, tonnes	8.4	19.7
Number of loading ports in Europe	11	3
Insurance costs†, £ per tonne	0.24	0.04
Value of goods in transit†, £ per tonne	2	1

Figure 3.3 Increase in Containerisation [9]

3.2 The Container Crane

3.2.1 Introduction

A ship-to-shore crane is the largest crane used in the operation of the maritime shipping industry [10] and is a common sight in many maritime ports worldwide. Ship-to-shore cranes are designed and constructed for the main function of loading and unloading containers from a container vessel. The crane is controlled by an operator within a cabin, which is attached to the trolley suspended from a beam traversing the span of the crane.

Figure 3.4 Liebherr STS Container Crane [1]

3.2.2 Brief History

In 1959, the world's first high speed container crane was established - considerably reducing ship turnaround time [11]. Since the loading cycle is repeated many thousands of times, reduction of the length of this cycle has major and direct impact on the productivity of these ports and consequent beneficial economic outcomes [12]. Significant improvements and advancements have been made over time to container cranes - but all modern cranes are direct descendants of this first crane and the blueprint for modern cranes has stayed relatively unchanged [13].

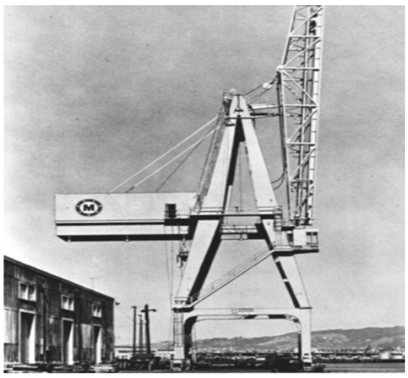

Figure 3.5 The First Container Crane [12]

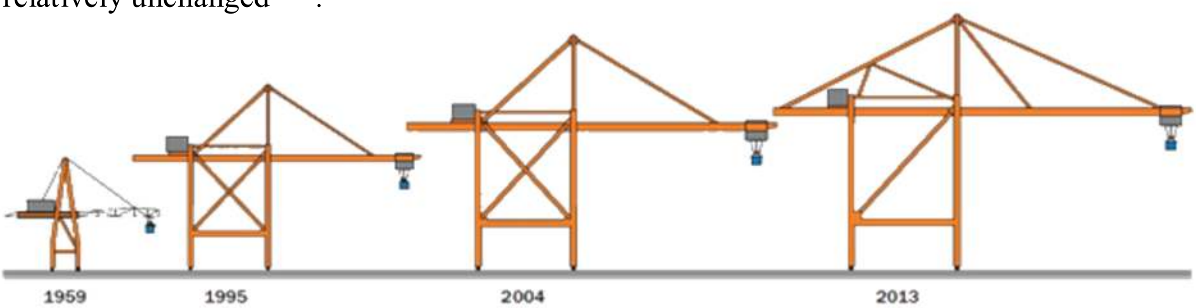

Figure 3.6 Container Crane Size Increase [14]

3.3 Challenges

3.3.1 Productivity

The accelerated growth of the maritime transport industry has meant container vessels and cranes have consistently increased in size to manage demand. In the 45 years since the first crane was designed, the dimensions of the cranes and their lifting capacities have more than doubled [15]. The driving force behind the expanding crane sizes has been the building of bigger container ships, which can carry more containers. Today, any port wishing to be at the forefront of container handling is reduced to a minimum operational capacity during the time that a ship is docked in the berth [16].The transfer of cargo between ships and ground transportation remains an expensive and time consuming process, driving a growing requirement for larger cranes.

Figure 3.7 Trend Towards Increasing Crane Size [1]

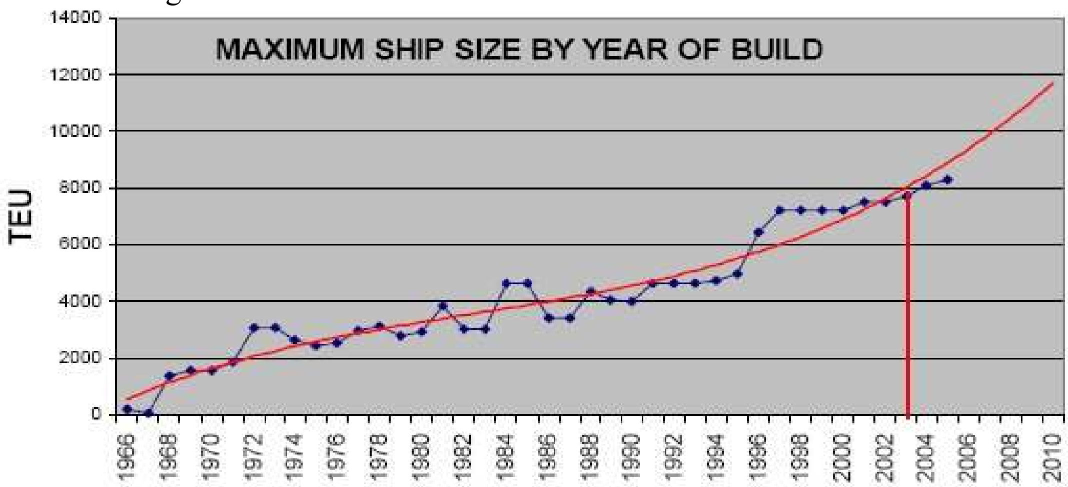

Figure 3.8 Growing Container Ship Sizes [11]

3.3.2 Quay Infrastructure

Currently very conservative methods are utilised in the calculation of container crane wind loads and, in many cases, these methods have been found to be impractical and also inaccurate. This approach can lead to a higher crane mass structure and consequently the quay infrastructure must be modified, which can prove very costly.

Figure 3.9 High Crane Mass Structure [1]

The crane structure member sizes can be reduced if the wind loads on the structure are proven to be less than those currently calculated, thereby yielding enormous benefits for design and energy efficiency. Furthermore, if the wheel loadings on the quay rails can be reduced, then the quay infrastructure can be designed with greater competence.

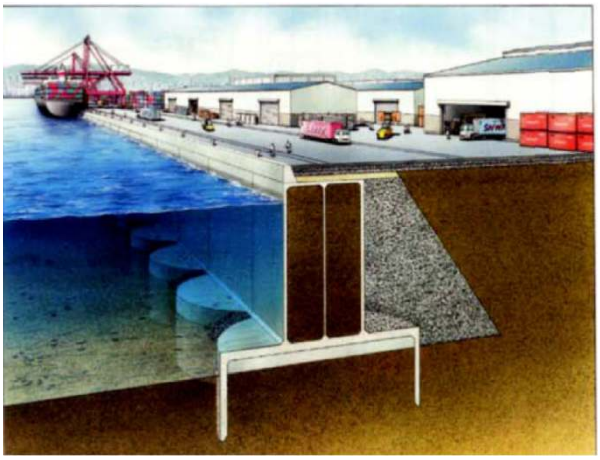

Figure 3.10 Quay Foundations [17]

Figure 3.11 Plastically Yielded Crane Legs due to Inadequate foundations [18]

3.3.3 Wind-Induced Failure of Crane Components

Container cranes, at their highest point reaching well over 100m, are especially exposed to severe windstorms and thus the wind load acting on the structure is substantial. In many cases, cranes have been severely damaged and even overturned due to losing their stability - as graphically demonstrated in Figure 3.13 [19].

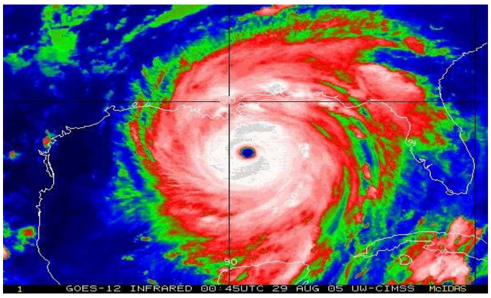

Figure 3.12 Increasing Storm Intensity [20]

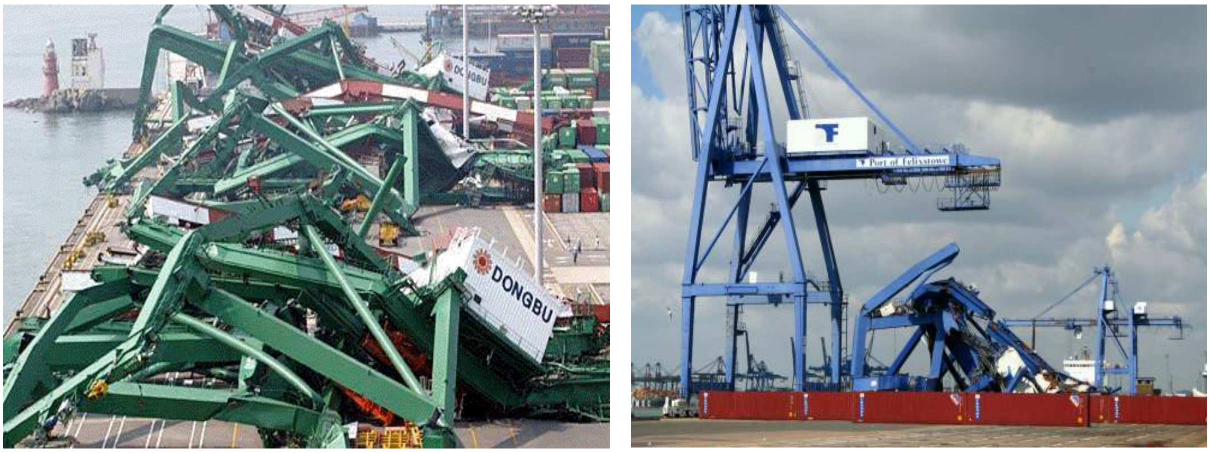

Figure 3.13 Crane Failure due to Wind-Induced Loading [19]

Crane safety devices, such as the tie-down system, prevent the crane from overturning and being pushed along the quay during extreme weather. However, studies and investigations of wind induced collapses of these cranes have determined that crane tie-down systems are the primary cause of failure and are found to be lacking in their mechanical response - failing at a fraction of the design load [21].

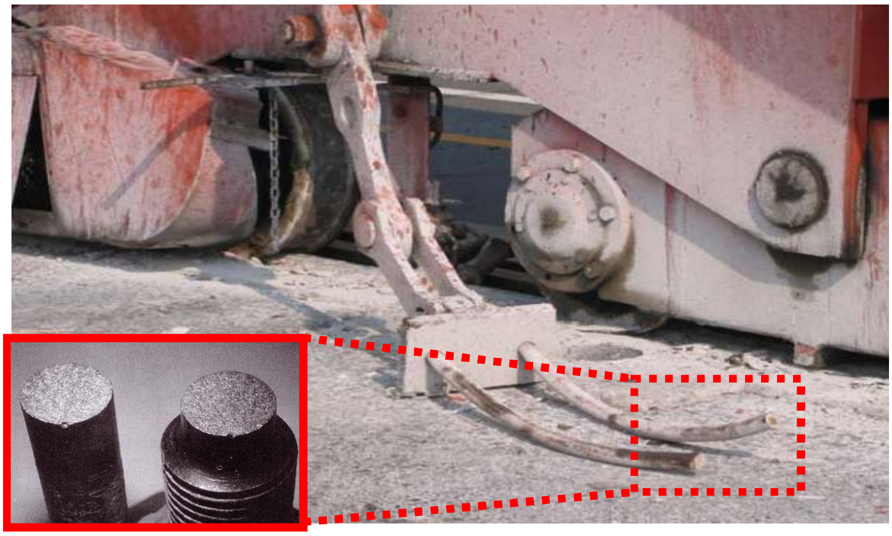

Figure 3.14 Mechanical Failure of Component [19]

The currently applied systems are cumbersome for crane workers attempting to set equal tension on these tie-down mechanisms and, due to deflection of the crane from wind loading, can lead to unequal tensile loads on the turnbuckles and give rise to a potential failure mechanism. In a study by maritime insurance provider TT Club, it was estimated that 34% of global asset claims are container crane related. Clearly, there is a requirement for improved safety and operation for container cranes [22].

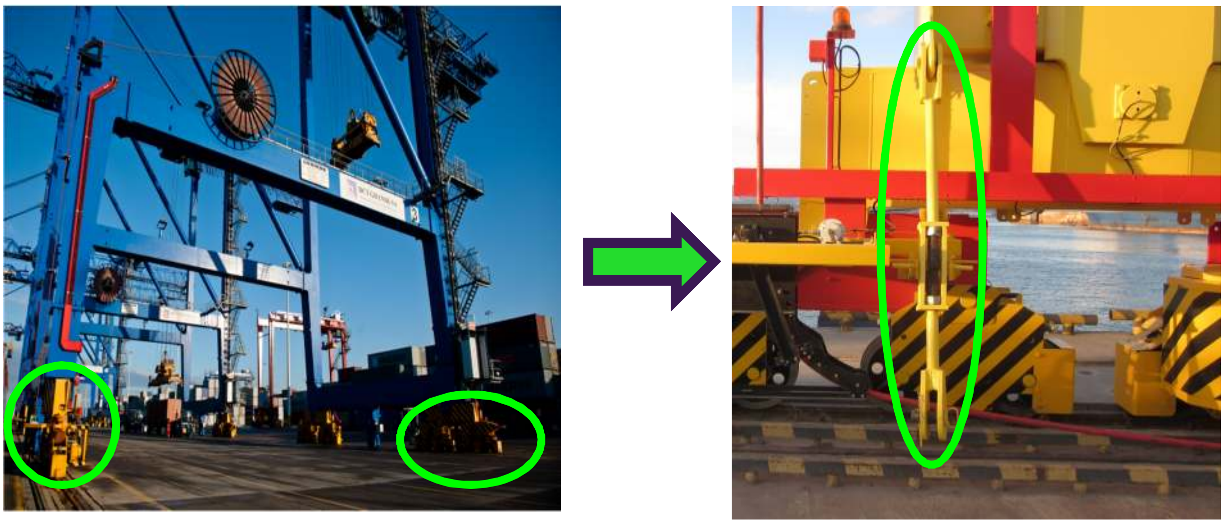

Figure 3.15 Current Crane Tie-Down System [1]

3.3.4 Emerging Technology

One area, in which there is particularly growing interest in the design of these cranes, is the application of numerical analysis techniques such as computational fluid analysis (CFD). However little published literature and research in this area exists - as is also the case for validation measures undertaken. The author's work in both CFD and experimental validation thus forms the backbone for this dissertation.

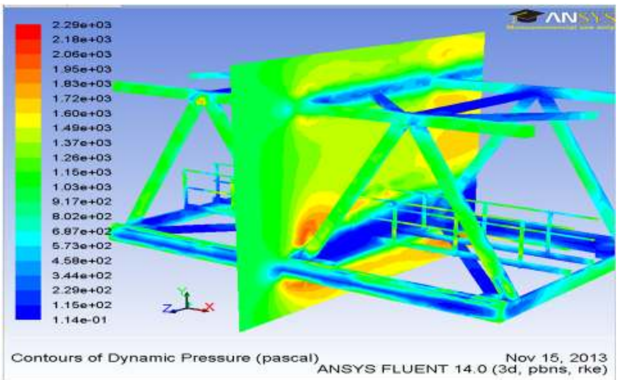

Figure 3.16 Computational Fluid Dynamics Application – B.Hand 2013

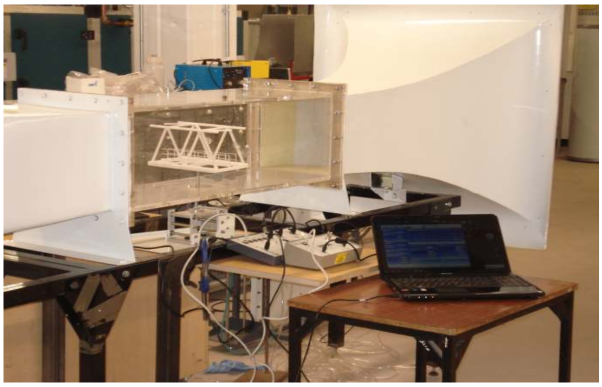

Figure 3.17 Validation via Wind Tunnel Test Studies – B.Hand 2014

4 Computational Fluid Dynamics Application

Computational fluid dynamics (CFD) analysis is the solution of the primary equations of fluid motion using numerical methods [23]. The section of flow and constraining boundaries are segregated into numerous small volumes or cells. The equations describing the conservation of mass, momentum and energy are calculated in each cell. Over the past ten years or so, there have been increasingly rapid advances in the area of CFD, especially in the development of improved numerical algorithms [24]. These advances have led to a large variety of numerical methods of diverse degrees of sophistication and precision.

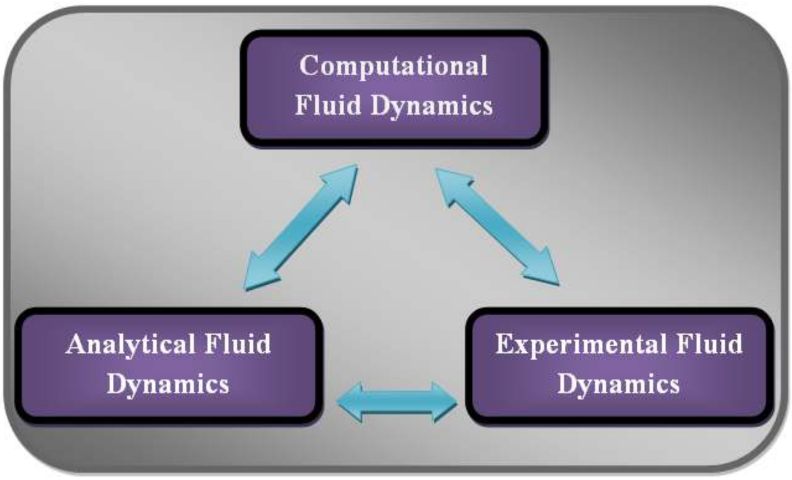

Figure 4.1 Fundamental Structure for Solution of Fluid Dynamic Problems - B. Hand 2013

4.1 Computational Approach

There are many advantages to using CFD - it complements experimental and analytical methods by delivering an alternative cost effective means of simulating real fluid flows. Developments in CFD (See Figure 4.2) make it a very appealing practical design tool in modern engineering practice [25]. CFD is thus steadily attracting more attention and awareness.

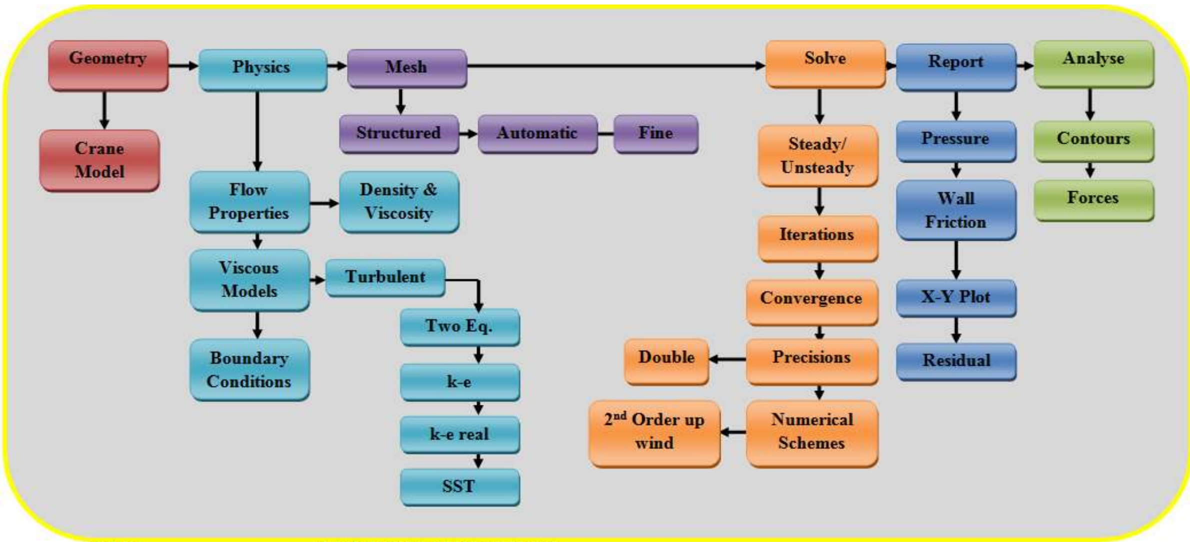

Figure 4.2 CFD Analysis Methodology - B.Hand 2013

CFD analysis was conducted by the author on a critical section of the crane structure - a repeating lattice section of the crane derrick boom (Figure 4.4). The complex nature of the lattice structure makes it very difficult to calculate accurately wind load - the results from the undertaken analysis are to be compared with current crane design standards.

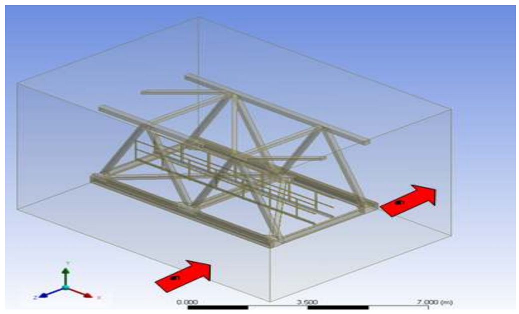

Figure 4.3 CFD Model Geometry – B.Hand 2013

Figure 4.4 Crane Derrick Boom Structure – Photo by B.Hand 2013

4.2 Computational Mesh Quality/Accuracy

Mesh generation is one of the most important steps during the pre-process stage of the CFD process. Model mathematical accuracy is highly dependent on the quality of the mesh developed. *"Both numerical stability and accuracy could be affected by a poor quality grid"* [26]. In the developed CFD models, extensive analysis was undertaken by the author on the CFD mesh to ensure optimal achievement of the most accurate results.

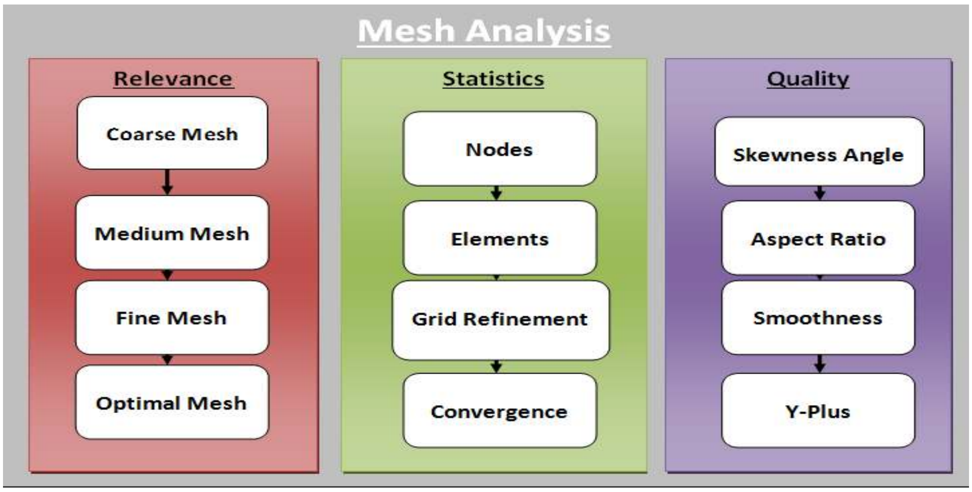

Figure 4.5 Mesh Analysis Undertaken - B.Hand 2014

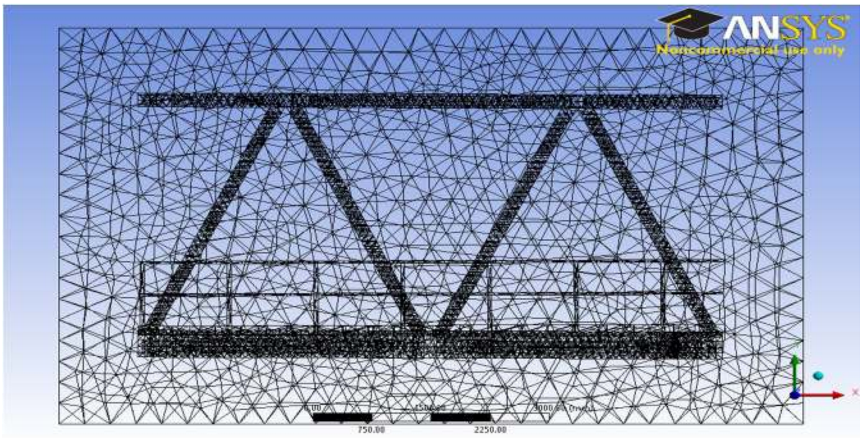

Figure 4.6 CFD Mesh generated on Critical Lattice Structure - B.Hand 2014

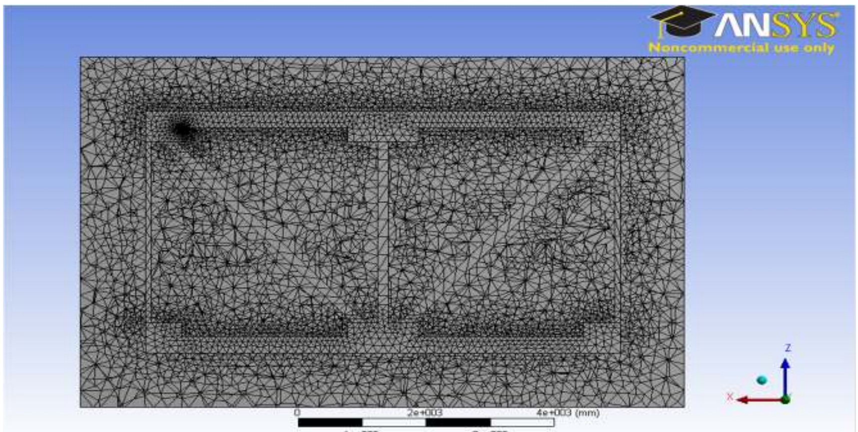

Figure 4.7 Section showing Mesh Detail - B.Hand 2014

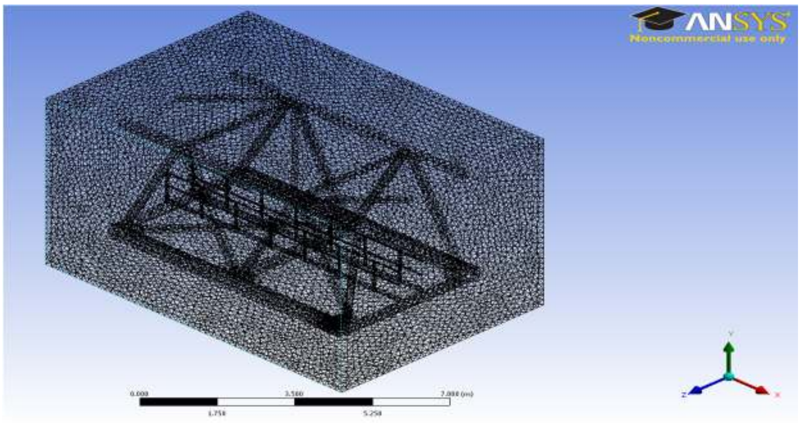

Figure 4.8 3D Mesh Intensity Detail - B.Hand 2014

Table 4.1 CFD Mesh Statistical Analysis - B.Hand 2014

Grid Elements Aspect Ratio				
Mesh Density	**Minimum**	**Maximum**	**Average**	**Standard Derivation**
Coarse	1.1706	10591	3.100	34.869
Medium	1.1669	364.85	2.288	3.248
Fine	1.1713	61642	2.119	88.095
Well Refined	1.1659	217.11	1.941	1.089

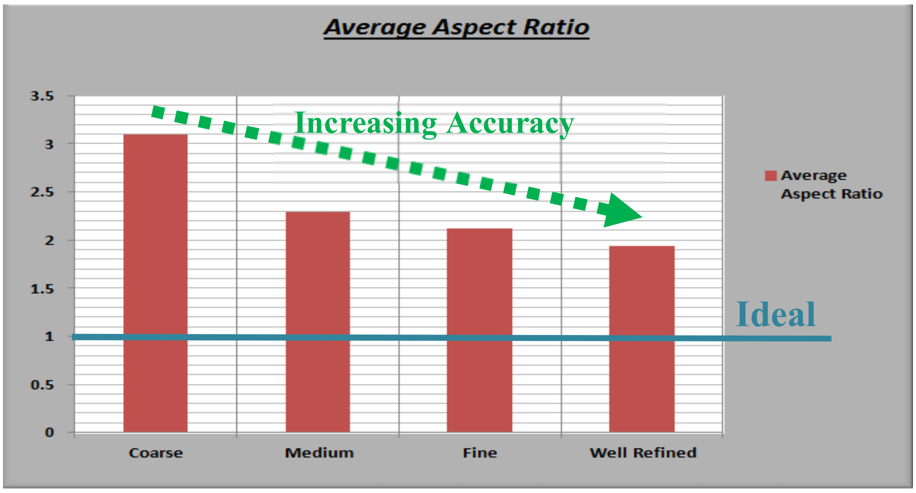

Figure 4.9 Optimal CFD Mesh Quality- B.Hand 2014

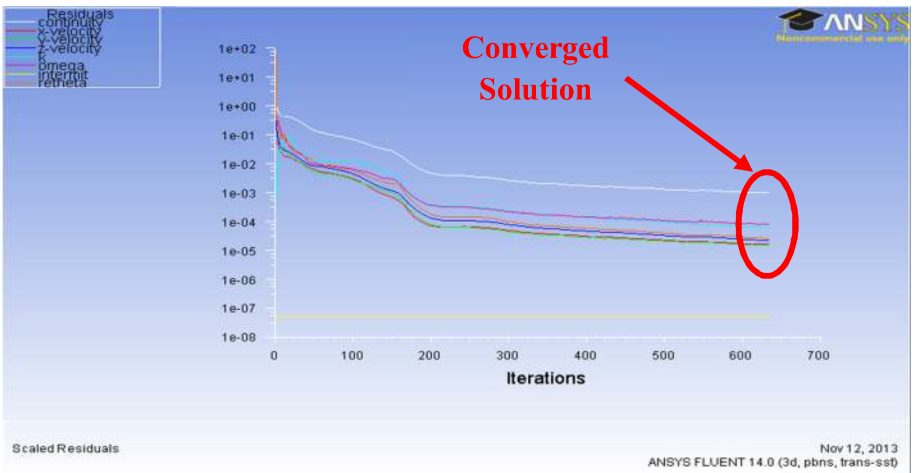

Figure 4.10 Iterative Analysis undertaken- B.Hand 2014

Note - Refer to Appendix: B for full mesh quality measures undertaken.

4.3 Applicable CFD Model Algorithm

The next and most integral part of the CFD analysis procedure is to research, analyse, choose and apply CFD mathematical model algorithms to accurately calculate results for the undertaken analysis. To achieve this, the author systematically analysed and compared three appropriate models for suitability for the developing analysis.

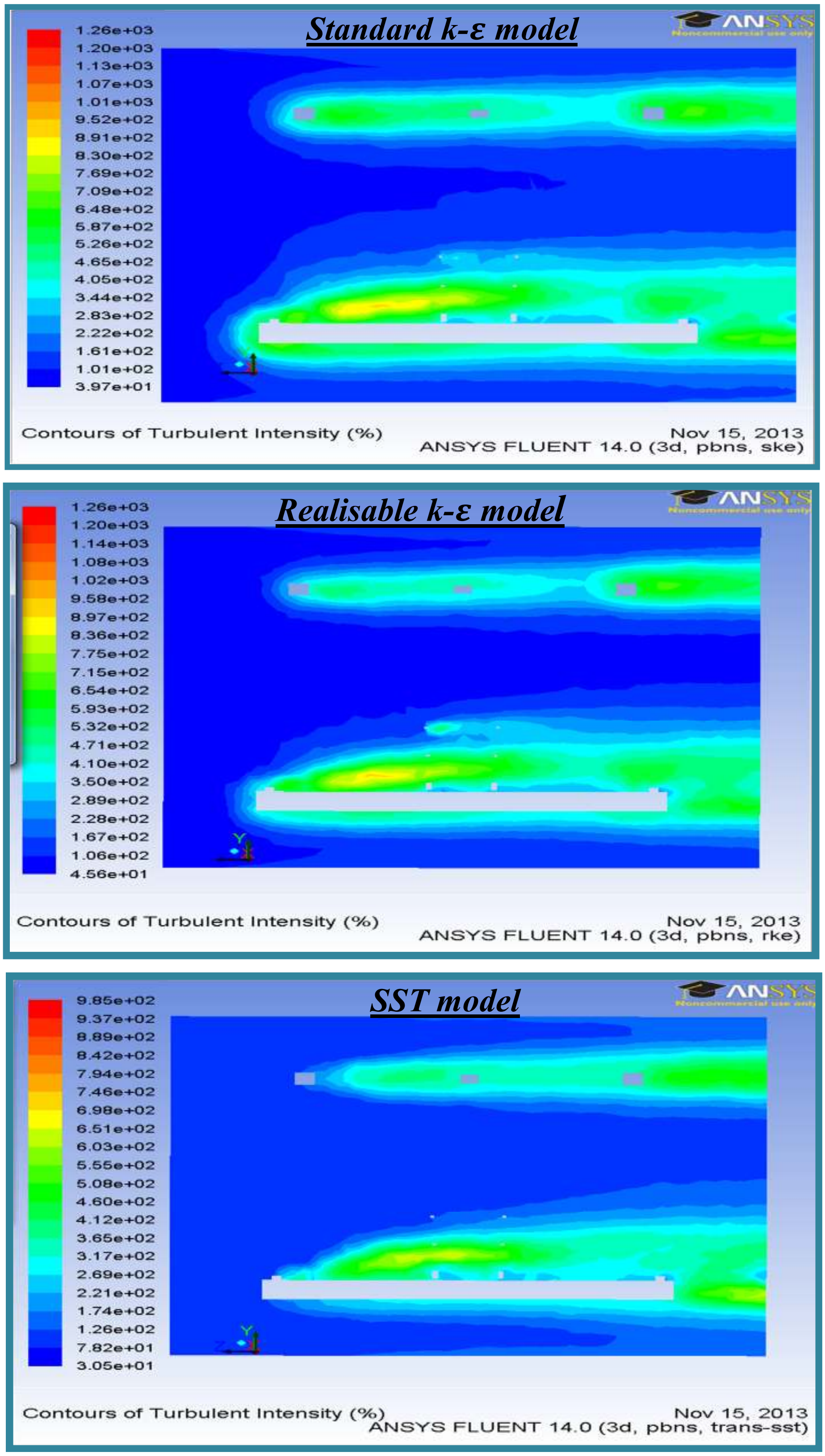

Figure 4.11 Diagrammatic Comparison of CFD Model Selection - B.Hand 2013

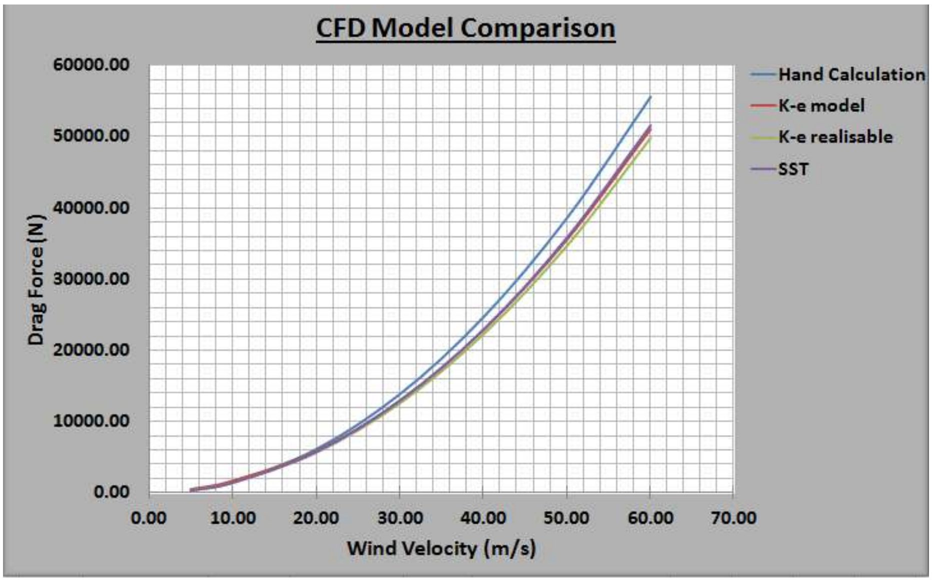

Figure 4.12 Graphical CFD Model Comparison - B.Hand 2014

This CFD model comparison allowed the most suitable model to be chosen for this analysis. Grid independence studies were conducted on the generated CFD mesh to ensure the results were convergent. Model mesh density was refined to achieve strict convergence criteria.

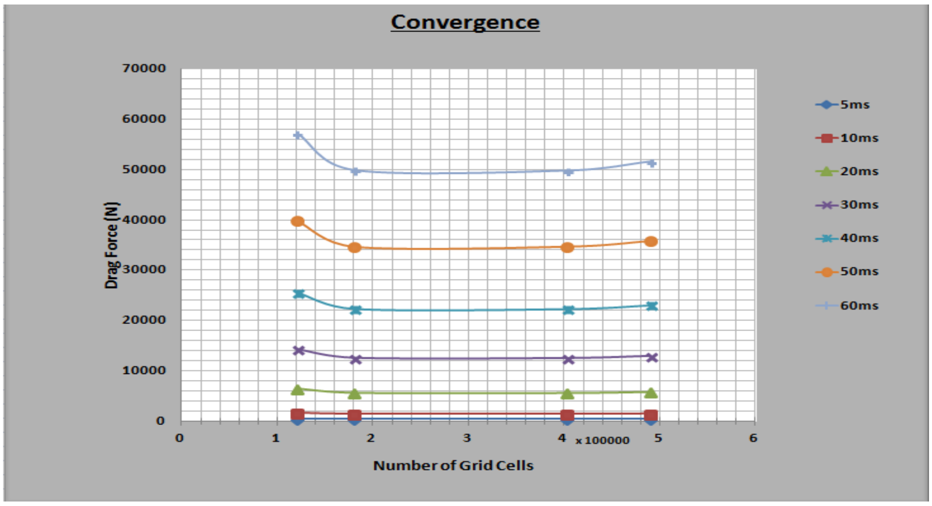

Figure 4.13 Developed Model Converged Results - B. Hand 2014

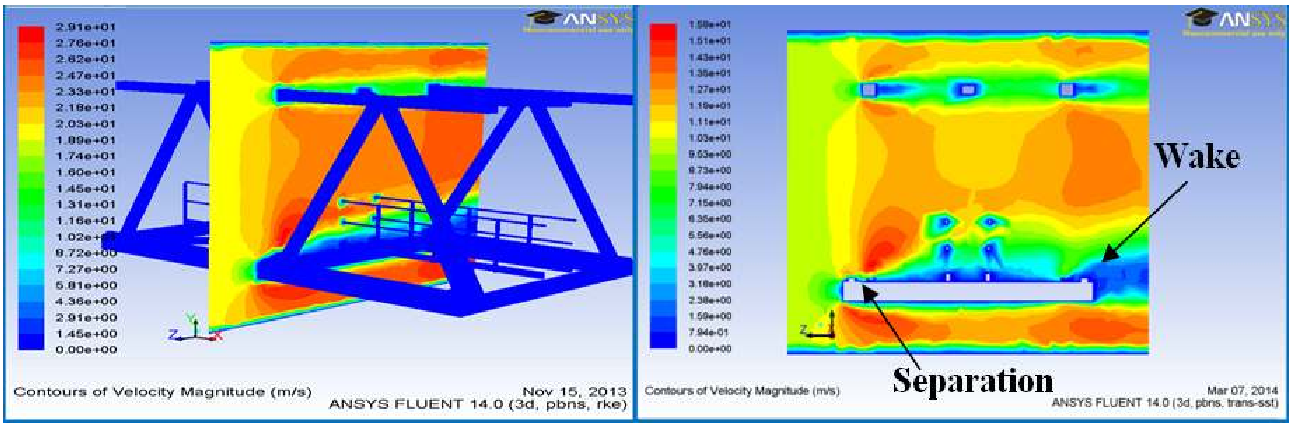

Figure 4.14 Boundary Layer Separation and Wake Region - B.Hand 2014

4.5 Numerical Results

Examination of the CFD results on the boom section reveals a considerable concentration of static pressure on the bottom section of the boom (Figure 4.16). This static pressure concentration is mainly caused by the shape of the rectangular faced section of the concerned I-beam box section (See Figure 4.17), critically required for the rigidity and strength of the structure.

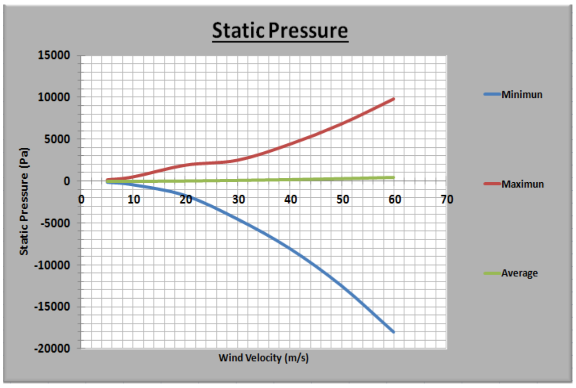

Figure 4.15 Static Pressure on Section - B.Hand 2014

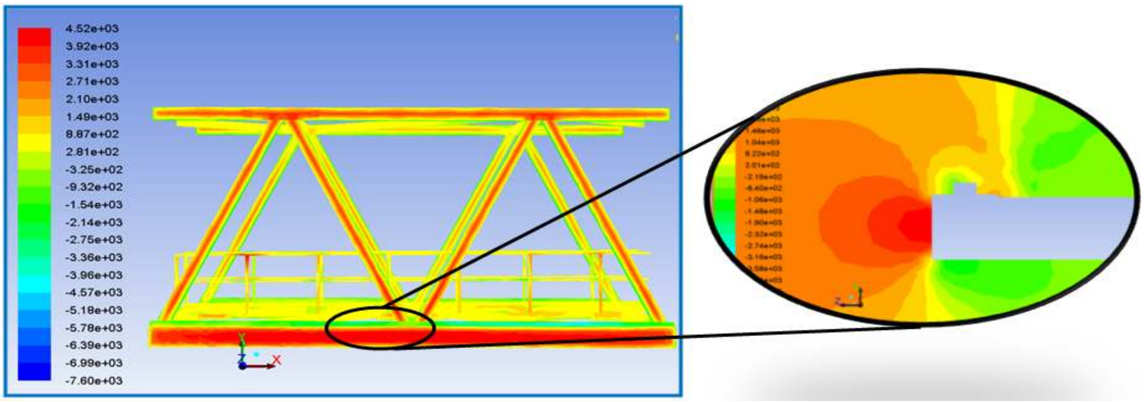

Figure 4.16 Static Pressure (Pa) - B.Hand 2014

The static pressure developing on the structure varies greatly with wind velocity. At two main set points of 20m/s and 40m/s, the maximum pressure is 0.78K KPa and 2.02 KPa respectively. Flow separation and wake formation is observed - mainly occurring around this part of the structure. Examination of generated CFD models leads to the conclusion that this separation is initiated by the relatively sharp corners on the beam. One minor but reasonably straightforward design modification is to ensure a well defined filleted edge is present at this location – thereby delaying the flow separation point to further downstream and improving the structure aerodynamics.

Figure 4.17 Structure Geometry - Photo by B.Hand 2013

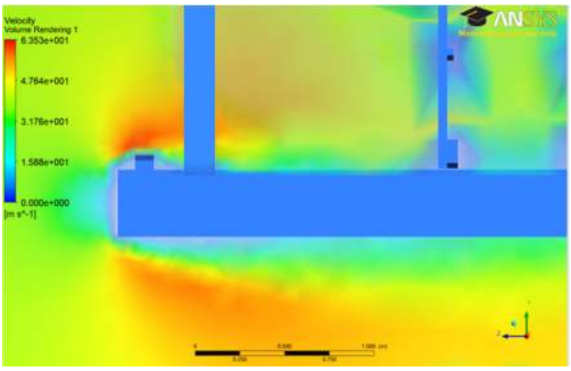

Figure 4.18 Flow Separation - B.Hand 2014

5 Wind Tunnel Testing

5.1 Overview

Wind tunnel testing on a scaled model was determined to be the best method to validate the CFD results found from the analysis. Even though this type of testing has been utilised since the early twentieth century, engineers and designers today, equipped with state of the art computers, still rely on the testing of models to verify computer data and determine baseline performance [26].

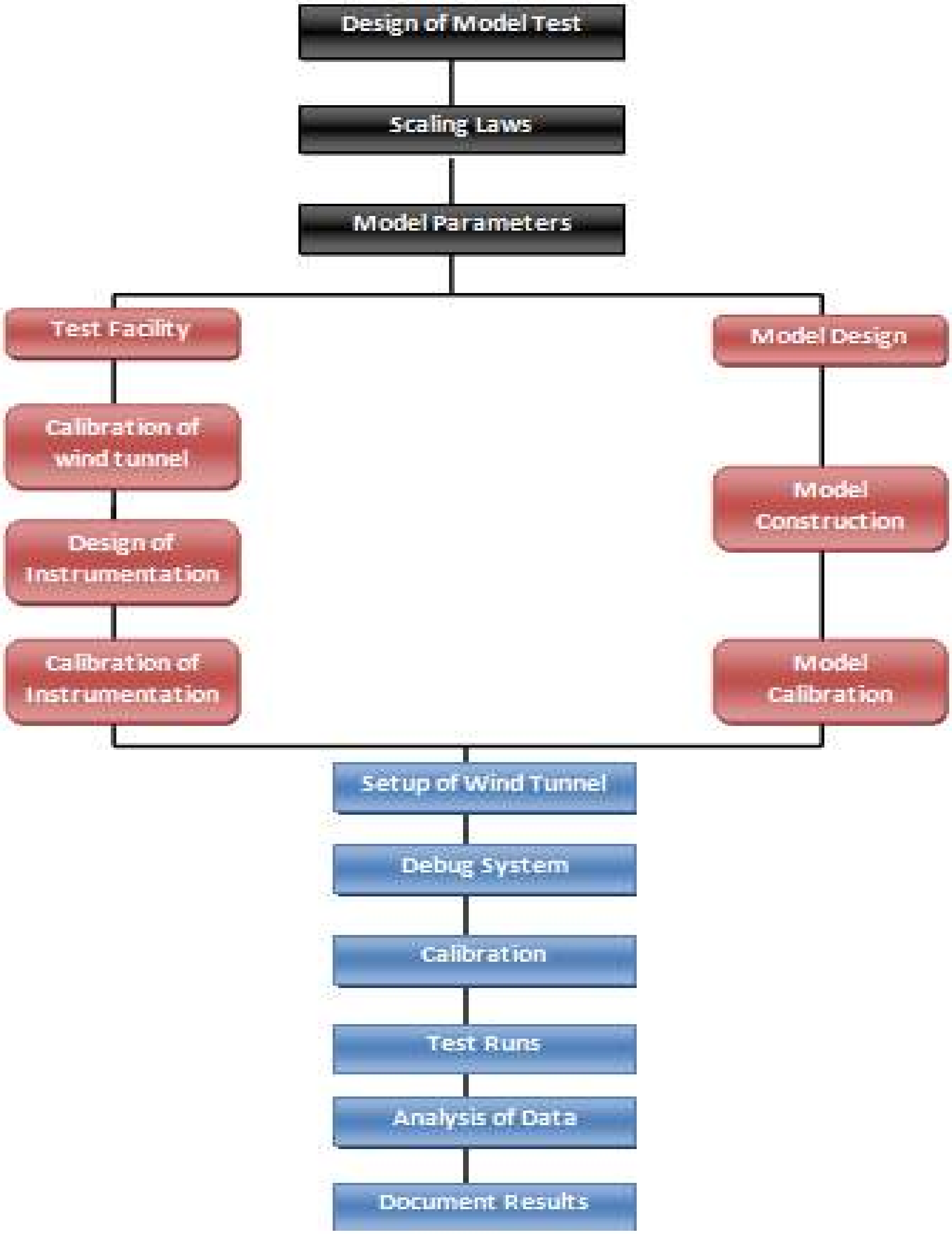

Figure 5.1 Wind Tunnel Test Methodology Adopted- B.Hand 2014

5.2 Scale Model Similitude Theory

5.2.1 Scaling Laws

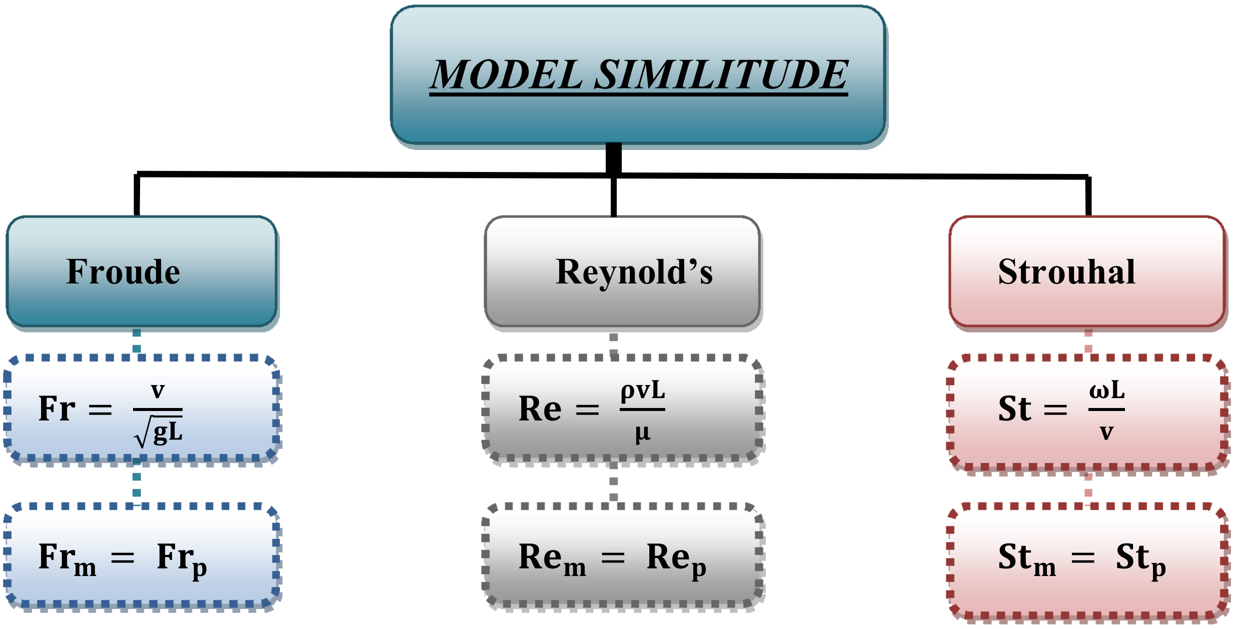

Figure 5.2 Applicable Scaling Laws for Model Testing - B.Hand 2014

Testing is carried out on a scaled model according primary to Froude's Scaling Law.

Table 5.1 Froude Scaling Factors - B.Hand 2014

Variable	Unit	Scale Factor	Model : Prototype
Length	L	λ	1:28
Force	MLT^{-2}	λ^3	1:21,952
Velocity	LT^{-1}	$\lambda^{\frac{1}{2}}$	1: 5.292

It is impossible to achieve both Froude and Reynold's scaling simultaneously in a specific model test but, taking specific scaling conditions, the testing can be undertaken independent of Reynold's number.

5.2.2 Model Test Conditions

1. The model will have sharp edges so flow separation occurs.
2. The flow stream must be turbulent.
3. Reynold's number must be kept sufficiently high.

5.3 Physical Model

5.3.1 Scaling Conditions

A 1/28 scaled model of the critical crane section was generated by the development of a detailed 3D CAD solid model by the author. The developed solid model enabled the physical production of the scaled wind tunnel model (ABS material) on the college advanced rapid prototyping facility.

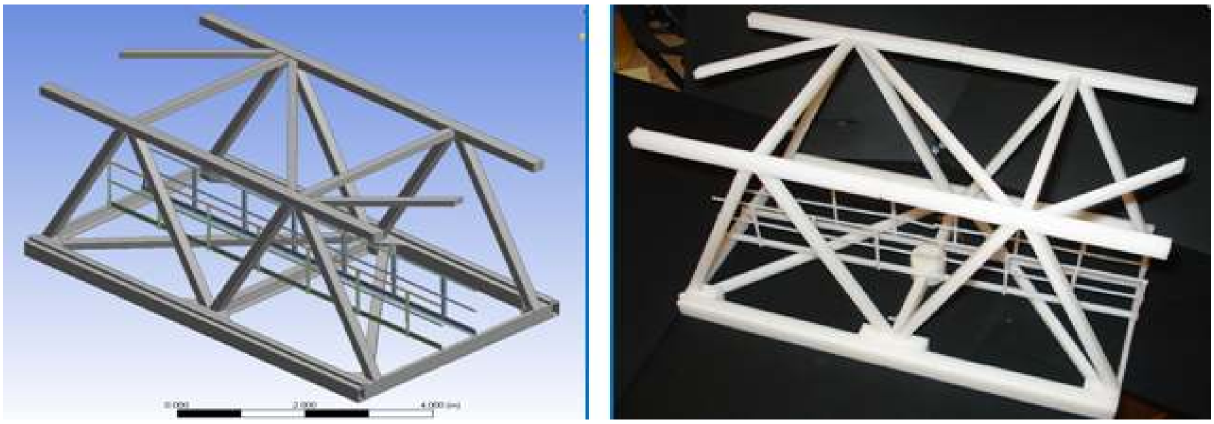

Figure 5.3 3D CAD Generated 3D Solid Model and Physical Rapid Prototyped Model (ABS material) - B.Hand 2014

Table 5.2 ABS Material Properties [29]

Young's Modulus *(E)*	Possions Ratio (ν)	Shear Modulus *(G)*	Density (ρ)	Yield Strength (S_y)	Tensile Strength (S_u)
3.1 GPa	0.38	950.277 MPa	1060 $\frac{\text{Kg}}{\text{m}^3}$	40.33MPa	40 MPa

In-depth design analysis was conducted by the author to ensure that the model would be capable of withstanding the drag forces created from wind tunnel testing. This pre-testing structural analysis was undertaken through finite element analysis. Further minor design modifications to facilitate practical testing were made to the model. (See Figure 5.4)

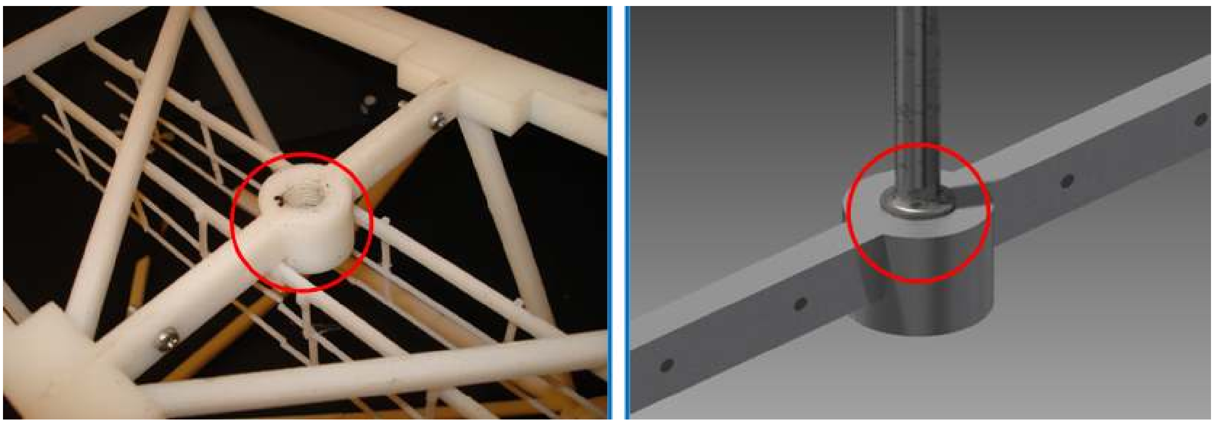

Figure 5.4 Developed Scale Model Testing Attachment Design and Implementation - B.Hand 2014

5.3.2 Finite Element Analysis

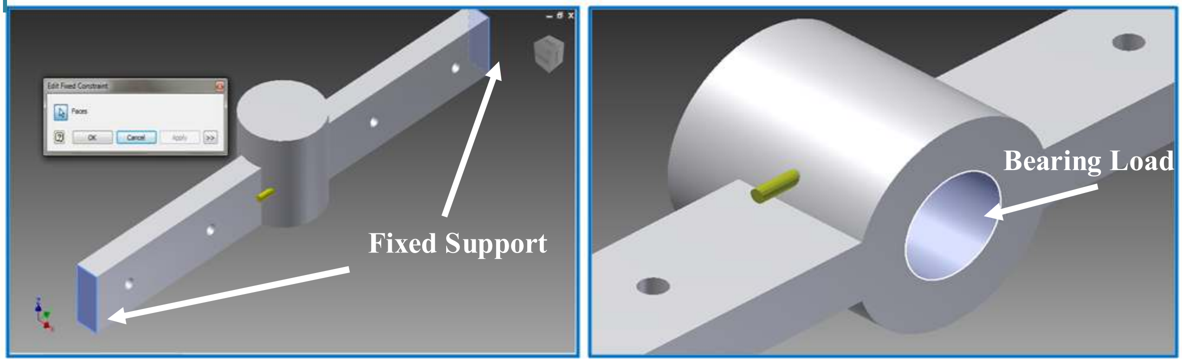

Figure 5.5 Analysis Boundary Conditions – B.Hand 2014

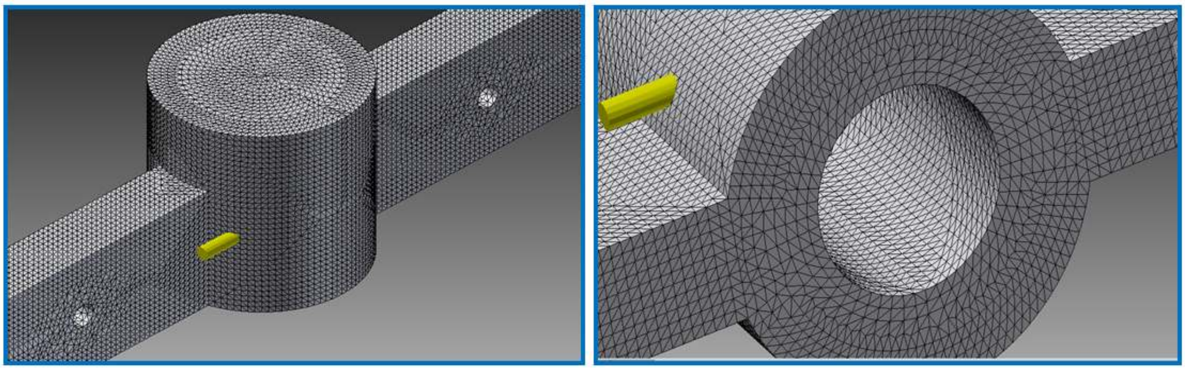

Figure 5.6 Design Mesh Detail – B.Hand 2014

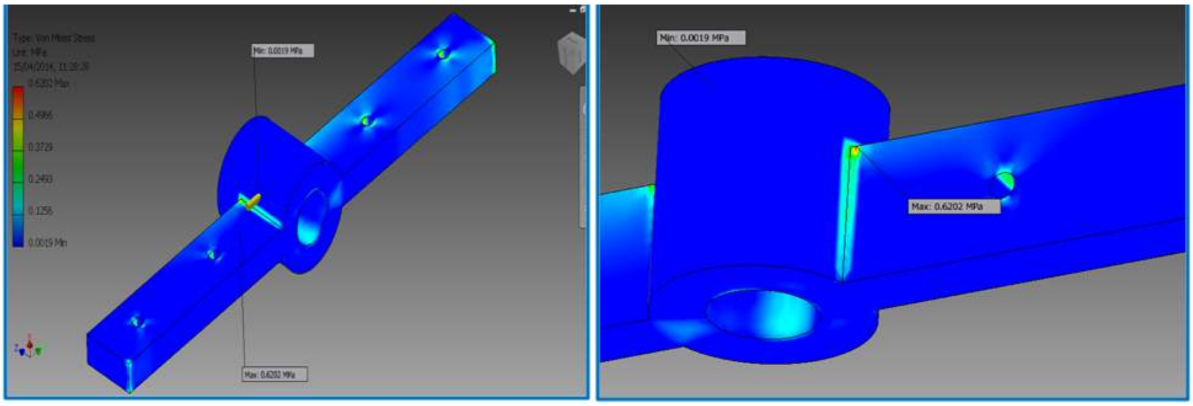

Figure 5.7 Equivalent Stress on Testing Model Design (MPa) - B.Hand 2014

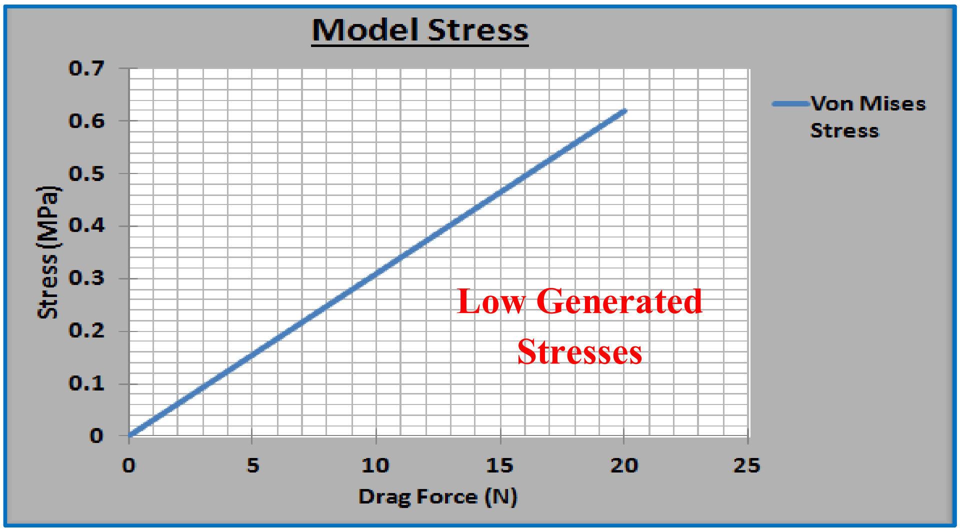

Figure 5.8 Equivalent Stress vs Predicted Drag Force for Design – B.Hand 2014

5.4 Wind Tunnel Test

The wind tunnel model testing was carried out using the college's open circuit type subsonic wind tunnel with a working test section of 300mm × 300mm. The air enters the tunnel through a carefully shaped inlet - the working section is transparent giving full visibility during the testing (See Figure 5.9).

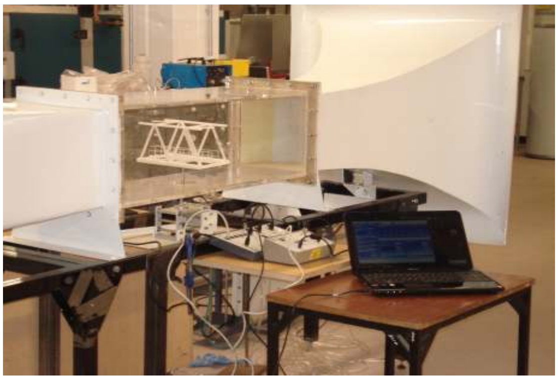

Figure 5.9 Wind Tunnel Test Facility – B.Hand 2014

"To gain accurate and trustworthy data from a testing apparatus, a proper data acquisition system is required" [27].Data acquisition (DAQ) is the method of measuring an electrical generated signal such as a voltage from a device known as a transducer. In this case, the load cell on the force balance is connected to a data acquisition system - the VDAS (Versatile Data Acquisition System) - which is compatible with the wind tunnel load cell. This system offers many advantages such as reducing the time needed to physically collect data and also lower the chance of errors taking place when inputting data to a computer manually. The system can also allow for high speed data collection.

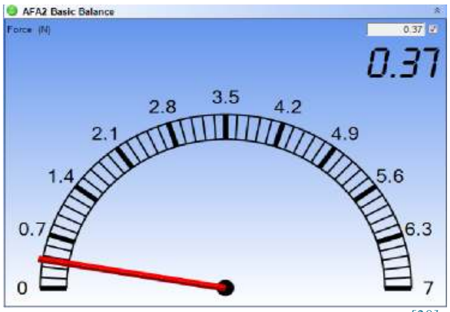

Figure 5.10 Data Acquisition System [28]

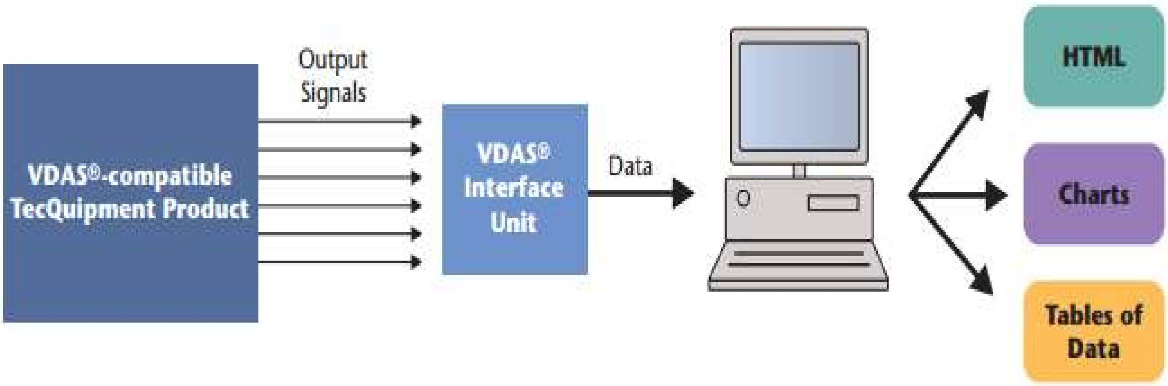

Figure 5.11 VDAS System [28]

Note - Refer to Appendix: C for Calibration procedures undertaken and numerical results

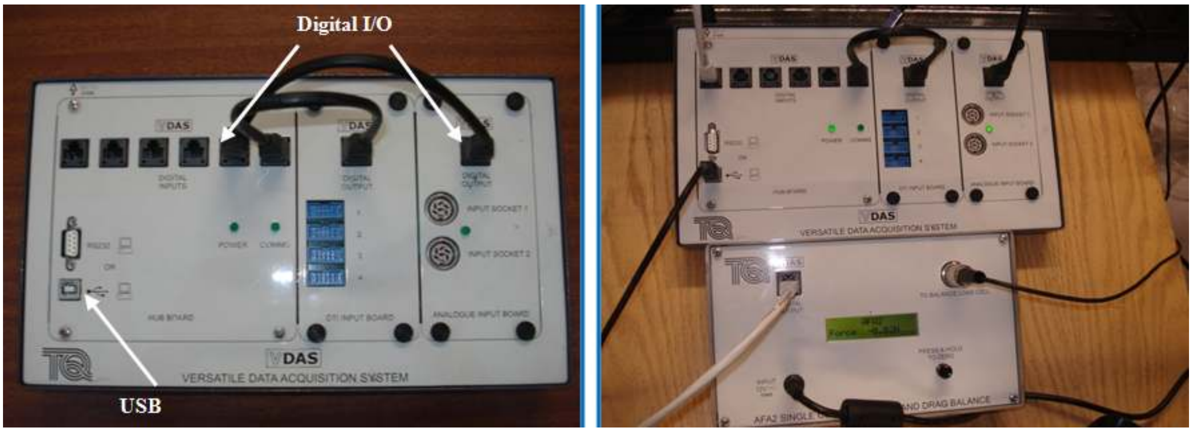

Figure 5.12 Data Acquisition System Setup – B.Hand 2014

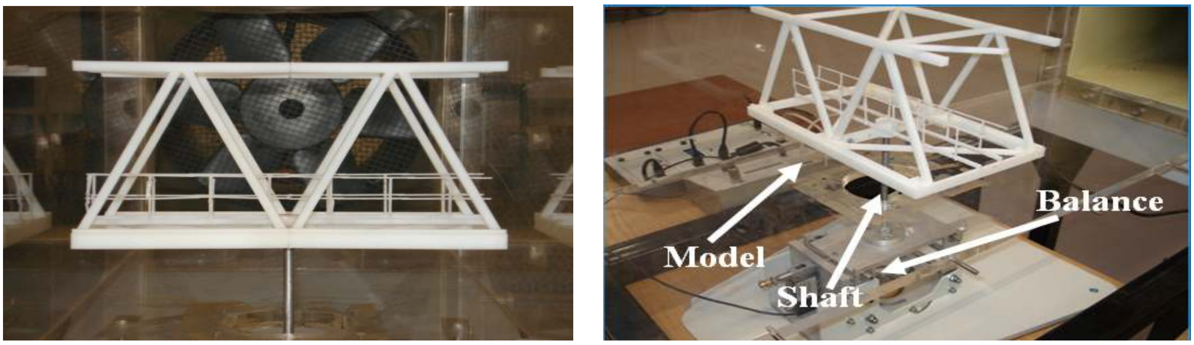

Figure 5.13 Wind Tunnel Model – B.Hand 2014

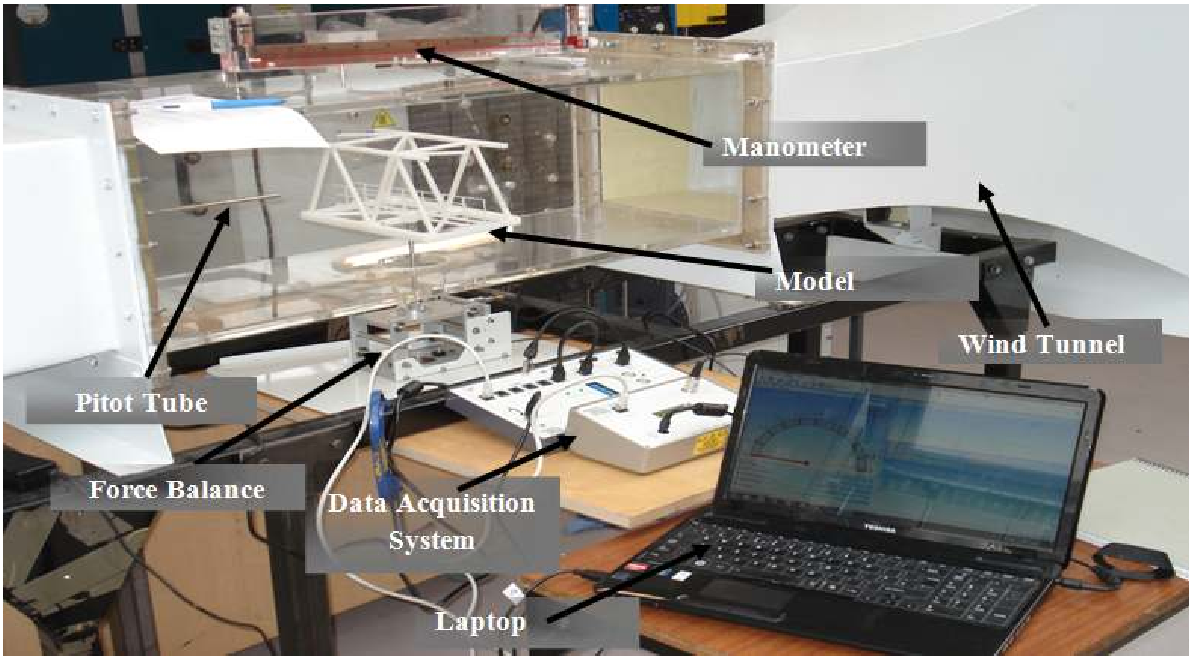

Figure 5.14 Wind Tunnel Test Setup – B.Hand 2014

Using the developed and commissioned experimental setup shown in Figures 5.12, 5.13 and 5.14, baseline wind tunnel testing commenced on the scale model.

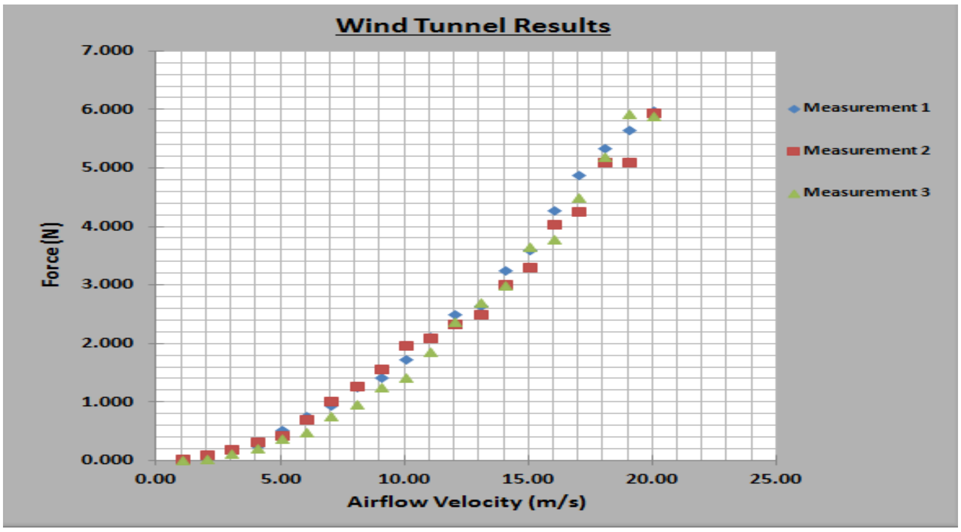

Figure 5.15 Recorded Model Drag Results – B.Hand 2014

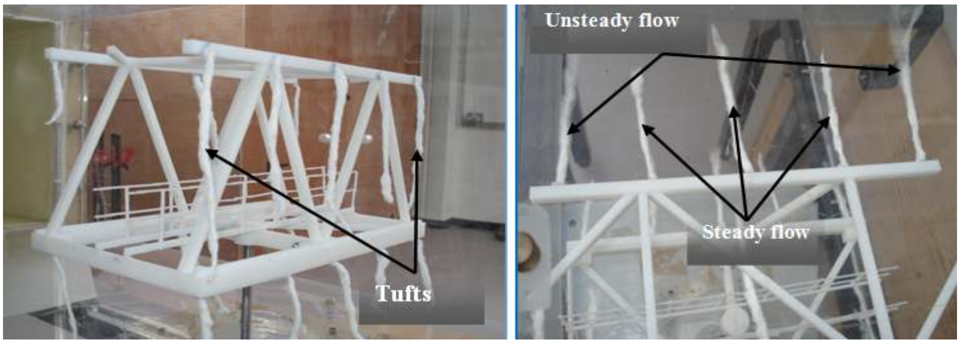

Figure 5.16 Aerodynamic Analysis using Tufts – B.Hand 2014

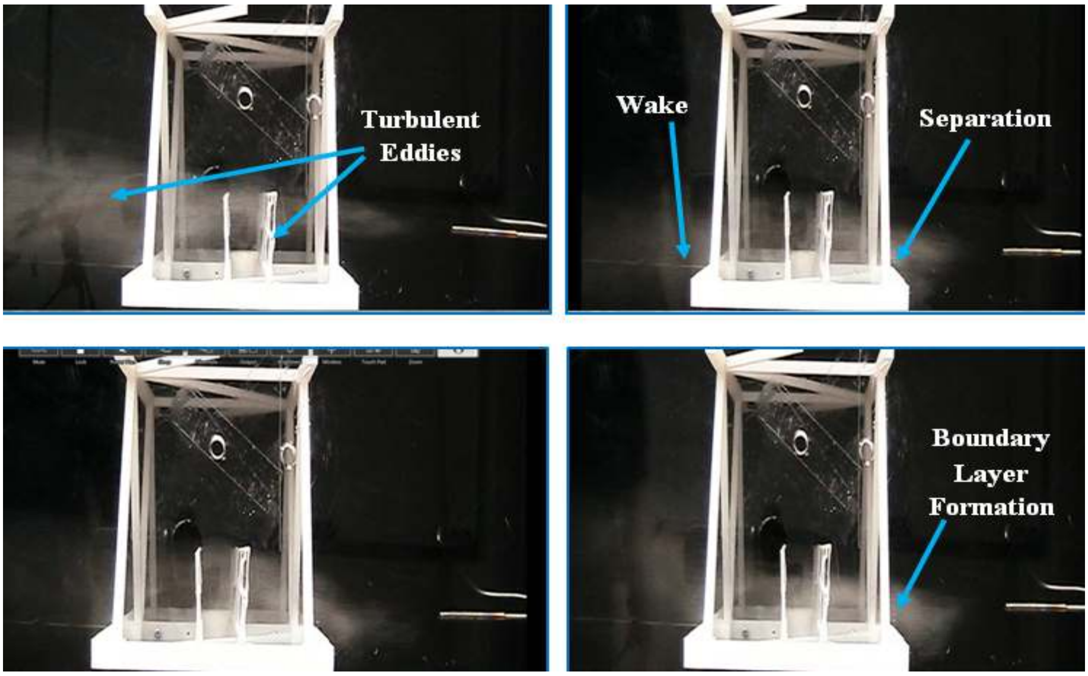

Figure 5.17 Wind Tunnel Airflow Visualisation Technique for Aerodynamic Analysis – B.Hand 2014

Comprehensive experimental analysis of the aerodynamic flow patterns around the structure, including smoke visualisation coupled aerodynamic tufts, was performed by the author.

On achievement of baseline results through wind tunnel testing on the physical model, corresponding CFD analysis and model results comparison was undertaken.

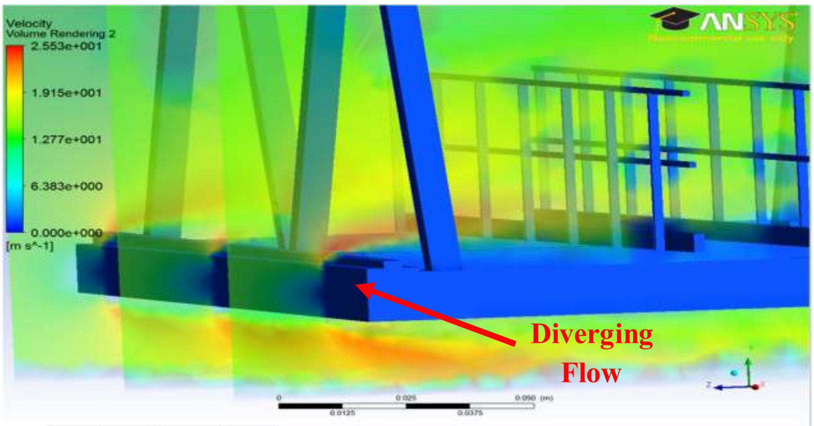

Figure 5.18 CFD Plot showing Rapid Velocity Distribution – B.Hand 2014

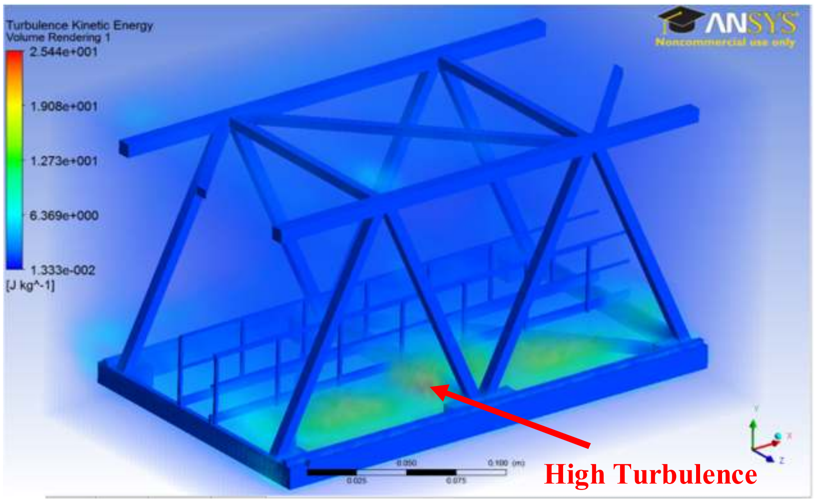

Figure 5.19 CFD Plot showing Turbulence Intensity on Model – B.Hand 2014

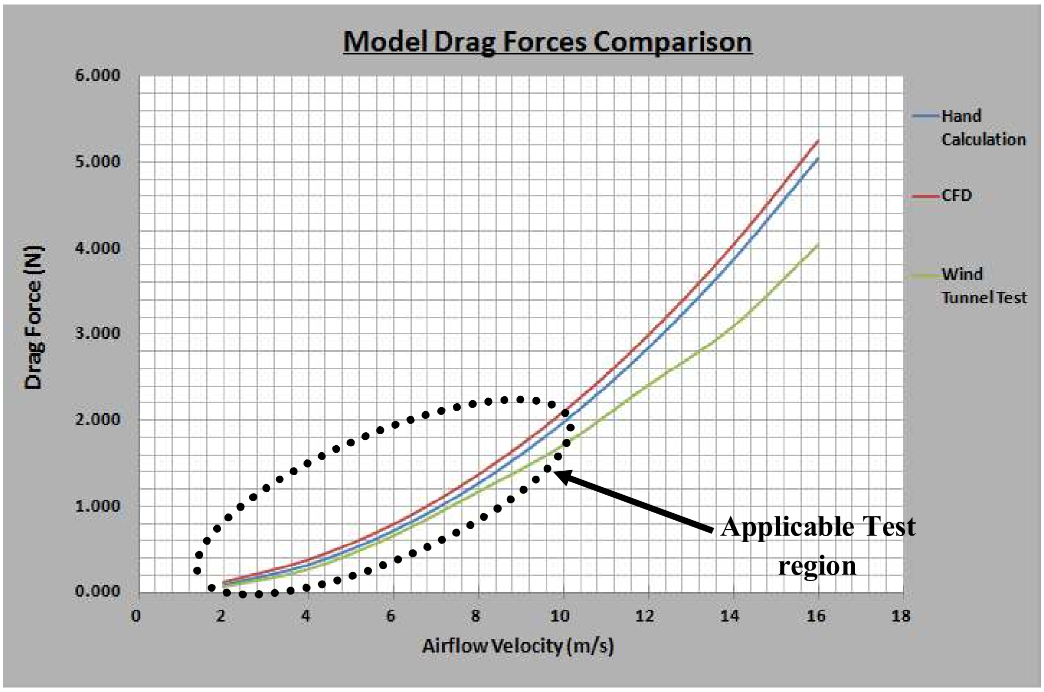

Figure 5.20 Comparison of Model Results – B.Hand 2014

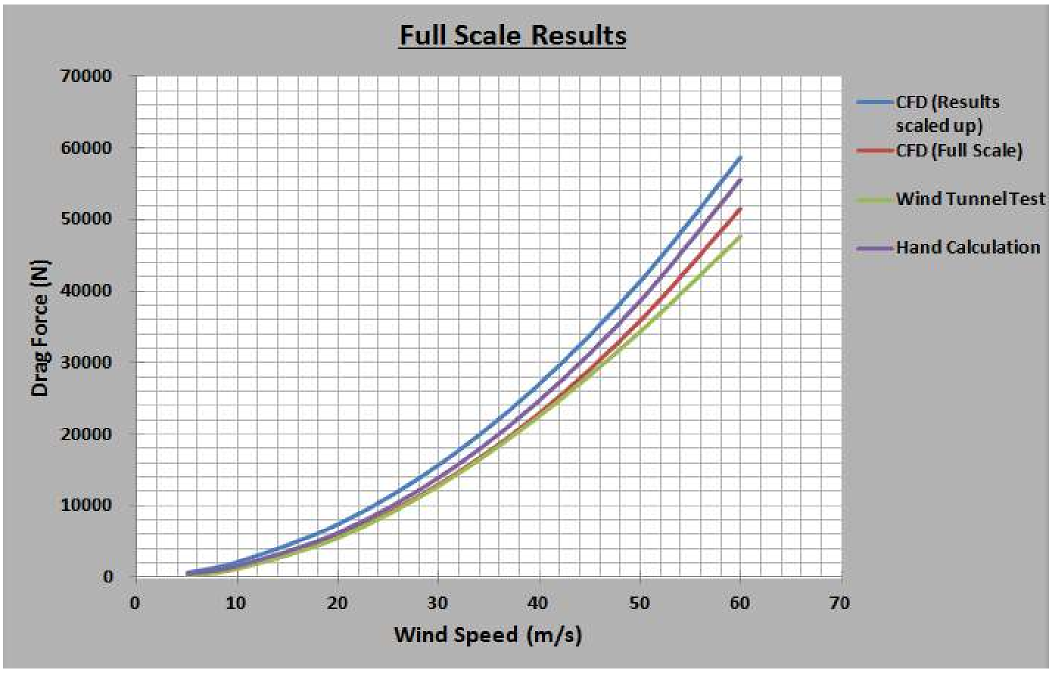

Figure 5.21 Full Scale Results Comparison – B.Hand 2014

Figure 5.21 shows the results for drag on the full scale crane structure with respect to the various analytical and experimental tools used. A significant deviation between the results in comparison with the current utilised standardised numerical approach is clearly observed.

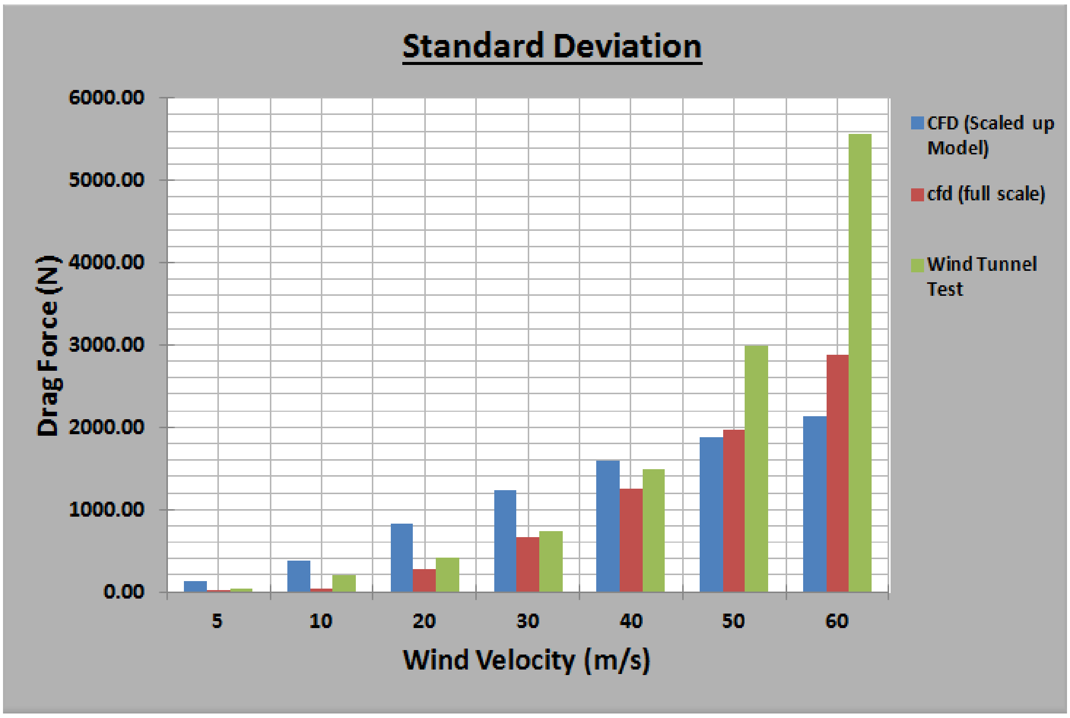

Figure 5.22 Deviation between Experimental and Numerical Results – B.Hand 2014

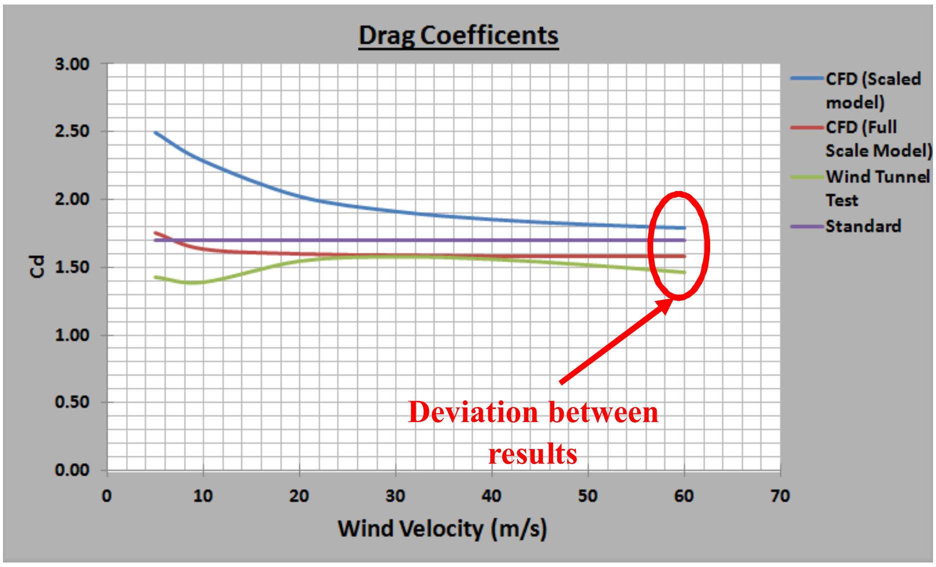

Figure 5.23 Drag Coefficients on Structure - B.Hand 2014

Generally, in analytical terms, the designer or analyst will mainly focus on the drag coefficient for the structure section and ultimately determine the wind force generated - so the need for accurate drag coefficient determination is paramount. Figure 5.23 shows a graphical representation of drag coefficients (C_d) computed from different means by the author with respect to the current standard approach. It was determined from this analysis that the (C_d) values were found to be significantly lower than those predicted by current standard approach. In effect, the wind loads calculated for these structures are being substantially overestimated. Achievement of lower force values confers further benefits to the designer - including optimal use of material and better control of factor of safety values applied to the structure. The reduction in values is also advantageous to the goal of minimisation of the overall weight of cranes - an increasing concern for designers of the foundations of quays and supporting structure at the base of the cranes as these cranes continue to increase in size.

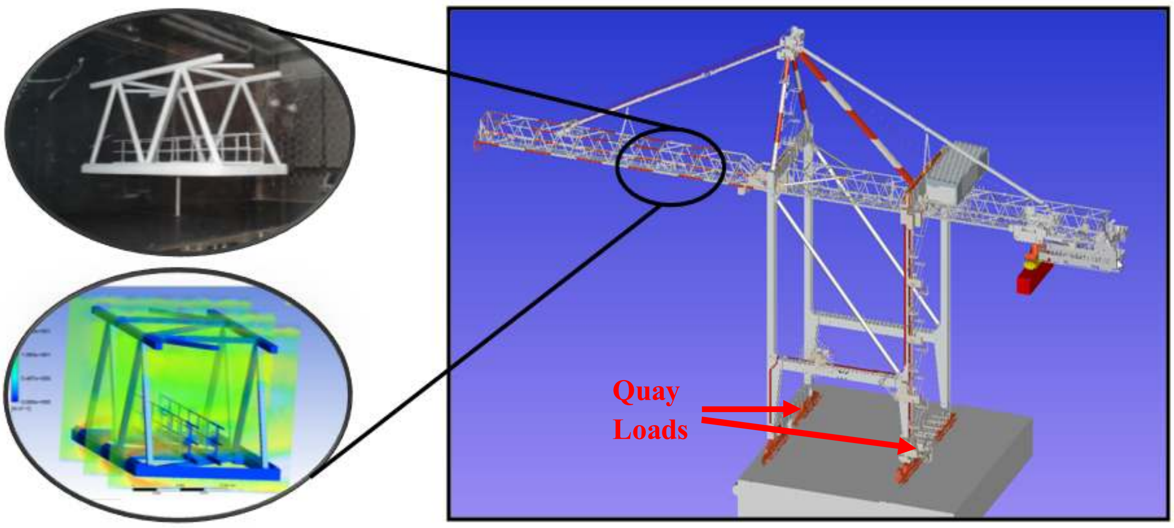

Figure 5.24 CFD and Wind Tunnel Results Prediction of Lower C_d Values – B Hand 2014

6 Design Optimisation

6.1 Overview

The potential for design optimisation is examined by the author in relation to critical crane tie-down anchor system, which is significantly affected by fluctuating wind loading. The crane tie down system prevents the crane from becoming detached during high winds or storms and resists the uplift forces created from wind flow over the crane. The current system has problems - it is cumbersome for the crane workers to set equal tension on these tie-down mechanisms and, due to deflection of the crane from wind loading, can lead to unequal tensile loads on the turnbuckles and give rise to a potential failure mechanism.

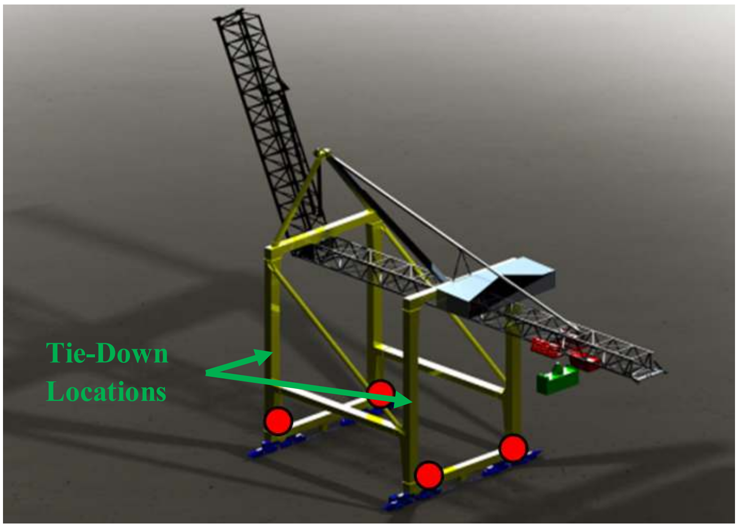

Figure 6.1 Location of Crane Tie-Downs B.Hand 2014

Figure 6.2 Current Tie-Down Design – B.Hand. 2014

A redesign of this critical crane component was undertaken. A systematic design approach was adopted by the author to achieve design optimisation of the component (Figure 6.3 depicts key aspects of the systematic design - extended versions are given in Appendix D).

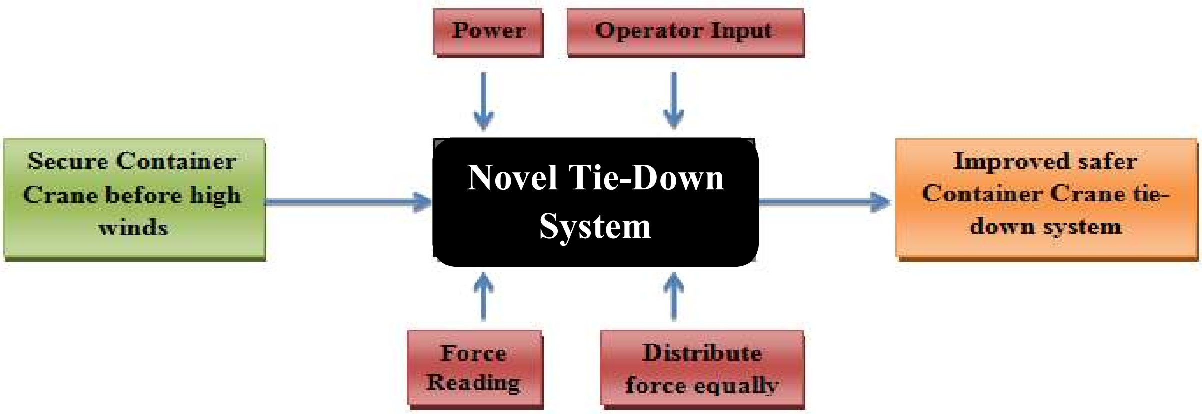

Figure 6.3 Primary Input and Outputs for Design - B.Hand 2014

6.2 Systematic Design

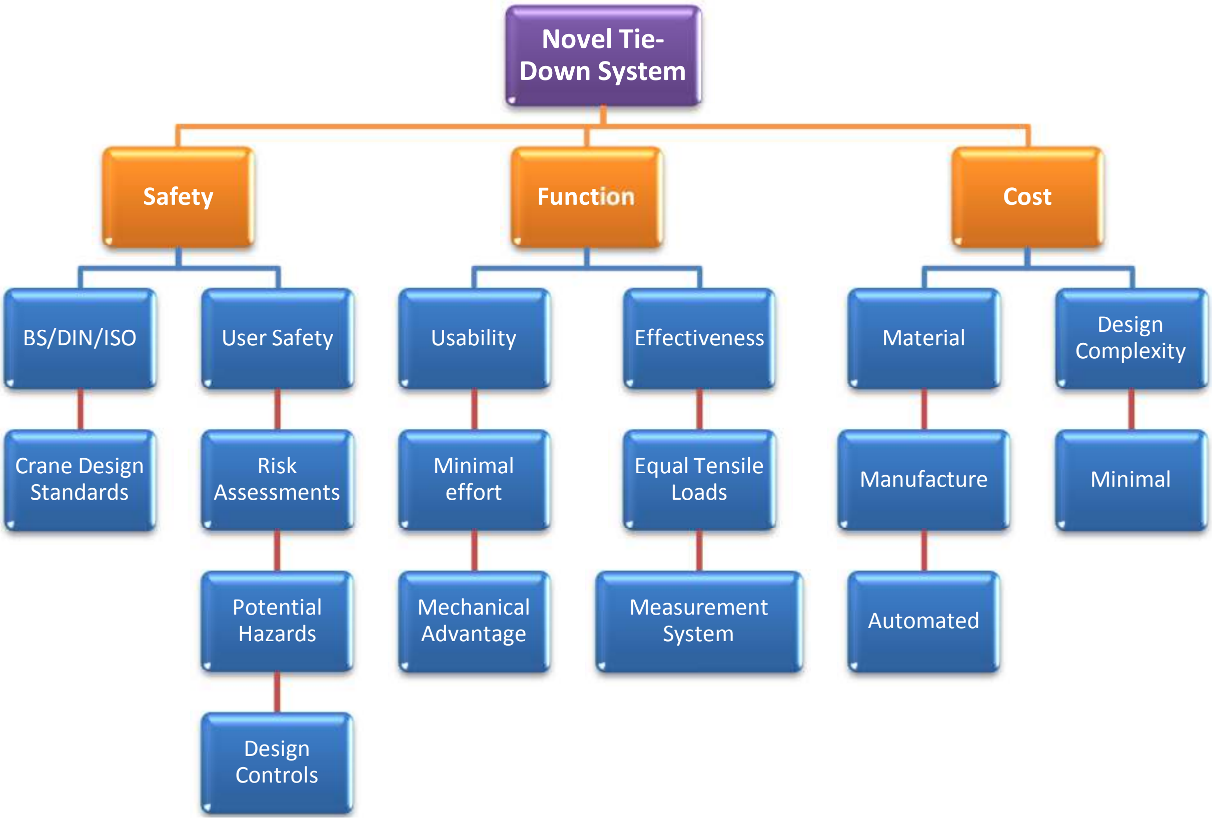

Figure 6.4 Design Requirements - B.Hand 2014

6.2.1 Design Iterations

A number of diverse designs concepts were investigated by the author to determine the most suitable design for this purpose. (Outlined in Appendix D is the rating table upon which the optimum design was chosen).

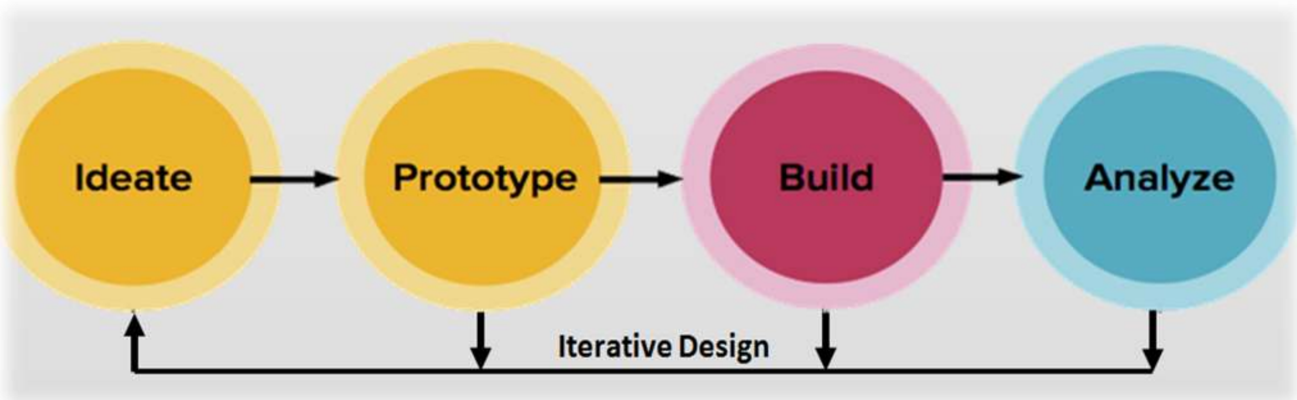

Figure 6.5 Iterative Design Approach - B.Hand 2014

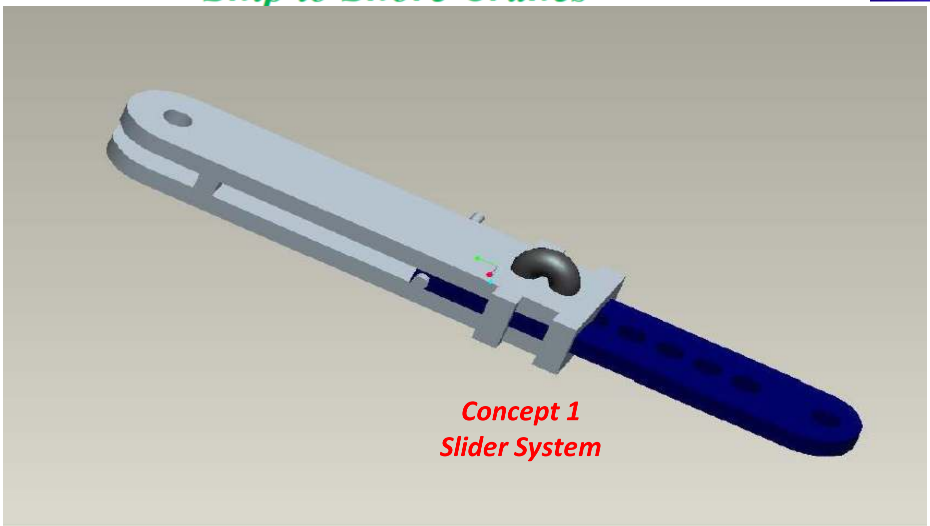

Figure 6.6 Design Concept 1 - B.Hand 2014

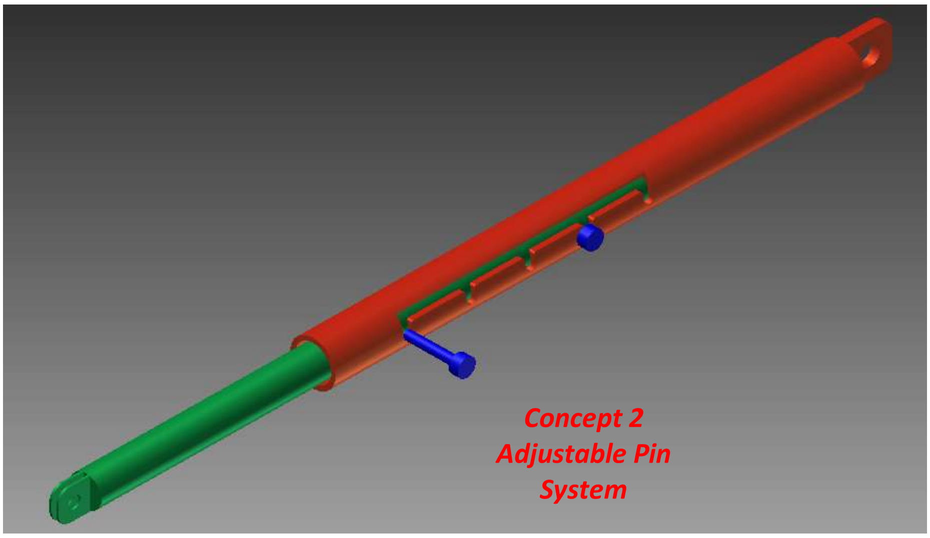

Figure 6.7 Design Concept 2 - B.Hand 2014

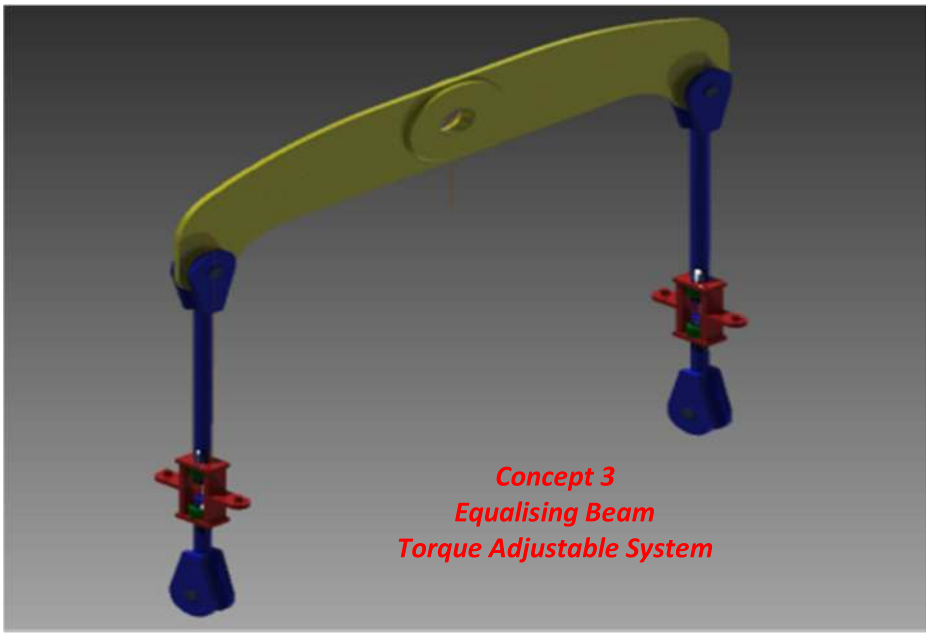

Figure 6.8 Design Concept 3 - B.Hand 2014

The adopted systematic design approach concluded Design Concept 3 to be the most suitable design solution for this application - See Figure 6.9 for Solid Model Depiction of Function and Operation of this novel Tie Down System - (Outlined also in Appendix D is the material selection process used for the design).

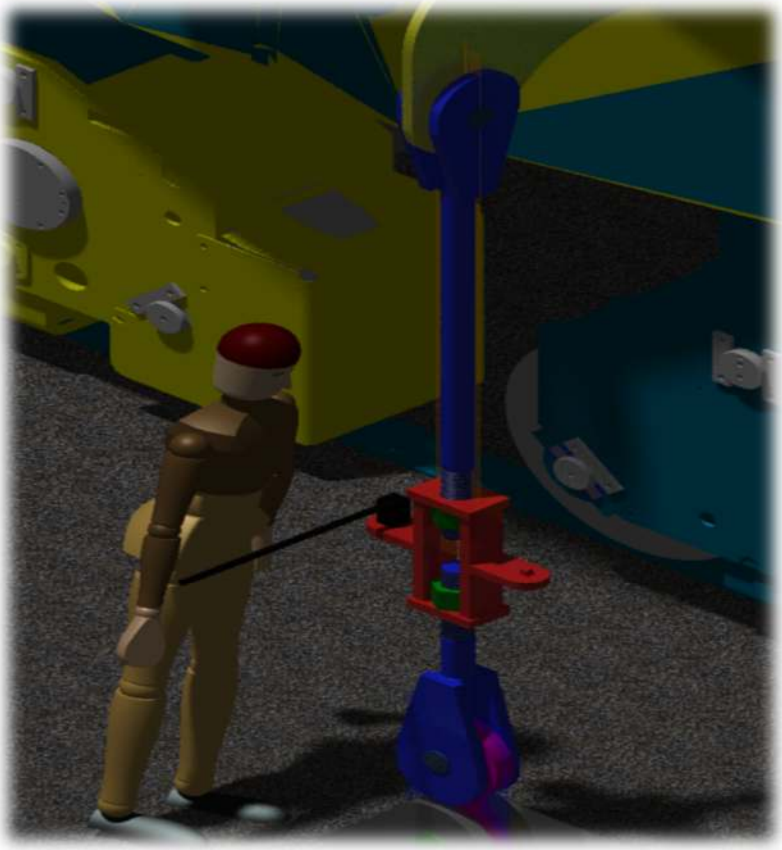

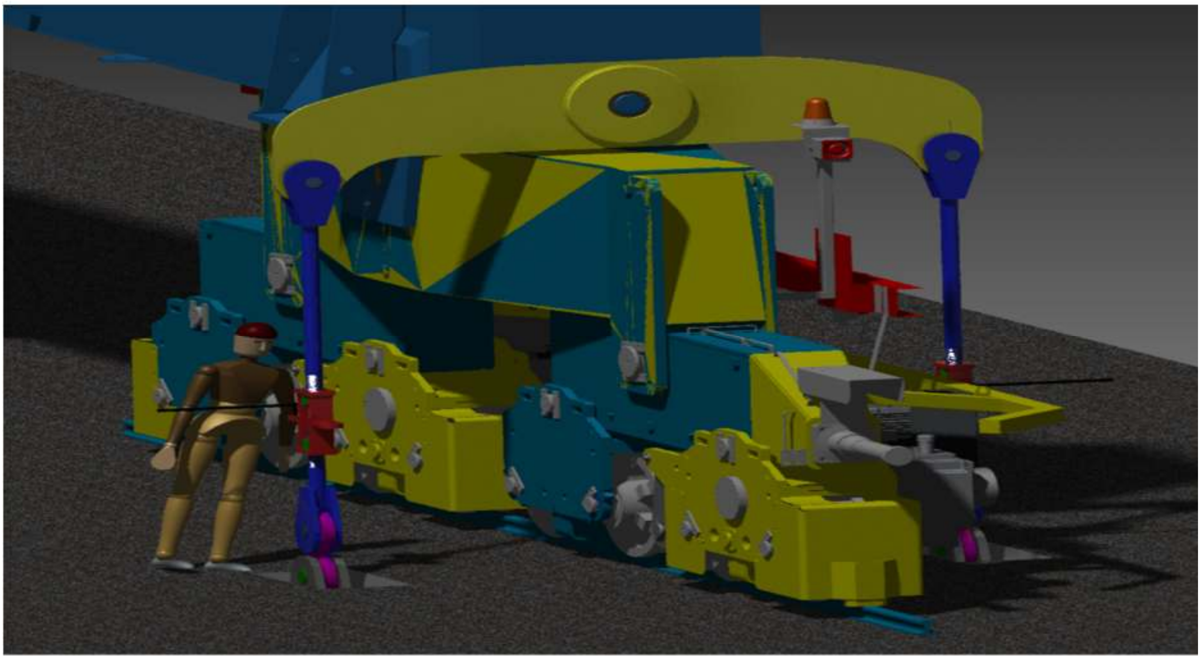

Figure 6.9 Proposed Novel Crane Tie-down Design Function and Operation - B.Hand 2014

6.2.2 Functional Analysis

To ensure the novel tie-down design was mechanically and structurally safe with a suitable factor of safety, the design was implemented in accordance with the standard BS 2573 Pt 1: 1983 Rules For Design of Cranes : Specification for Classification stress Calculations and design criteria for structures. This standard contains a set of rules for carrying out calculations and applying factors for allowable stresses to be used for the grade of materials. Critically and centrally, design calculations were conducted to allow the determination of the maximum uplift force the tie-downs would have to resist - derived from the author developed wind tunnel testing and CFD analysis.

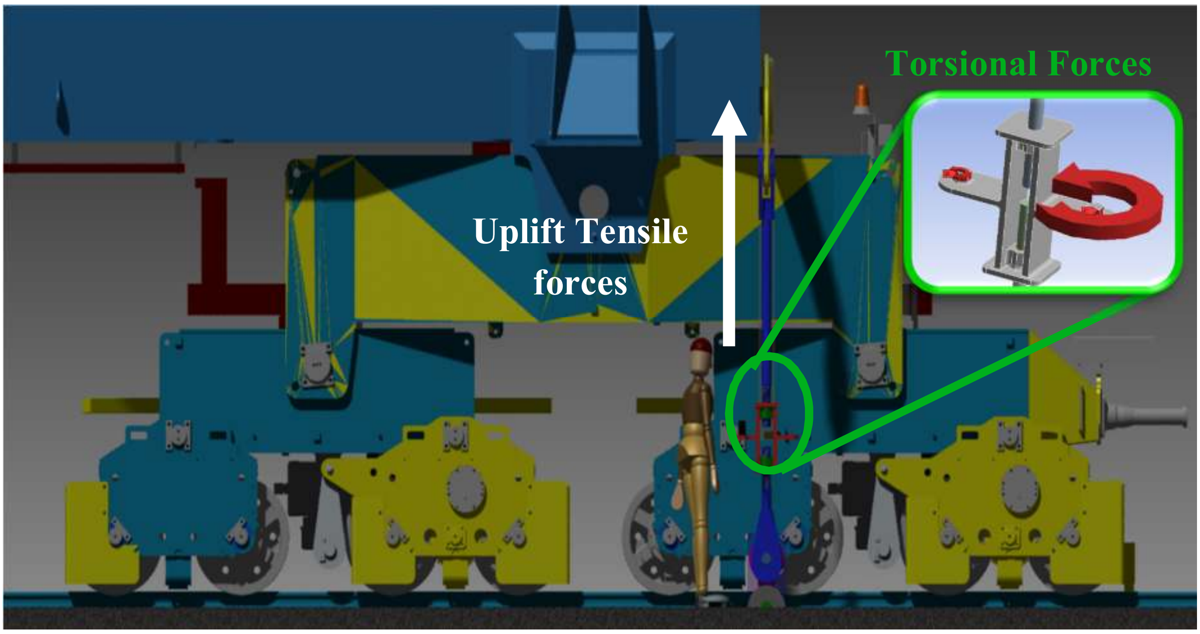

Figure 6.10 Design Load Analysis - B.Hand 2014

Figure 6.11 Effective generation of tensile loads via effective torque setting – B.Hand 2014

6.3 Finite Element Analysis (FEA)

FEA was carried out by the author on the developed tie-down mechanism in two loading situations - (1) in direct loading situation while under a tensile load and (2) during the tightening phase where a torque is applied on the turnbuckle. This analysis allows examination of the stresses and deflections in the design and to determine if these values are within acceptable limits for the design.

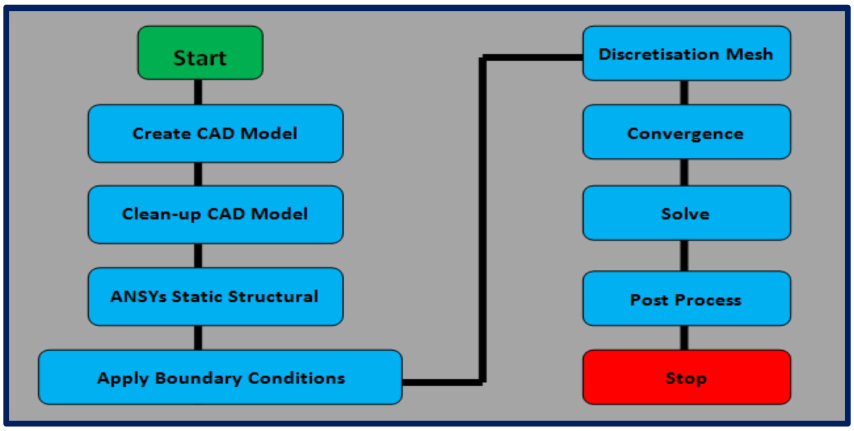

Figure 6.12 Finite Element Analysis Methodology - B.Hand. 2014

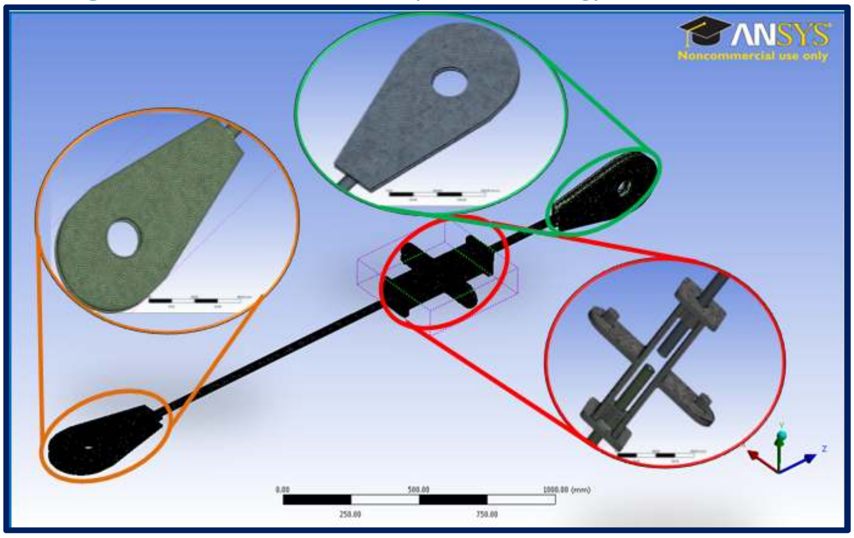

Figure 6.13 FEA Mesh Detail on Developed Tie-Down System - B.Hand 2014

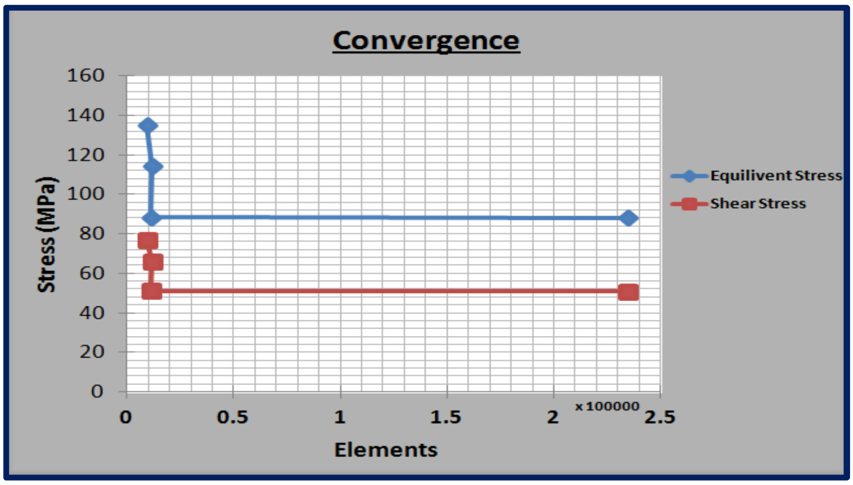

Figure 6.14 Convergence of FEA Results - B.Hand 2014

6.3.1 Torsional Loading Analysis

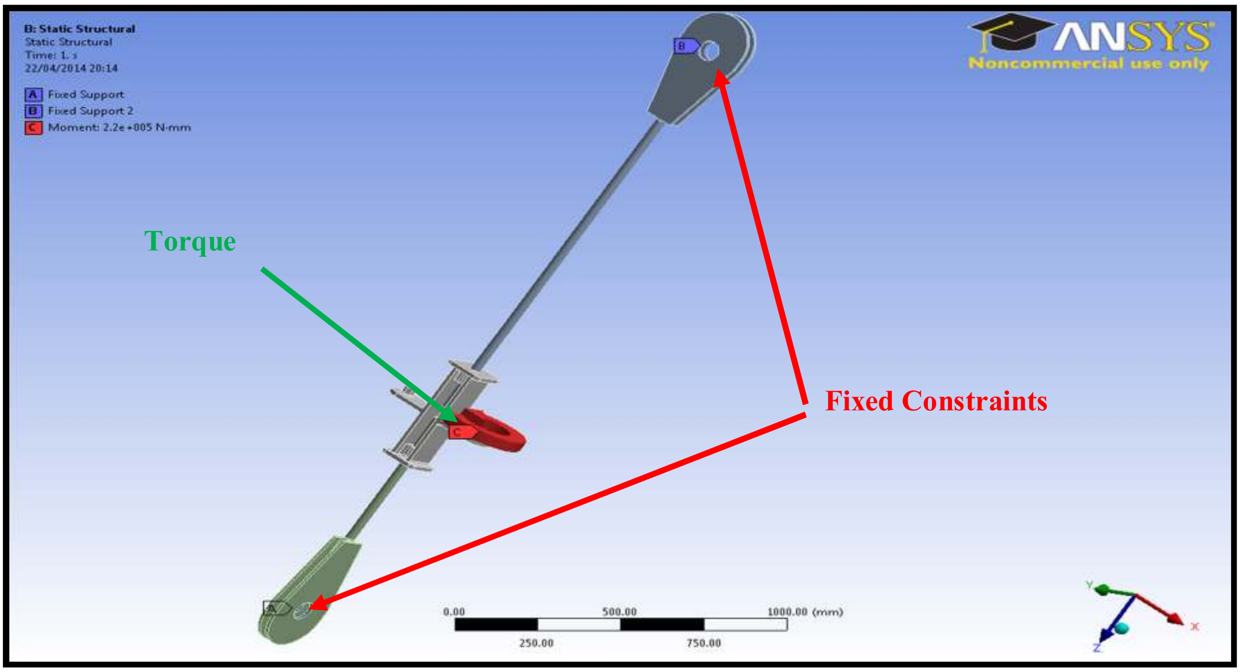

Figure 6.15 Boundary Conditions for Torque Applied Load Case - B.Hand 2014

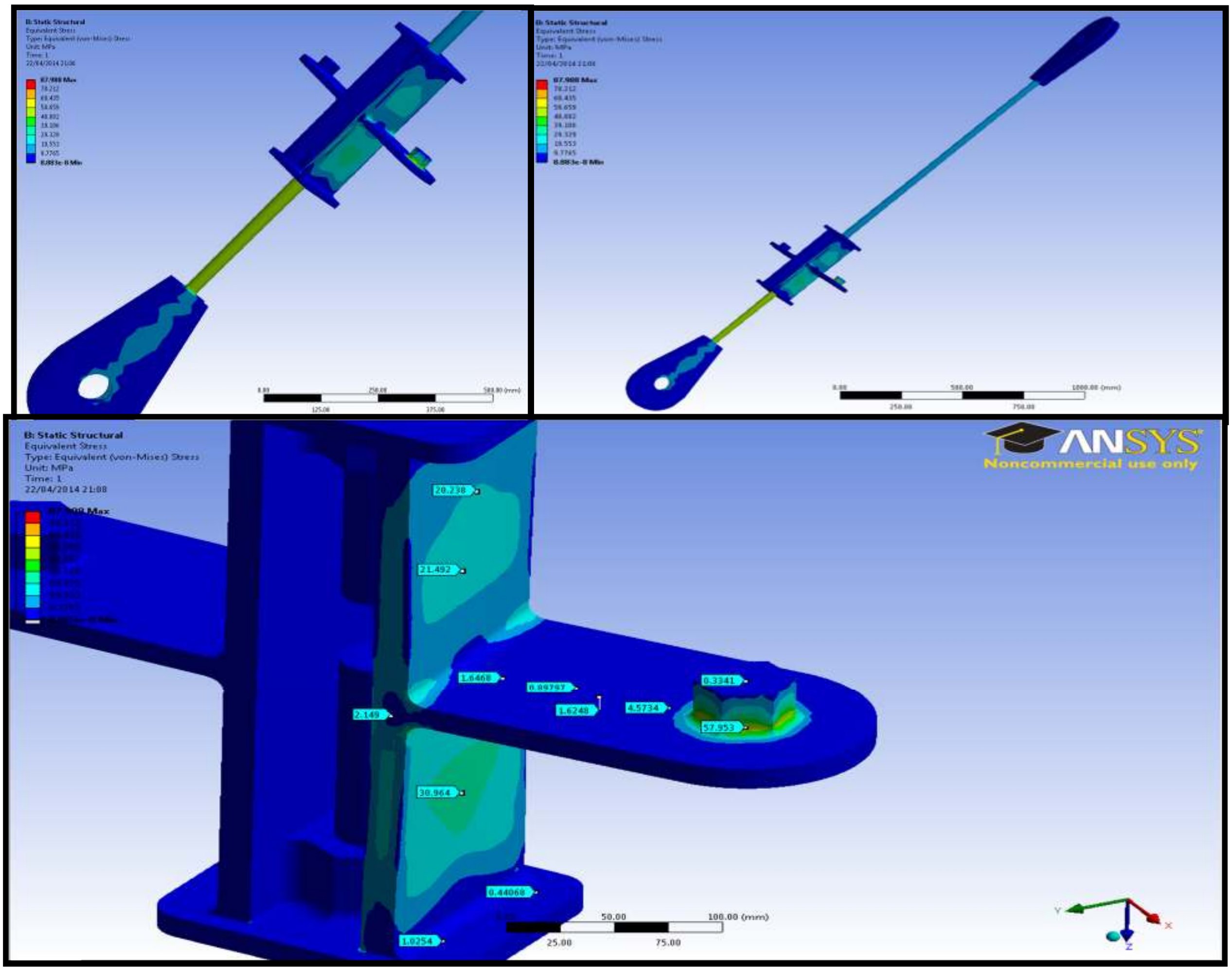

Figure 6.16 Equivalent Stress (MPa) - B.Hand 2014

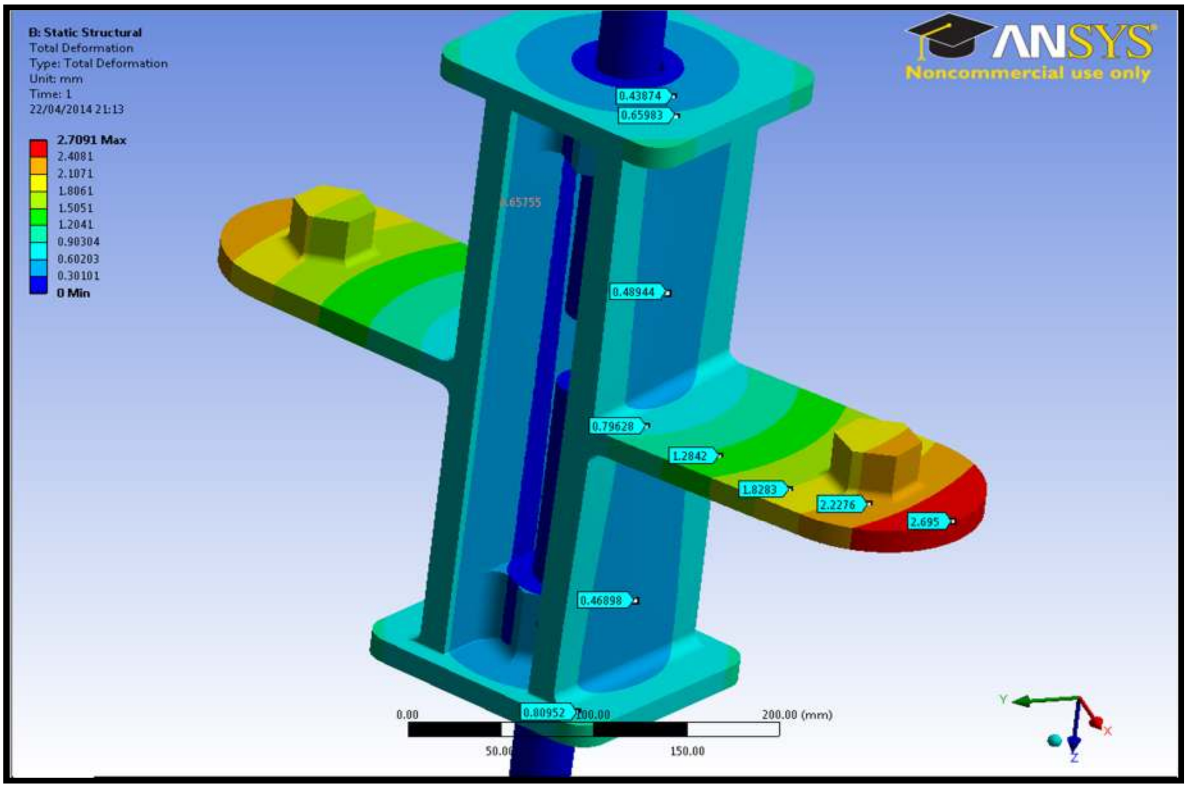

Figure 6.17 Displacement (mm) due to Applied Torque - B.Hand 2014

6.3.2 Direct Tensile Loading Analysis

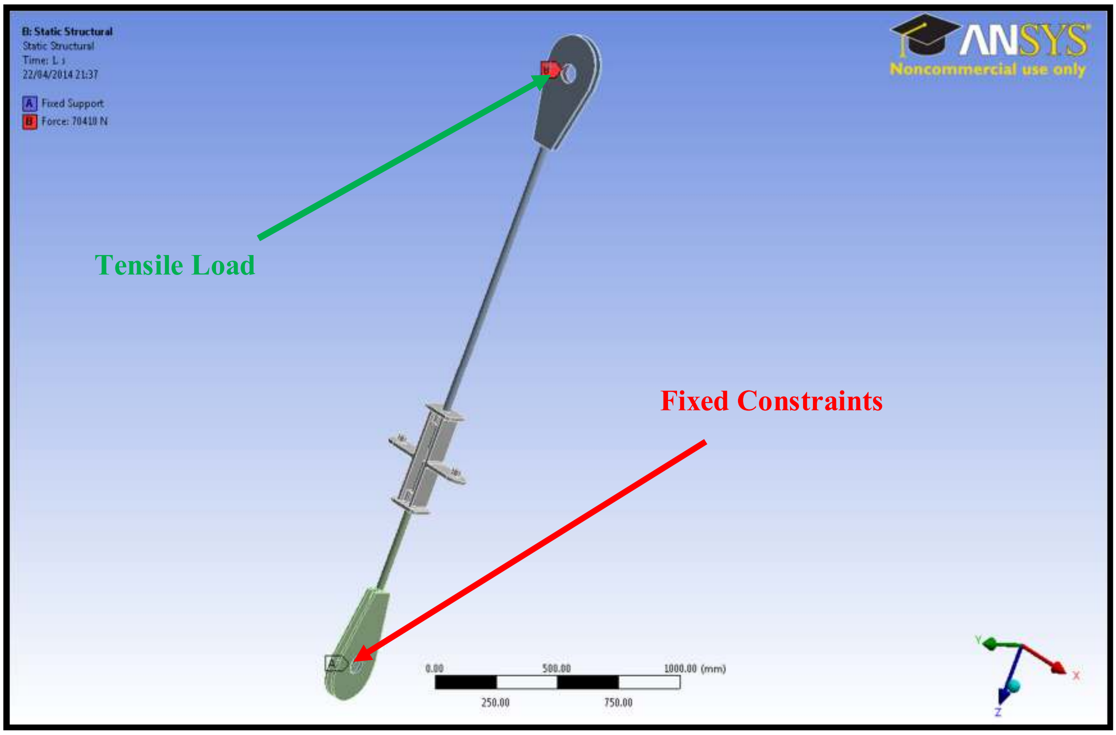

Figure 6.18 Boundary Conditions for Direct Tensile Load Case - B.Hand 2014

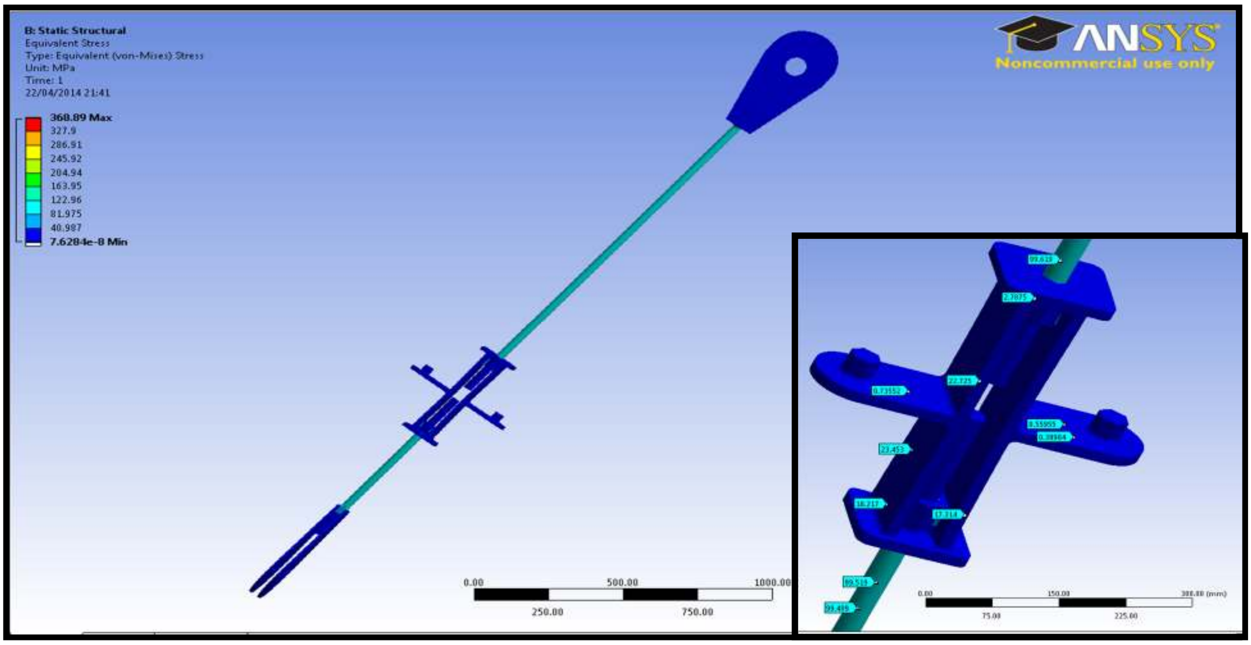

Figure 6.19 Equivalent Stress (MPa) for Direct Tension Load Case - B.Hand 2014

6.3.2 FEA Results

Table 6.1 FEA Primary Torque Results - B.Hand 2014

Torque Applied Load Case			
Parameter	Maximum Equivalent Stress	Maximum Shear Stress	Max Displacement
Magnitude	87.98 MPa	50.796 MPa	2.709 mm
FOS	4	3.5	Low Displacement

Table 6.2 FEA Primary Tensile Load Results – B.Hand 2014

Direct Tensile Load Case			
Parameter	Maximum Equivalent Stress	Maximum Shear Stress	Max Displacement
Magnitude	96.62 MPa	49.81 MPa	0.934 mm
FOS	3.7	3.6	Low Displacement

Examination of the results from the undertaken FEA analysis loads cases determined that critical stresses and displacements on the new product were within acceptable limits. Photoelasticity testing was then undertaken to experimentally validate the developed finite element models used to determine these critical design parameters.

6.4 Photoelasticity Analysis

6.4.1 Outline

Photoelasticity is an experimental technique used to determine the stress distribution in a part where common mathematical procedures can become tedious and unpredictable. Photoelasticity gives a full body picture of the stress distribution in a component unlike that possible with analytical calculations. One of the primary advantages of this method is that it is a full field measurement and allows the determination of the critical stress concentration points in a model and is very much suited to irregular shapes and geometries such as in this particular design case.

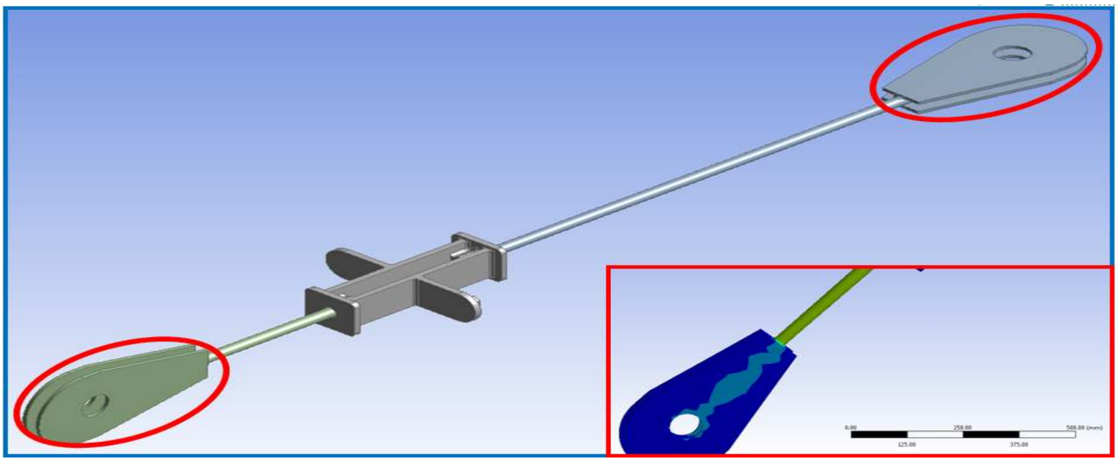

Figure 6.20 Photoelastic Design Analysis - B.Hand 2014

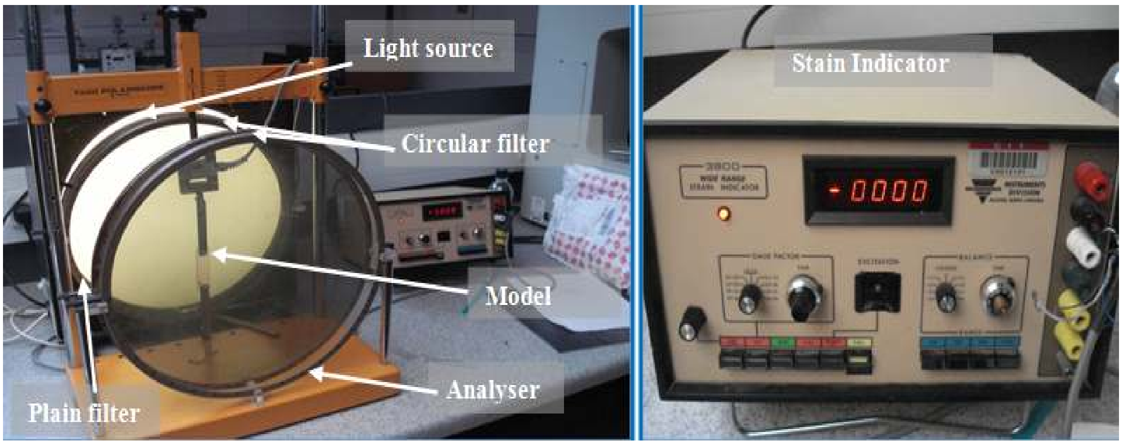

Figure 6.21 College Terco Photoelastic Test Rig - B.Hand 2014

Calibration test pieces and a physical test piece were machined by the author from PSM birefringent material. Careful attention had to be paid in the manufacture of both calibration and test pieces to the speed of machining of the material as chipping would create stress raisers - furthermore, heat generated had to be adequately alleviated.

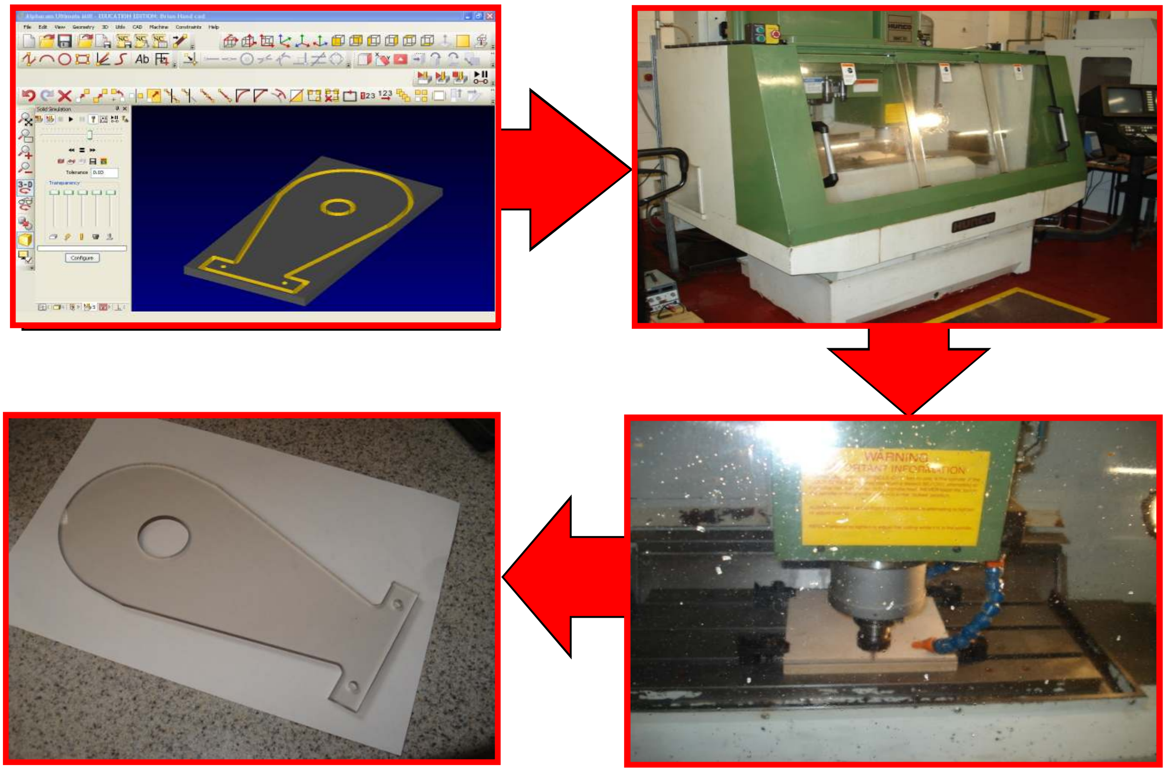

Figure 6.22 Photoelastic Test Piece Generation – B.Hand 2014

A customised testpiece support rig was designed and manufactured by the author in order to achieve a realistic and practical recreation in the photoelastic test apparatus of the loading of the tie- down system.

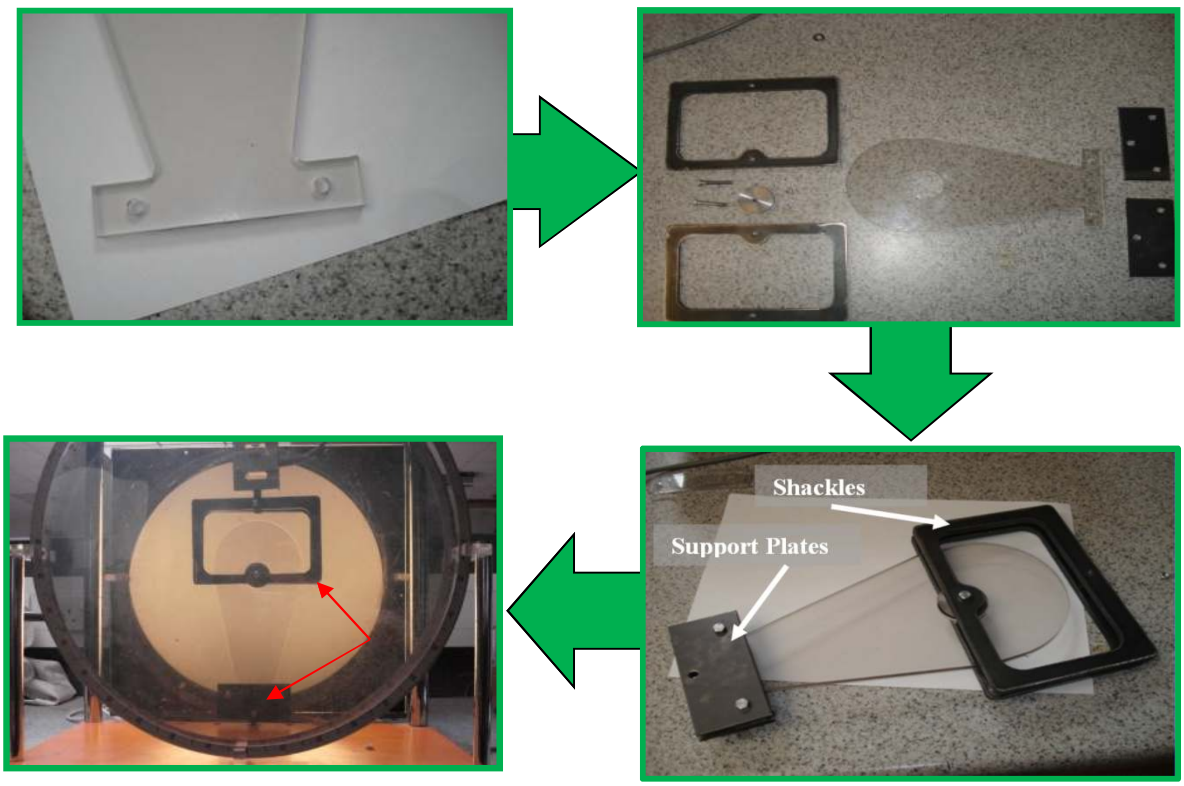

Figure 6.23 Support Rig Development - B.Hand 2014

6.4.2 Testing

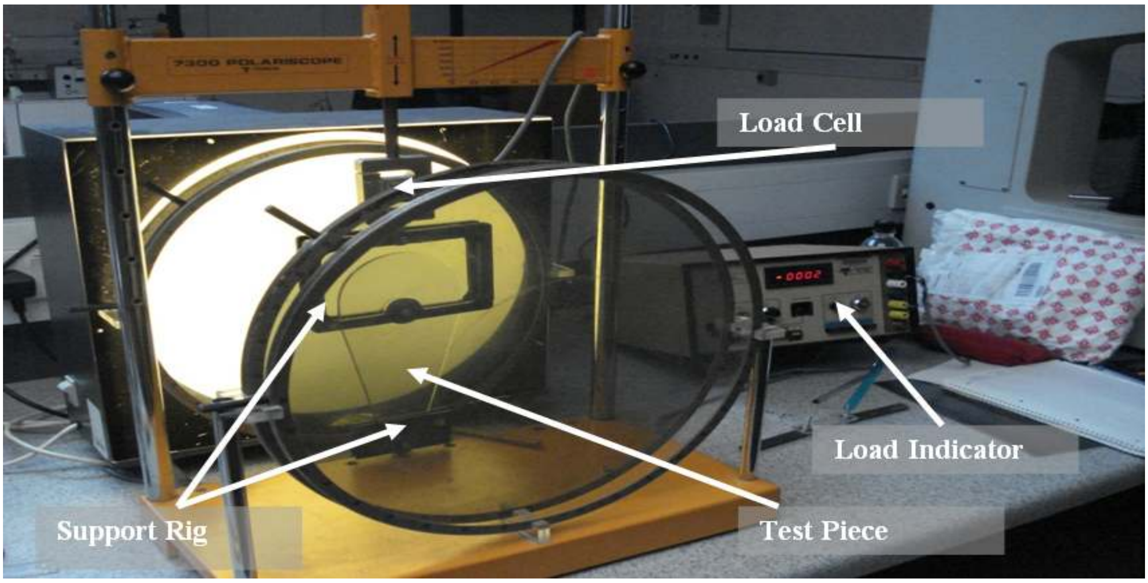

Figure 6.24 Photoelastic Test Setup - B.Hand 2014

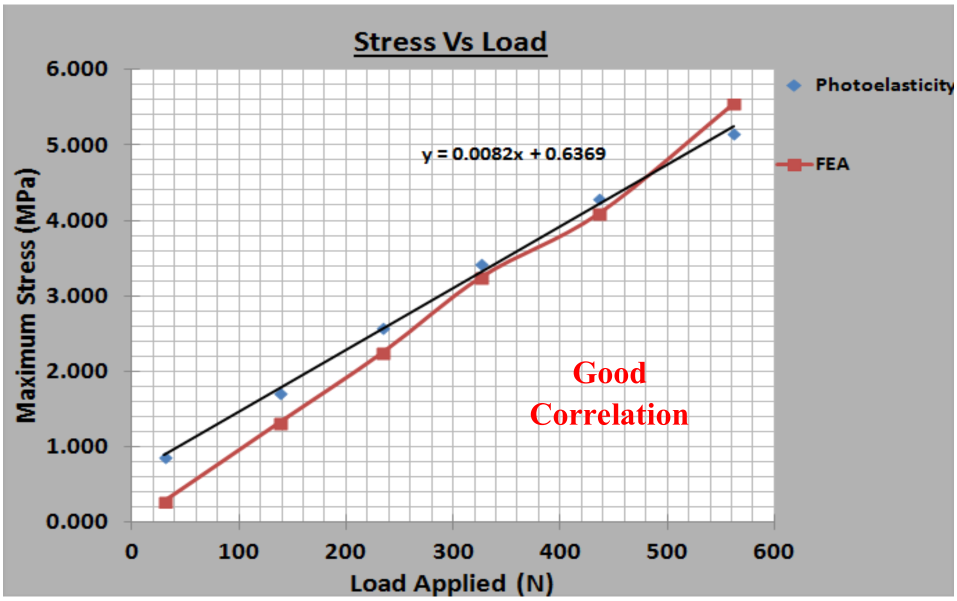

Figure 6.25 Graphical Comparison of FEA and Photoelasticity Results – B.Hand 2014

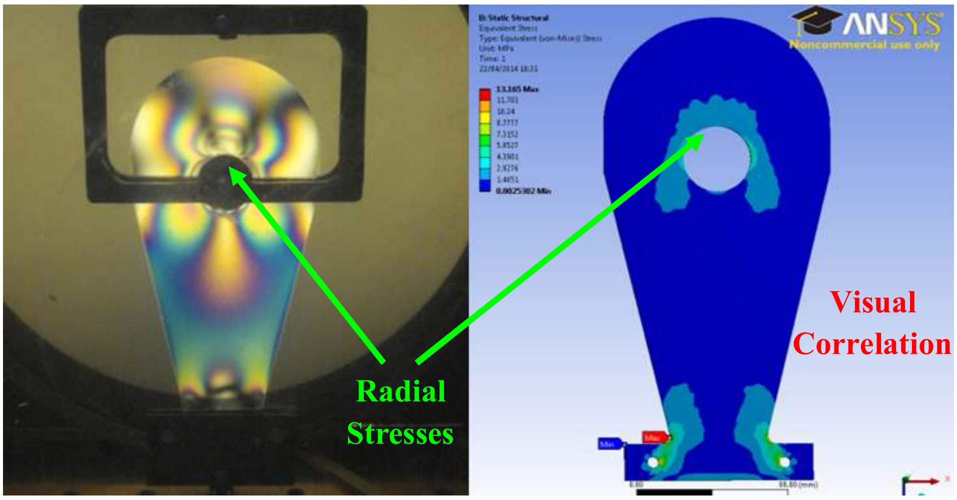

Figure 6.26 Diagrammatic Comparison of FEA and Photoelascity Techniques – B.Hand 2014

6.5 Prototype Development

6.5.1 Manufacture/Instrumentation

Good correlation was achieved between finite element analytical and photoelastic experimental results (See Figures 6.25 and 6.26), leading to a high degree of confidence in the underlying design calculations for the developing novel tie-down system.

To examine the functionality of the redesign, a prototype of the tie-down was manufactured as shown in Figure 6.27. (Further details of prototype manufacture are in Appendix D).

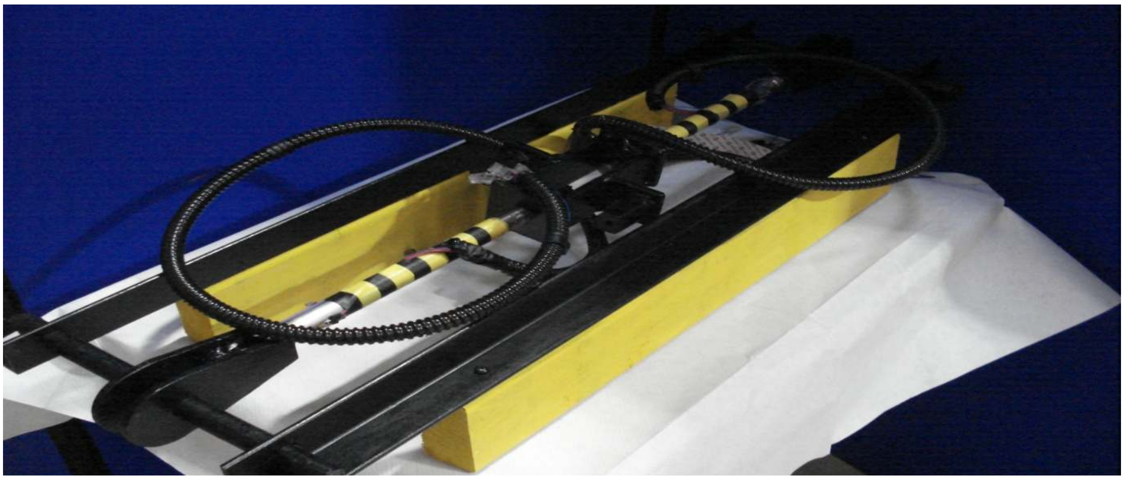

Figure 6.27 Manufactured Tie-Down Prototype in Developed Proof of Concept Test Rig - B.Hand 2014

A Tie-Down Prototype Proof of Concept Test Rig was also designed, developed and commissioned (see Figure 6.27).

Bonded strain gauges were applied to the prototype (see Figure 6.28) to experimentally measure the torque to tensile force generated in the design.

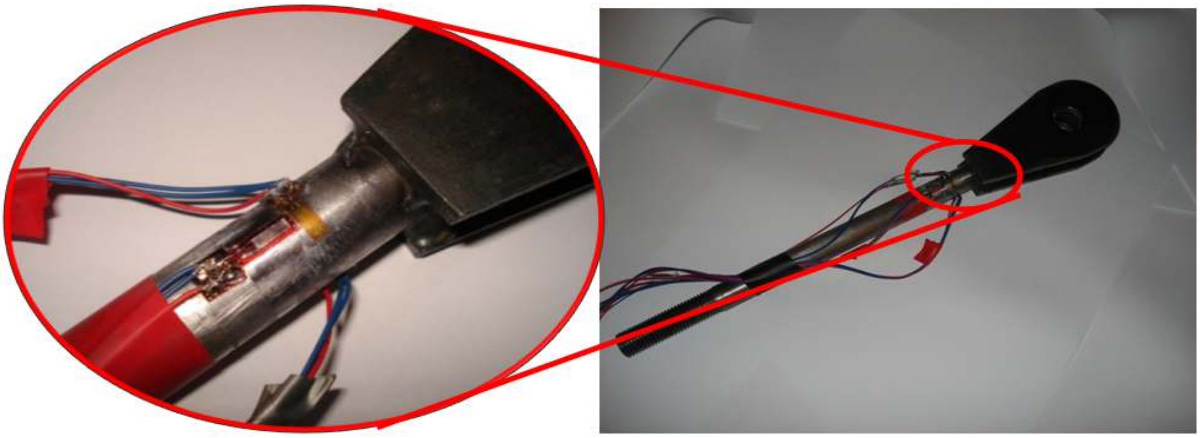

Figure 6.28 Proof of Concept Experimental Strain Gauge Configuration Detail - B.Hand 2014


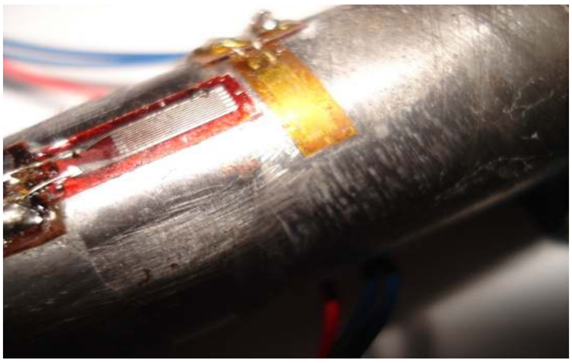

Figure 6.29 Mounted Load Cell Arrangement - B.Hand 2014

6.5.2 Prototype Testing

Using compatible experimental test software *Strain Smart,* the loading of the prototype was undertaken and experimental measurement recorded and analysed.

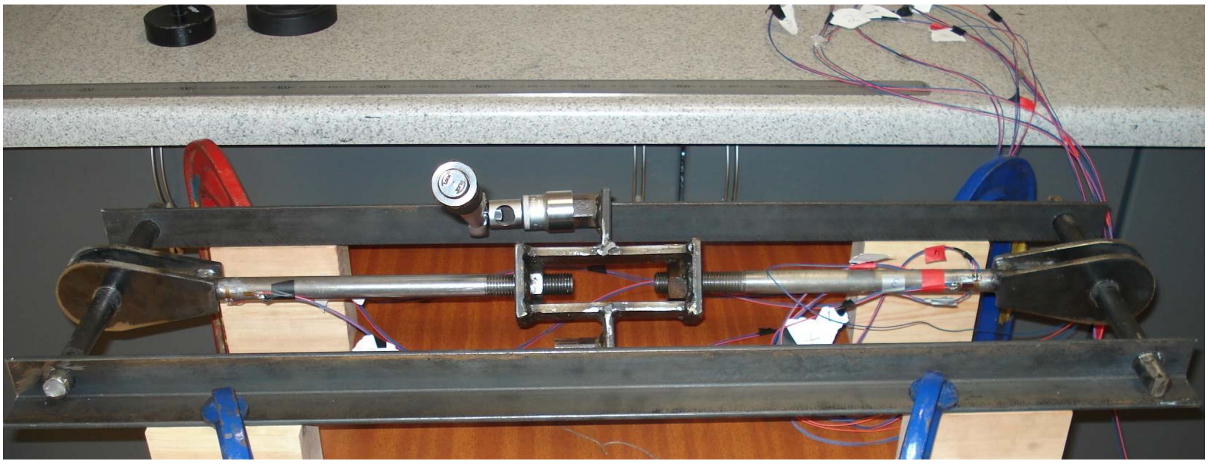

Figure 6.30 Experimental Test Rig Torque Application and Force Measurement Configuration - B.Hand 2014

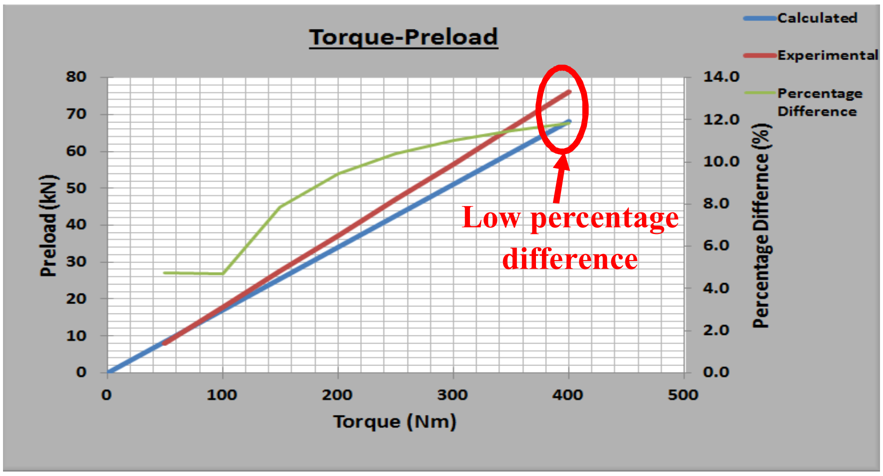

Figure 6.31 Graphical Comparison of Experimental and Calculated Torque to Pre-Load Conversion B.Hand 2014

Good correlation (see Figure 6.31) was achieved between experimental and calculated torque to pre-load conversion in the developed prototype tie-down system.

7. Financial/Commercial Benefits

Port performance is influenced by a number of container terminal operations including:

- Vessel berthing operation
- Crane unloading/loading operation
- Delivery operation by trucks
- Storage operation

The STS crane operation is the most important operation for port terminal logistics - it has been estimated that STS crane operation constitutes 70% of vessel berthing time [30]. Any improvements in this efficiency have very significant implications for effectiveness and turnaround of a major port.

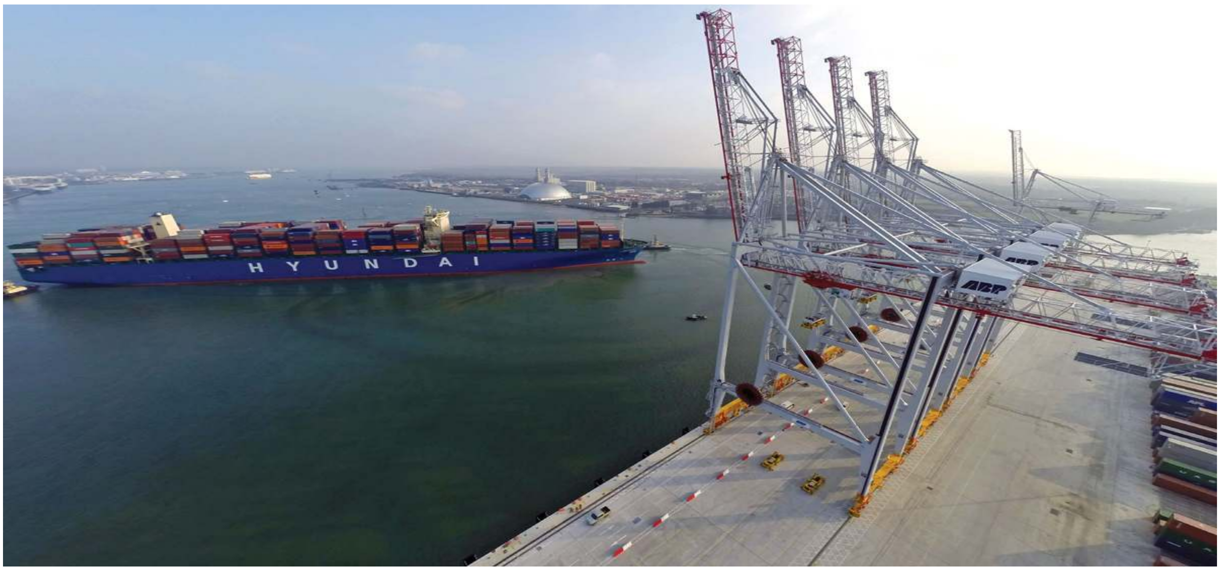

Figure 7.1 Efficient STS Cranes are Crucial for Effective Port Operations [1]

Based on the in-depth analysis and validation undertaken, it has been established that current wind load structure calculations are overestimated by almost 15%, a very significant figure indeed. The analysis has also determined areas in which structure wind loads can be reduced further by streamlining and modifying geometry, while still maintaining structural integrity.

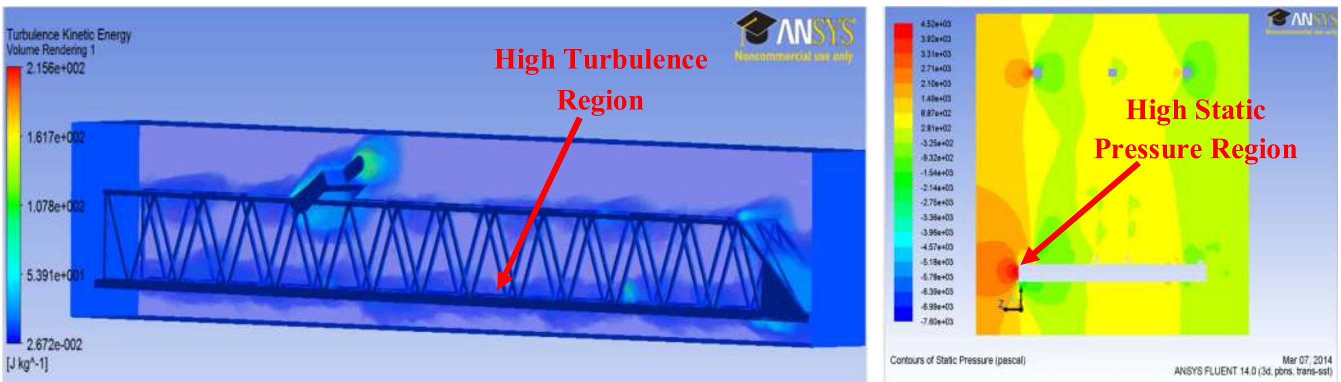

Figure 7.2 Use of CFD to Reduce STS Crane Wind Loads - B.Hand 2014

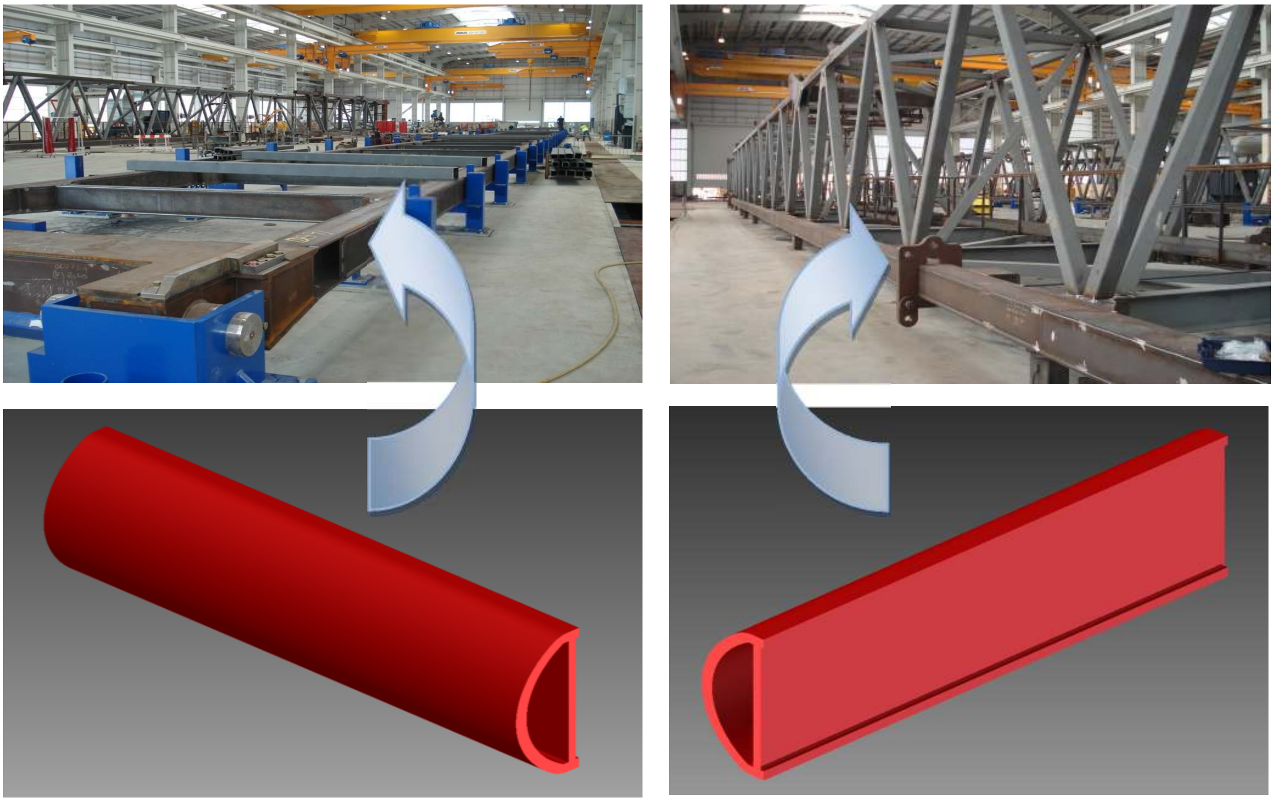

Figure 7.3 Concept Drag Reduction Configuration Attachment - B.Hand 2014

STS cranes are the workhorses in port operations - being used around the clock. Any improvements in design and efficiency will have significant associated benefits.

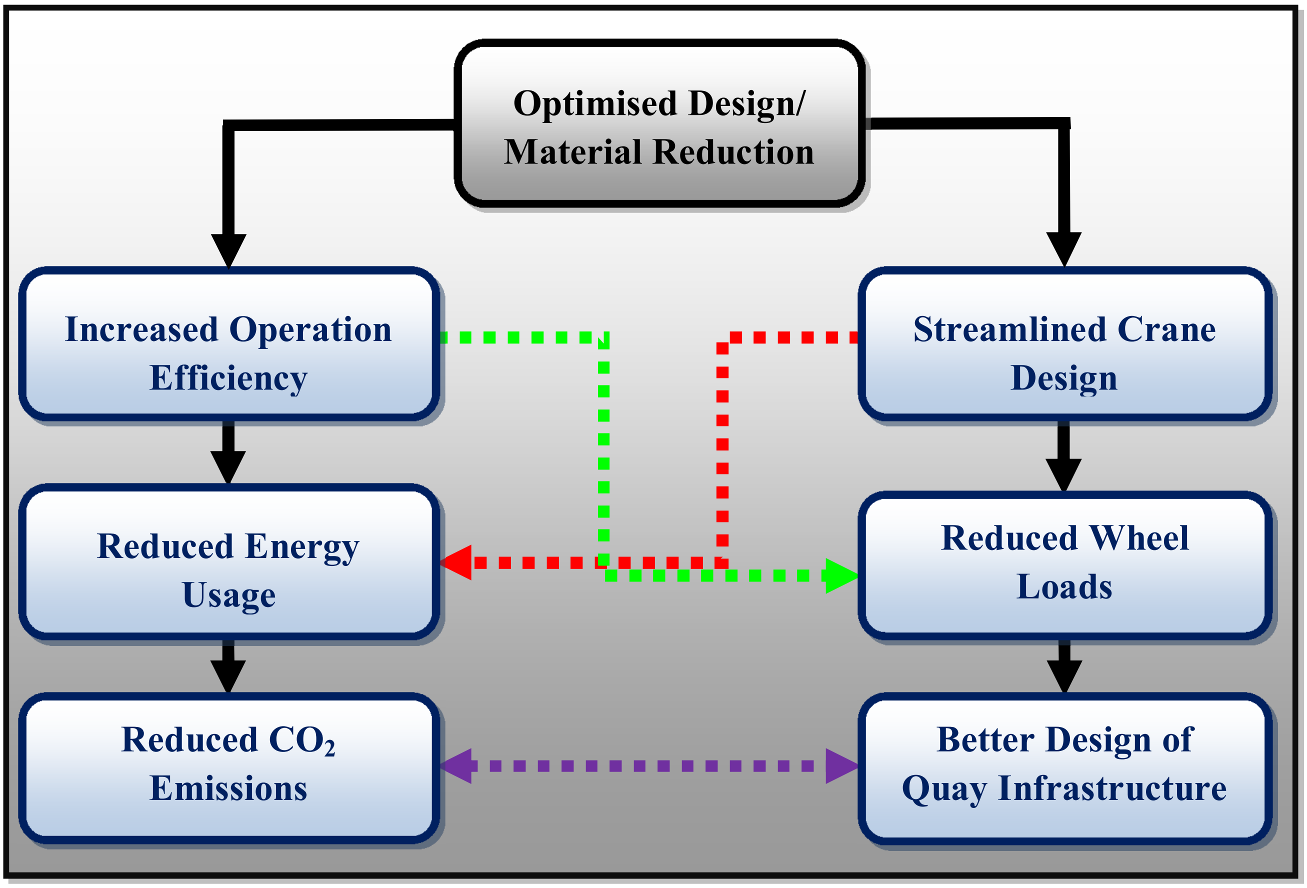

Figure 7.4 Benefits from Optimised Design and Efficiency - B.Hand 2014

A comprehensive case study was undertaken by the author to quantify the potential savings and efficiency gains from the conducted analyses. Table 7.1 summaries the case study on three typical sized cranes currently produced with increased concentration on larger cranes (See Appendix D for dimensions). Operational data was received from Liebherr in relation to current cranes operating in ports worldwide. Respective crane masses and energy consumption in moving these cranes along quays during operation were acquired.

Figure 7.5 STS Crane Movements along Quay [1]

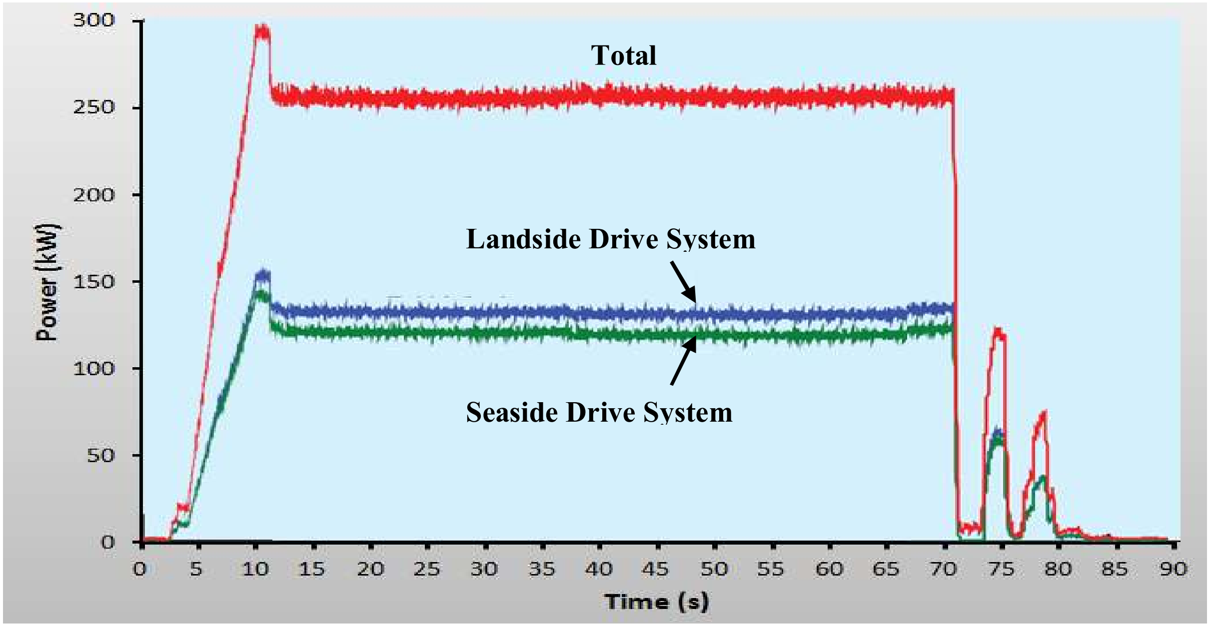

Figure 7.6 Typical Power-Time Graph of STS Crane during Movement Operation along Quay - B.Hand 2014

Based on experimental and numerical analyses, substantial material savings were determined. Mathematical spreadsheets were created to calculate energy consumption during crane movements along quays via numerical integration methods. It was established that, on average, the cranes operated in this manner for 1,000 hrs annually and accordingly significant savings in energy and reductions in CO_2 emissions were found due to reduced mass.

Table 7.1 Material/Energy Consumption Saving and CO_2 Emissions Reduction - B.Hand 2014

Crane Model Size	Average Crane Mass[A] (T)	Material Saving (T)	Material Cost Saving[B] (£)	Average Annual Energy Consumption[A] (kW/h/year)	Annual Energy Saving (kW/h/year)	Annual Energy Cost Saving[C] (£/year)	Reduction in CO_2 Emissions[D] (Kg CO_2/kWh/year)
Panamax	725	21.30	9,585.0	102,011.58	9,181.04	835.47	3,947.85
Post-Panamax	930	36.50	16,425.0	136,275.50	12,264.79	1,116.10	5,273.86
Super Post-Panamax	1,300	78.00	35,100.0	208,333.50	18,750.02	1,706.25	8,062.51

[A] STS Crane Operational Data [31]
[B] S355 Structural Grade Steel – £450/tonne [32]
[C] Port Operation Energy Cost – £0.091/kWh [33]
[D] CO_2 Emission per kW/h – 0.43 Kg/kWh [34]

Significant savings in energy and running costs are determined for each crane configuration relative to size. CO_2 emissions from the global shipping industry account for around one billion tonnes a year and must be reduced considerably over the coming years [35]. The study undertaken by the author demonstrates that emissions can be reduced greatly by introducing the desired changes acquired from the analysis. These benefits are amplified as STS cranes gain predominance in ports worldwide.

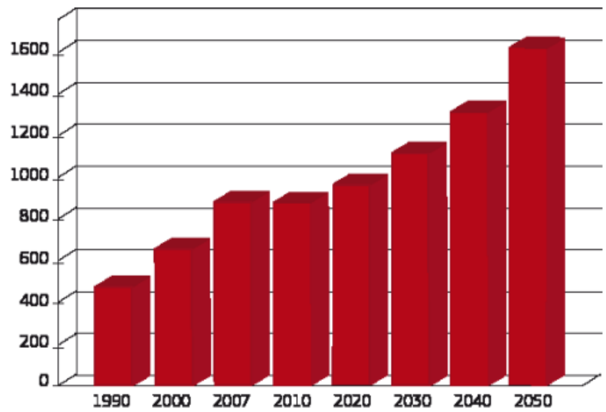

Figure 7.7 Estimated CO_2 emissions in million tonnes per year for maritime transport industry [35]

Figure 7.8 Predominance of STS Cranes Enables Major Reduction in Energy Usage and CO_2 Emissions in Maritime Industry [1]

Conclusion

The initial challenge of this project has been comprehensively achieved – full numerical and experimental critical crane section wind loading analysis has been conducted and validated with results showing good correlation.

A principal finding from this investigation is that both of the employed numerical and experimental methodologies predicted drag coefficients to be significantly lower for this type of structure than those predicted in the current standards based design approach. This finding raises a significant question mark in relation to the suitability of the current standards in relation to their accuracy of quantifying wind loading on these structures. This study conclusion thus provides evidence to support the opinion of crane designers that current standards are not entirely suitable for container crane geometry.

The study also points to the accuracy of CFD analysis in the application of crane design and the many benefits associated with this software for an engineer or designer wishing to diverge from the standardised approach. From the analysis and testing, it was established that significant potential savings could be found from optimised design in the form of reduction in energy and material usage. This saving is critically important to port operations worldwide as major ports are expected to increase output significantly in the coming years and must comply with strict legislation especially with CO_2 emissions targets as finite fossil fuels resources continue to exponentially decline and the price of energy correspondingly increases.

Figure 8.1 Liebherr Super Post-Panamax STS Container Cranes Operating at Port of Southampton, United Kingdom [1]

Extensive progress has been made in improving the safety and design functionality of an important crane component, which is highly influenced by fluctuating wind loads (using the tools and design philosophy investigated and advanced by the author).

A novel tie-down system, incorporating equalising beam and torque adjustable features, has been designed and developed. The developed system is specifically designed to prevent unequal tensile loads on the turnbuckles and consequent potential failure mechanisms, which for ship to shore cranes can be life threatening, function disruptive, crane/quay structure damaging and hugely costly. Prototype manufacture and proof of concept testing of the novel tie-down system has been successfully undertaken.

Recommendations for future work include further advanced analysis of STS container crane geometry and investigation into application of drag reduction measures. More extensive validation testing, manufacture and implementation of working tie-down system is to be undertaken.

All project findings and results have been presented to the Liebherr Group on conclusion of the project. Liebherr response has been very positive - particularly with respect to the work undertaken in structural CFD analysis and wind tunnel testing and the potential for implementation of these methodologies into the design process (Appendix-A outlines the response from the Liebherr Chief Design Engineer).

The application of numerical analysis and model testing in STS container crane design has proven to be a very challenging but also greatly rewarding opus. The work undertaken by the author indicates the importance of these growing technologies as a very powerful and practical design tool - pointing the way forward to exciting and beneficial innovations in maritime crane development.

Figure 8.2 Future Innovations in Maritime STS Container Crane Designs [5]

References

[1] Liebherr Group, 2013. Production site in Killarney (Ireland): Liebherr Container Cranes. Available Online at http://www.liebherr.com/en-GB/35279.wfw. [Accessed 24th October, 2013].

[2] Hamedi. M, 2010. Containership Load Planning With Crane Operations: Faculty of the Graduate School of the University of Maryland: Chapter 1: Introduction: *Containerisation.* Page 1.

[3] Graham.C, 2005. *Containerization and the Decline of South Street Seaport*: Fordham University: The Jesuit University of New York: Decline 1870-1960. Available Online at. http://www.fordham.edu/academics/colleges__graduate_s/undergraduate_colleg/fordham_college_at_l/special_programs/honors_program/seaportproject/decl/containerization.html. [Accessed 21th October, 2013].

[4] World Shipping Council (WSC), 2013. About the Industry: History of Containerization: *Before Container shipping.* Available Online at http://www.worldshipping.org/about-the-industry/history-of-containerization/before-container-shipping. [Accessed 16th October, 2013].

[5] Joyce.B, 2012. Federal Reserve Bank of Richmond: Publications: Current Publications: Economic History: *The Voyage to Containerization:* How a North Carolina trucker freed world trade. Page 39.

[6] Container Handbook, 2013. 1 History : 1.*1 History of the Container*. Available Online at. http://www.containerhandbuch.de/chb_e/stra/index.html?/chb_e/stra/stra_01_01_00.html. [Accessed 22nd October, 2013].

[7] Rodrigue. JP & Notteboom. T, 2007. The future of containerization: Box logistics in light of global supply chains: Proceedings of the 2007. International Association of Maritime Economists (IAME) Conference, July, Athens: 1.Introduction: *1.1 Looking Back at Fifty Years of Containerization*. Page 2.

[8] UN (United Nations), 2005. Economic and Social Commission for Asia and the Pacific: monograph Series on Managing Globalization: Regional Shipping and Port: Development strategies: (Container Traffic Forecast): Container Trade Growth 3.2 *Global Container Forecasts*. Page 28-29.

[9] Financial Press, 2013. *Economy: Free exchange*: The humble hero. Available Online at. http://financialpress.com/2013/05/19/free-exchange-the-humble-hero/. [Accessed 21th October, 2013].

[10] Marine Insight, 2010. *Container-Gantry-Crane-Construction-and-Operation*. Available Online at http://www.marineinsight.com/marine/container-gantry-crane-construction-and-operation/. [Accessed 24th October, 2013].

[11] ASME (The American Society of Mechanical Engineers), 2013. About ASME: Who we are: Engineering history: Landmarks: *PACECO Container Crane*. Available Online at https://www.asme.org/about-asme/who-we-are/engineering-history/landmarks/85-paceco-container-crane. [Accessed 23th October, 2013].

[12] ASME (The American Society of Mechanical Engineers), 1983. Dedicates an International Historic Mechanical Engineering Landmark: *The PACECO container crane: The World's First High Speed, Dockside Container Crane:* Encinal Terminals – Alameda, California: May 5th 1983: Introduction. Pages 3-5.

[13] Ceccarelli. M, 2004. International Symposium on History of Machines and Mechanisms. Coulomb and applied Mechanics: *Evolution of Container Crane Industry*: Page 231-232 ISBN 1-4020-2203-4.Printed by Kluer Acedemic Publishers.

[14] International Maritime Organisation (IMO), 2012. Maritime Knowledge Centre: " Sharing Maritime Knowledge": International Shipping Facts and Figures – Information Resources on Trade, Safety, Security, Environment: *2.1. Shipping and the global economy*. Page 7.

[15] Luck.K & Modler.L, 1990. Getriebetechnik- Analyse, Synthese, Optimierung. Printed by Springer – Verlag Wien, New York.

[16] Zrnic N, Petkovic Z & Bosnjak S, 2005. Automation of Ship-To-Shore Container Cranes: A Review of the State-of-the-Art: Faculty of Mechanical Engineering: University of Belgrade: Introduction: FME Transactions: Page 111.

[17] MLIT (Ministry of Land, Infrastructure and Transport), 2001. Niigata Research and Engineering Office for Port and Airport Hokuriku Regional Development Bureau: The Development of the Suction foundation: 3. Applicable structures-Possible applications

[18] GEER, 2002. Port Facilities and Artificial Islands: 3.2.3 Damage to Port Structure and adjacent Facilities: Plastically yielded crane legs due to about 2 m of spreading between crane rails as a consequence of lateral caisson displacement. Available Online at http://www.geerassociation.org/GEER_Post%20EQ%20Reports/Kobe_1995/ch3-2.html. [Accessed 24th October, 2013].

[19] Lee .S.J & Kang .J, H, 2007. *Wind Load on a container crane located in atmospheric boundary layers*: Journal of Wind Engineering and Industrial Aerodynamics 96 193-208: Department of Mechanical Engineering, Pohang University of Science and Technology, Hyoja-dong. Pohany 790-784,South Korea: 1 Introduction: Published by Elsevier Ltd.

[20] UCAR (University Corporation for Atmospheric Research), 2007. News Centre: News Releases: NCAR News Release: *Frequency of Atlantic Hurricanes Doubled Over Last Century; Climate Change Suspected*: Greg Holland: Available Online at: http://www.ucar.edu/news/releases/2007/hurricanefrequency.shtml. [Accessed 10th November 2013].

[21] McCarthy. P & Vazifdar.F, 2004. Liftech Consultants: ASCE PORTS 2004 Conference :Houston, Texas. *Securing Cranes for Storm Wind: Uncertainties and Recommendations*: Background: Page 1

[22] TT Club, 2011. *Recommended minimum safety specifications for quay container cranes* A joint initiative from TT Club, ICHCA International and Port Equipment Manufacturers Association: 1 Introduction: Page 6. ISBN 978-1-85330-0349 Available Online at: http://www.ttclub.com/fileadmin/uploads/tt-club/Publications___Resources/Annual_Reports/Recommended%20minimum%20safety%20specifications%20for%20quay%20cranes%2020110607.pdf. [Accessed 28th November 2013].

[23] HSE (Health & Safety Executive), 2001. *Review of model testing requirements for FPSO's*: Prepared by BMT Fluid Mechanics Ltd for the Health and Safety Executive: Offshore Technology Report 2000/123: ISBN 0 7176 2046 8: Printed and Published by the Health & Safety Excutitive.

[24] Cakir,M 2012. CFD Study on Aerodynamic Effects of a Rear Wing/Spoiler on a Passenger Vehicle: Master Thesis: Submitted in Partial Fulfilment of the Requirements For the Degree of Master of Science In Mechanical Engineering In the School of Engineering at Santa Clara University, December 2012 Santa Clara, California: Chapter 1: Automobile Aerodynamics: 1.4.3 *Friction Drag*. Page 7.

[25] Moin P & Kim J, 2012. Stanford University: Centre for Turbulence Research: Tackling Turbulence with Supercomputers: Available Online at: http://www.stanford.edu/group/ctr/articles/tackle.html. [Accessed 12th April 2014].

[26] Moonena P, Blockena. B, Roelsa S. & Carmelieta J., 2006. *Numerical modelling of the flow conditions in a closed-circuit low-speed wind tunnel:* Journal of Wind Engineering and Industrial Aerodynamics 94 (2006) 699–723. Introduction. Published by Elsevier Ltd.

[27] Smith S, 2002. Recent advances in digital data acquisition technology. Sound and Vibration, 36(3), Pages 18-21.

[28] TecQuipment, 2013. *Aerodynamics: Basic Lift and Drag Balance*: AFA2: Measures lift and drag forces on models in a TecQuipment Subsonic Wind Tunnel (AF100): PE/bs/db/0313.

[29] CES (Cambridge Engineering Selector) 2014. Material Selection Database.

[30] Yang K, 2012. *The Influence of the Quay Crane Travelling Time for the Quay Crane Scheduling Problem.* Proceedings of the International MultiConference of Engineer's and Computer Scientists 2012 Vol II, IMECS 2012, March 14-16, Hong Kong: Introduction.

[31] Liebherr Group, 2014. Operational data and statistical port data obtained for project studies.

[32] Tata Steel 2012. *Advance® sections: CE marked structural sections BS 5950 version*: S355 Structural Steel. Available online at http://www.tatasteelconstruction.com/file_source/StaticFiles/section_plates_publications/sections_publications/Tata%20Steel%20Advance%20to%20BS5950%20Nov12.pdf

[33] GOV.UK, 2013. Statistics: *International Industrial Energy Prices*: Available online at https://www.gov.uk/government/statistical-data-sets/international-industrial-energy-prices. [Accessed 28th November 2013].

[34] Defra, 2012. 2012 Guidelines to Defra / *DECC's GHG Conversion Factors for Company Reporting*: https://www.gov.uk/government/uploads/system/uploads/attachment_data/file/69554/pb13773-ghg-conversion-factors-2012.pdf. [Accessed 28th November 2013].

[35] EC (European Commission), 2013. *Time for international action on CO_2 emissions from shipping*: The shipping sector's contribution to climate change: Rapid growth in CO_2 emissions from international shipping

Bibliography

[1] Andersson. B, Andersson. R, Hakansson. L, Sudiyo.R, Wachem. B.V & Hellstorm.L, 2012. *Computational Fluid Dynamics for Engineers*, Chapter 4: Turbulent Flow Modelling: 4.1 The Physics of fluid turbulence: 4.1.1 Characterises features of turbulent flow: Page 63-66: ISBN 978-1-107-01895-2 Printed by Cambridge University Press

[2] Ai Z.T & Mak C.M. 2013. *CFD simulation of flow and dispersion around an isolated building: Effect of inhomogeneous ABL and near-wall treatment*: Department of Building Services Engineering, The Hong Kong Polytechnic University, Hong Kong: 3. Near-wall treatments 3.1. Wall functions modified for rough surfaces: Page 570. Published by Elsevier:

[3] Altekar R.V, 2005.*Supply Chain Management: Concepts and Cases: Concept of Containerisation*: Page 266: Published by PHI Learning Pvt. Ltd.

[4] ASCE (American Society of Civil Engineers), 2012. *Wind Tunnel Testing for Buildings and Other Structures:* Chapter 6 Extreme Wind Climate: C 6.1.4 Hurricanes: ISBN 978-0-78-1228-2: Published by the American Society of Civil Engineers (ASCE)

[5] Bansal R. K, 2005. Text Book of Fluid Mechanics and Hydraulic Machines: Model Laws or Similarity: 12.9.2 Froude Model Law: Page 583: ISBN 81-7008-311-7: Published by Firewall Media:

[6] Bireswar M 2011,*Fluid Mechanics with Laboratory Manual*: Chapter 12 Dimensional Analysis and Similitude:12.3 Physical Similarity: Page 377-378: ISBN 978-81-203-4034-3: PHI Learning Pvt. Ltd.

[7] Bosniakov .S, 1998. Experience *in integrating CFD to the technology of testing models in wind tunnels:* Progress in Aerospace Sciences 34 (1998) 391Ð422: Power Unit Department, TsAGI, Zhukovsky 3, Moscow Region, Russia.

[8] Cebeci T, 2004.*Analysis of Turbulent Flows*: 2nd Edition Revised Edition: Chapter 4: General Behaviour of Turbulent Boundary Layer: 4.2 Composite Nature of Turbulent Boundary layer: Page 81-89: Published by Elsevier: ISBN 0-08-044350-8

[9] Coronado D, 2006.*Economic Impact of the Container Traffic at the Port of Algeciras Bay*: 1.2 Containerisation Process: Concepts, Resources and Relationships:1 Container Traffic from an economic perspective: 1.2.1 Containerisation and Intermodality Page 6: ISBN 978-3-540-36788-8: Published by Springer

[10] Defraeyea T, Blockenb B, Koninckxc E, Hespel P & Carmeliet J, 2010 *Aerodynamic study of different cyclist positions: CFD analysis and full-scale wind-tunnel tests*: 5 Conclusions. Page 1267: Published by Elsevier:

[11] Glabeke, G,2011. The influence of wind turbine induced turbulence on ultra light aircraft, a CFD Analysis: The Von Karmen Institute for Fluid Mechanics: Chapter 4 Turbulence: What is Turbulence: Pages 4-9.

[12] Gray D, 2000 *A First Course in Fluid Mechanics for Civil Engineers:* Chapter 15: Physical Models and Similarity: 15.1 Scale Model Testing: Page 437-439: ISBN 1-887201-11-4: Published by Water Resources Publications.

[13] Pickering M, 2009. *Human Powered Submarine Hull CFD*: Final Year MEng Engineering University of Bath: Department of Mechanical Engineering: Chapeter19. Accuracy Discussion: 19.1 Effectiveness of the CFD Model: Page 79.

[14] Samardzˇic .M, Isakovic´.J, Anastasijevic . Z ´& Marinkovski D, 2013. *Apparatus for measurement of pitch and yaw damping derivatives in high Reynolds number blow down wind tunnel: Measurement* 46 (2013) 2457–2466:

[15] Stathopoulos T, Charalambos C, & Baniotopoulos, 2007. *Wind Effects on Buildings and Design of Wind-Sensitive Structures*: 1.Introduction: Page 2-3 ISBN: 978-3-211-73075-1. Published by Springer.

[16] Tavoularis S,2005 *Measurement in Fluid Mechanics*: Chapter 6: Wind Tunnels : Fluid Mechanical Apparatus: ISBN 978-0-521-81518-5 : Page 155-156: Published Cambridge University Press.

Appendices

Appendix A - Project Feedback from Liebherr

LIEBHERR

Liebherr Container Cranes Ltd., Killarney, Co. Kerry, Republic of Ireland.

Liebherr Container Cranes Ltd.

Container Cranes.
Ship to Shore Gantry Cranes.

Attention: Brian Hand

Your ref.:	Our ref.:	Date:	From the desk of:
	Js	4th June, 2014	James Scanlon Telephone ++ 353 64 6670200 Fax ++ 353 64 6631602 james.scanlon@liebherr.com

RE: "An Analysis into wind Induced loading Effects on a STS crane and Investigation into Design Optimisation"

Dear Brian,

On behalf of Liebherr Container Cranes I would like to congratulate you upon completion of an outstanding final year project. In many respects the project is a true masterpiece with useful results which could be utilised to design/manufacture more efficient container handling equipment.

As the use of CFD and wind tunnel analysis for crane structural design is a new approach for Liebherr, the merits of adopting this technology are clear based on the results of your studies. The current standards typically used in the industry are deemed conservative when applied. The benefits of having more accurate drag coefficients for these complex structures will effectively streamline the efficiency of the crane's structural design with the following benefits;

- Lighter crane structures due to lower wind coefficient being applied.
- Reduce crane manufacture cost which will help increase market share.
- Greener crane design as less material required thus lowering the crane's carbon footprint.
- Lower wheel loading, thus help reduce demands on quay civil structures.
- Lower crane tie down and storm pin loadings.

The analysis/results outlined in your research report will prove beneficial for Liebherr to pioneer technical advancement in future projects for Quay Crane designs.

We again compliment you on your work produced to date on the above subject matter and wish you the very best for your future studies.

Yours faithfully,
LIEBHERR CONTAINER CRANES LTD.

James Scanlon

James Scanlon
(Chief Design Engineer)

Liebherr Container Cranes Ltd.,
Fossa, Killarney, Co. Kerry,
Republic of Ireland.
Telephone: + 353 64 6670200.
Fax: + 353 64 6631602, 6631474.
Web:www.liebherr.com

VAT No. IE 8Z92243K
Registered Office:
Fossa, Killarney, Co. Kerry.
Certificate of Incorporation
16968 Dublin, Ireland.

Directors:
P. O'Leary.
R. Ganser (German).
S. Mirakaj (German) Secretary.
C. McCarthy.

Appendix B – Extended CFD Analysis Versions

The Mesh

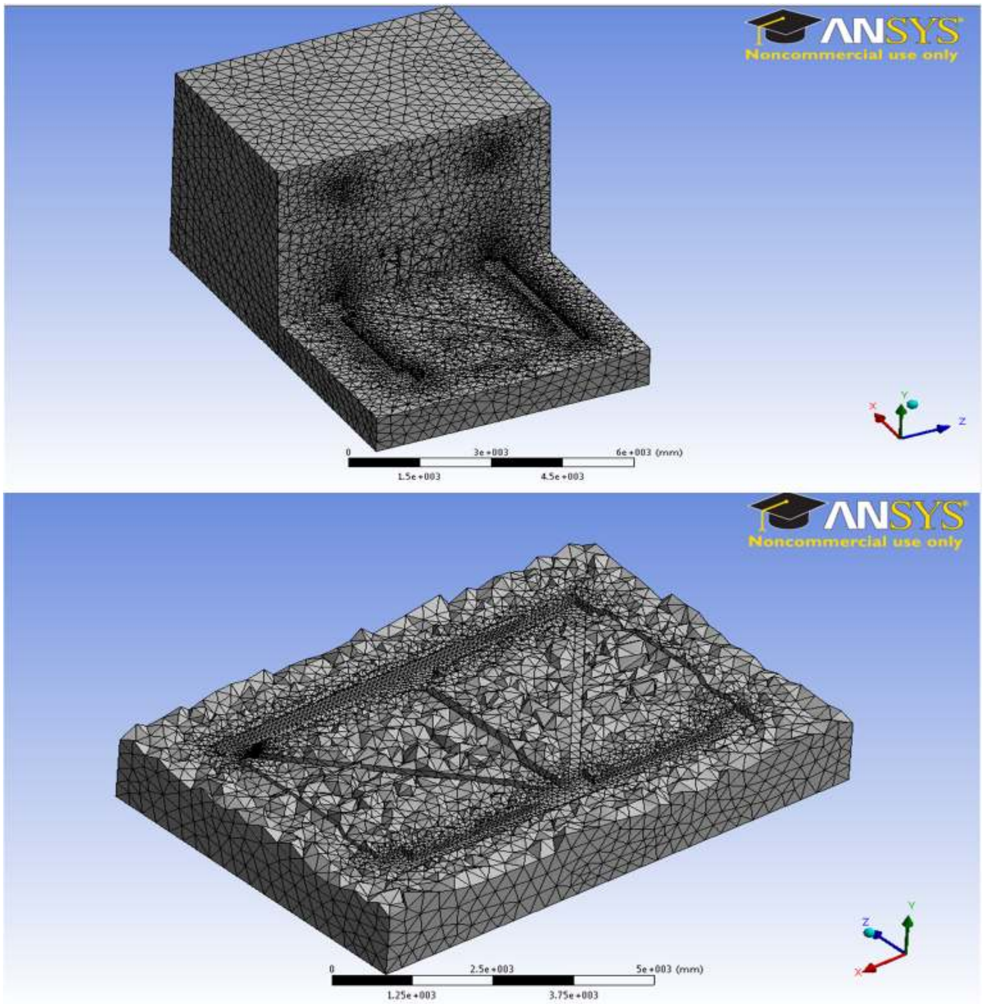

Figure B1 CFD Mesh Detailed Views – B.Hand 2014

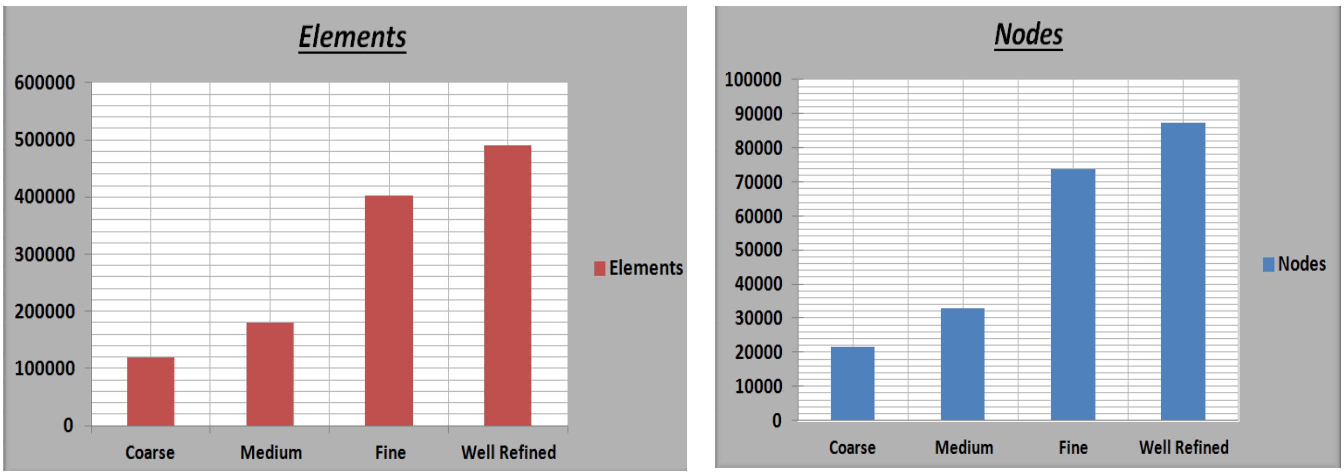

Figure B2 CFD Mesh Statistical Values – B.Hand 2014

Table B1 CFD Mesh Size variation – B.Hand 2014

Mesh Metric Sizes (m)				
Mesh Density	**Minimum**	**Maximum**	**Average**	**Standard Derivation**
Coarse	8.72E-04	0.999	0.725	0.202
Medium	2.44E-03	0.999	0.780	0.165
Fine	7.94E-03	1.000	0.822	0.119
Well Refined	6.72E-05	1.000	0.816	0.125

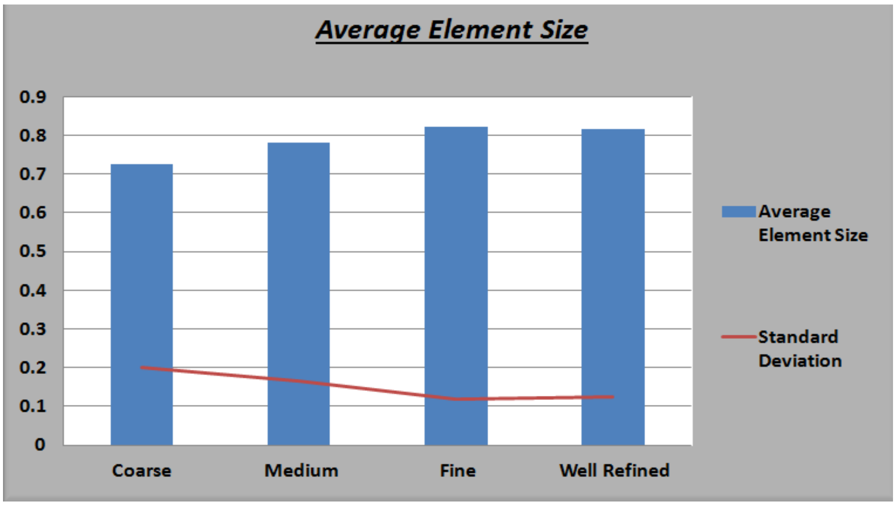

Figure B3 CFD Mesh Statistical Values – B.Hand 2014

Table B2 CFD Mesh Quality Analysis – B.Hand 2014

Grid Elements Skewness Values				
Mesh Density	**Minimum**	**Maximum**	**Average**	**Standard Derivation**
Coarse	1.33E-03	1.000	0.374	0.241
Medium	2.42E-04	1.000	0.299	0.197
Fine	4.53E-04	1.000	0.255	0.153
Well Refined	1.25E-03	1.000	0.246	0.145

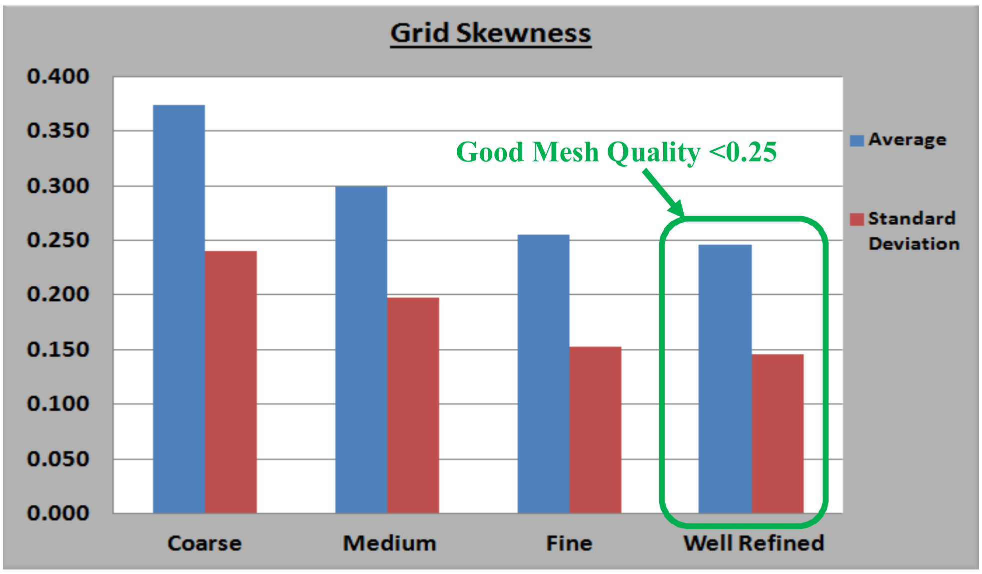

Figure B4 CFD Mesh Graphical Quality Analysis – B.Hand 2014

Appendix C – Extended Wind Tunnel Testing Versions

Calibration

Before any testing could be conducted, it was essential that the wind tunnel test equipment was calibrated before the experimentation had begun. It was imperative that the model received an even velocity distribution in the wind tunnel. To achieve this suitable experimentation was conducted to size the model.

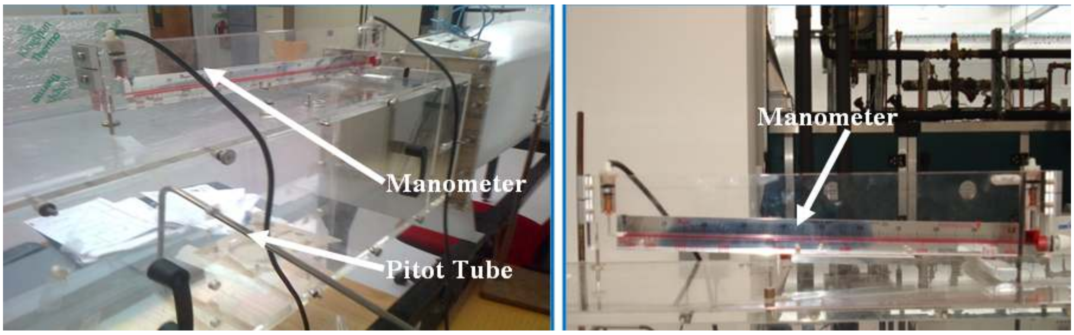

Figure C1 Velocity Measurement of Wind Tunnel – B.Hand 2014

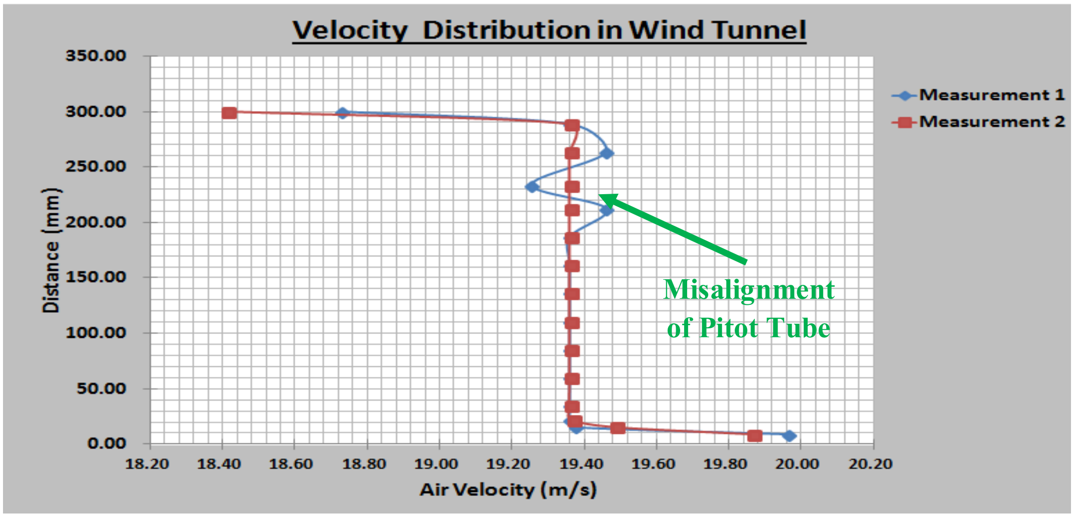

Figure C2 Wind Tunnel Velocity Measurement - B.Hand 2014

Combined with the experimental measurement, theoretical calculation of the wind tunnel boundary layer was established.

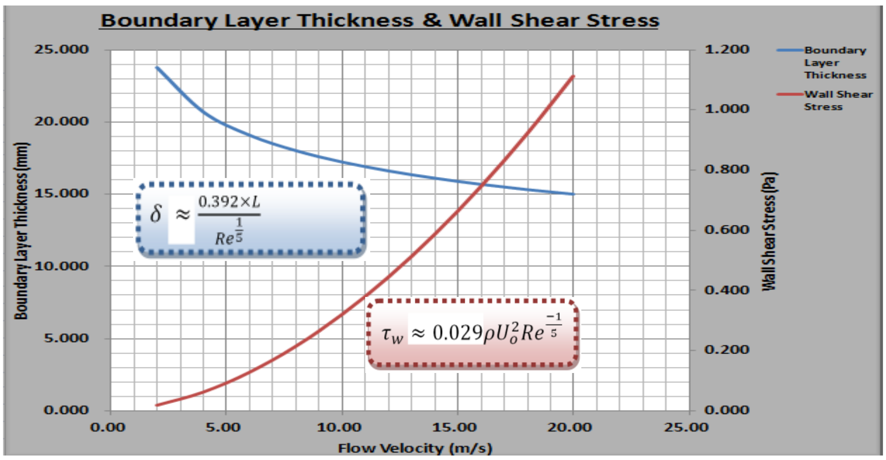

Figure C3 Calculated Wind Tunnel Boundary Layer - B.Hand 2014

Model Wind Tunnel Test Results

The testing on the model was conducted three times to ensure the utmost accuracy was guaranteed and possible sources of error could be eliminated. Shown in Table A1 are the results that were recorded from the testing. Mean and standard deviation between the results have been calculated.

Table C1 Recorded Wind Tunnel Results on Model - B.Hand 2014

	Measurement 1	Measurement 2	Measurement 3	Average	Standard Deviation (σ)
Velocity (m/s)	Drag Force (N)	Drag Force (N)	Drag Force (N)	Drag Force (N)	Drag Force (N)
1.00	0.008	0.034	0.018	0.020	0.013
2.00	0.069	0.102	0.041	0.071	0.031
3.00	0.168	0.208	0.132	0.169	0.038
4.00	0.251	0.333	0.230	0.271	0.054
5.00	0.523	0.449	0.377	0.449	0.073
6.00	0.764	0.724	0.496	0.661	0.144
7.00	0.946	1.018	0.778	0.914	0.123
8.00	1.256	1.283	0.974	1.171	0.171
9.00	1.415	1.580	1.269	1.421	0.155
10.00	1.736	1.970	1.428	1.711	0.272
11.00	2.106	2.099	1.866	2.024	0.137
12.00	2.494	2.354	2.377	2.408	0.075
13.00	2.653	2.515	2.712	2.627	0.101
14.00	3.244	3.026	2.998	3.089	0.135
15.00	3.595	3.308	3.663	3.522	0.188
16.00	4.269	4.046	3.793	4.036	0.238
17.00	4.884	4.272	4.500	4.552	0.310
18.00	5.347	5.116	5.200	5.221	0.117
19.00	5.648	5.116	5.938	5.567	0.417
20.00	5.981	5.955	5.904	5.947	0.039

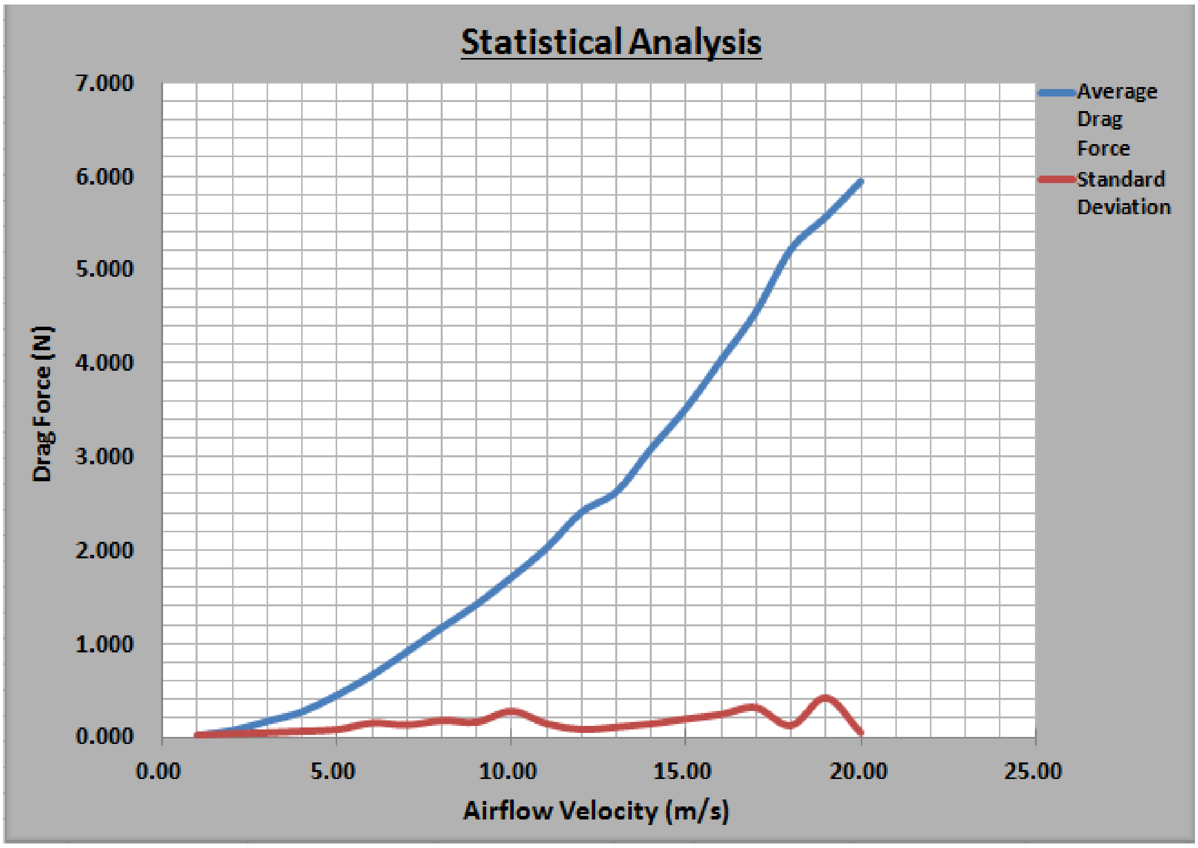

Figure C4 Statistical Analysis of Wind Tunnel Test Results - B.Hand 2014

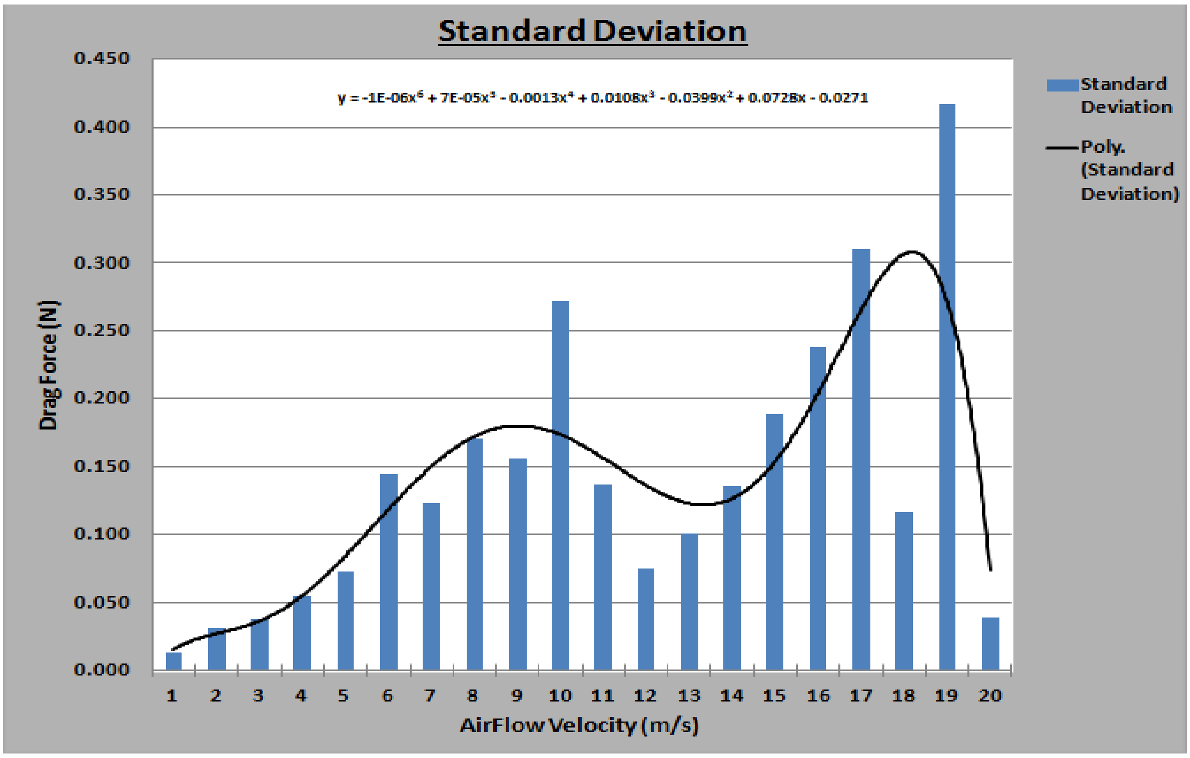

Figure C5 Standard Deviation of Wind Tunnel Test Results - B.Hand 2014

CFD Analysis of Wind Tunnel Model

Using the scaling capabilities in ANSYS Fluent 14, the full scale model was scaled down to the model size used in the wind tunnel by using a scaling factor of 28.

This approach allowed all the features of the model and the CFD mesh to be scaled without distortion.

The four grid types used in the full scale analysis were scaled down - to ensure the results achieved at the model scale were also grid independent.

Table C2 CFD Model Grid Independence Study - B.Hand 2014

Mesh Relevance	**Coarse**		**Medium**		**Fine**		**Enhanced**
Grid Elements	**119960**		**180067**		**402221**		**489858**
Wind Velocity	**Drag Force (N)**	**%**	**Drag Force (N)**	**%**	**Drag Force (N)**	**%**	**Drag Force (N)**
2	0.103	2.180	0.101	1.076	0.102	0.944	0.100
4	0.405	6.073	0.379	1.404	0.387	0.735	0.382
6	0.853	7.880	0.793	1.548	0.803	0.304	0.791
8	1.474	7.835	1.366	0.885	1.379	0.066	1.367
10	2.277	8.809	2.083	0.936	2.113	0.483	2.093
12	3.240	8.640	2.955	0.570	2.999	0.926	2.982
14	4.360	8.217	3.995	0.421	4.046	0.829	4.029
16	5.684	8.516	5.189	0.515	5.265	0.932	5.238
Overall Percent Difference (%)		**7.27**		**0.92**		**0.65**	

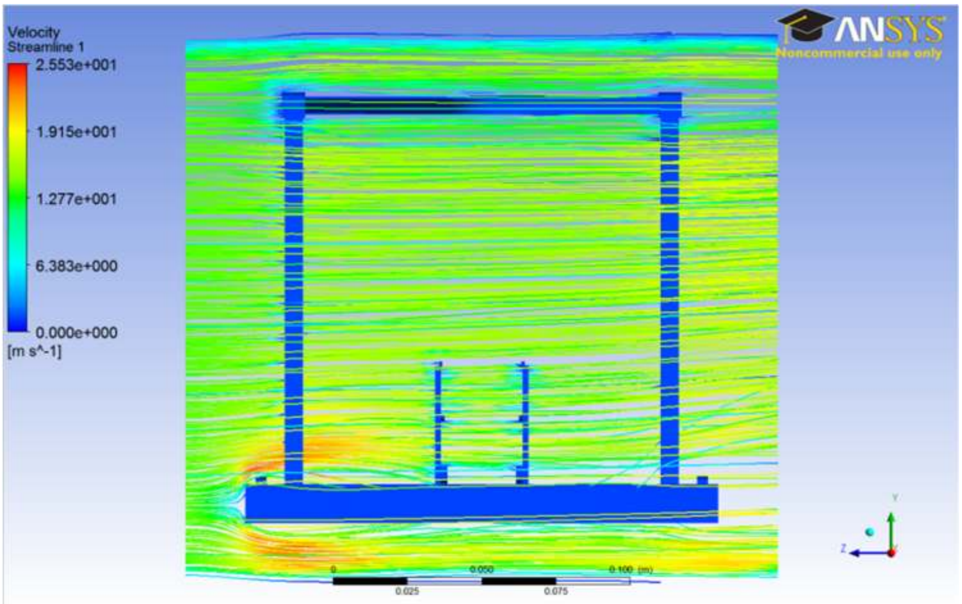

Figure C6 CFD Analysis of Wind Tunnel Model - B.Hand 2014

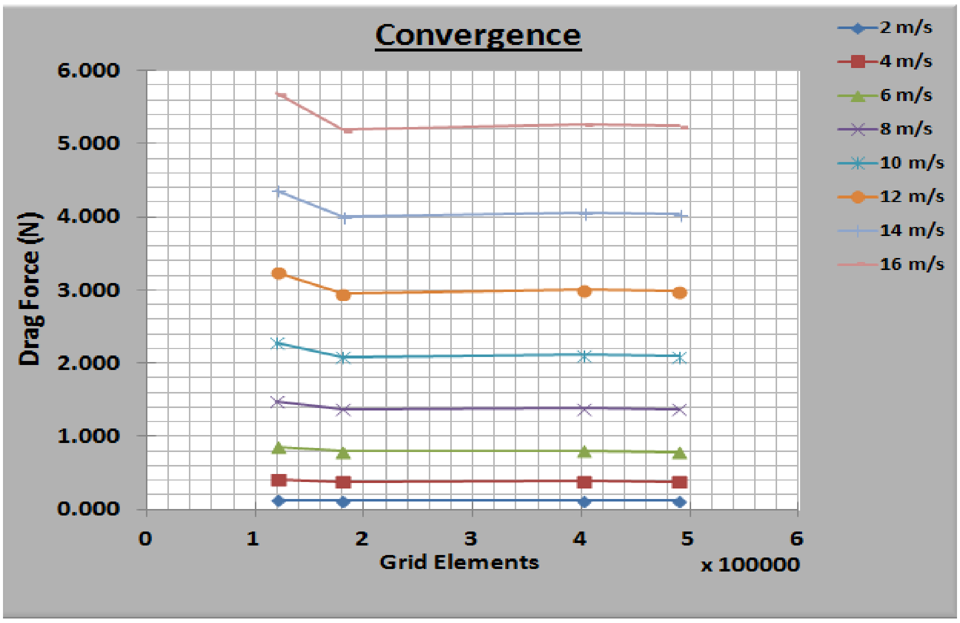

Figure C7 CFD Wind Tunnel Model Convergence of Results - B.Hand 2014

Model Results Comparison

After completing the post-processing of the results from the CFD model analysis, it was now possible to compare these results from the experimentally wind tunnel testing and the reference hand calculation as documented in Table A3.

Table C3 Model and CFD Results - B.Hand 2014

Airflow Velocity (m/s)	CFD Drag (N)	Difference (%)	σ	Wind Tunnel Test (N)	Difference (%)	σ	Hand Calculation (N)
2	0.100	26.904	0.015	0.071	9.898	0.006	0.079
4	0.382	21.079	0.047	0.271	14.023	0.031	0.315
6	0.791	11.476	0.058	0.661	6.810	0.034	0.709
8	1.367	8.407	0.075	1.171	7.130	0.064	1.261
10	2.093	6.230	0.087	1.711	13.156	0.183	1.970
12	2.982	5.119	0.103	2.408	15.125	0.303	2.837
14	4.029	4.329	0.118	3.089	20.007	0.546	3.862
16	5.238	3.849	0.137	4.036	19.981	0.713	5.044
Average		**10.924%**	**0.080N**		**13.266%**	**0.235N**	

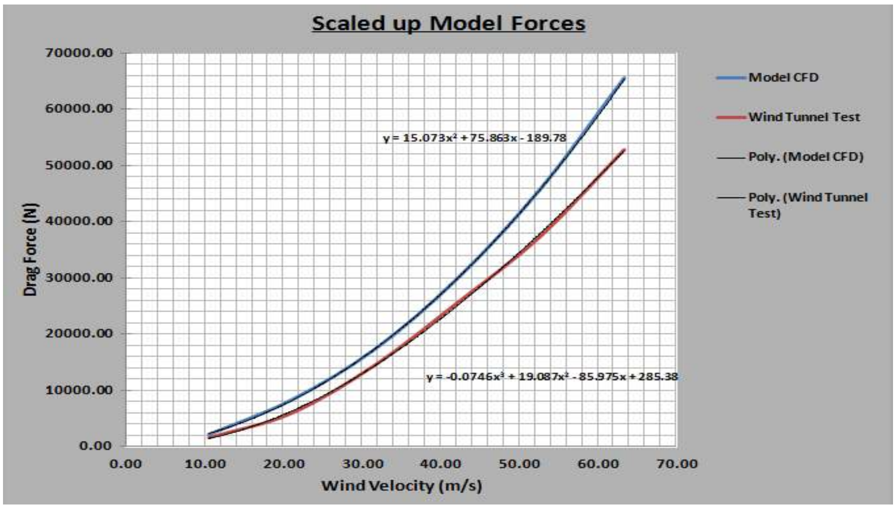

Figure C7 Curve Fitting Techniques Utilised - B.Hand 2014

Full Scale Results

Table C4 Full Scale Results for Crane Section - B.Hand 2014

Velocity (m/s)	CFD (Scaled up Model) (N)	CFD (Full Scale) (N)	Wind Tunnel Test (N)	Hand Calculation (N)
5	566.36	398.40	323.355	386.16
10	2076.15	1481.60	1259.73	1544.66
20	7356.68	5795.00	5603.88	6178.63
30	15651.81	12957.30	12870.23	13901.92
40	26961.54	22931.60	22611.18	24714.53
50	41285.87	35831.20	34379.13	38616.45
60	58624.8	51531.20	47726.48	55607.68

Table C5 Drag Coefficients Determined by Diverse Methods - B.Hand 2014

Wind Velocity (m/s)	CFD Model (Scaled up model) (C_D)	CFD (Full Scale) (C_D)	Wind Tunnel Test (C_D)	Hand Calculation (C_D)
5	2.49	1.75	1.42	1.70
10	2.28	1.63	1.39	1.70
20	2.02	1.59	1.54	1.70
30	1.91	1.58	1.57	1.70
40	1.85	1.58	1.56	1.70
50	1.82	1.58	1.51	1.70
60	1.79	1.58	1.46	1.70
Average	**2.03**	**1.61**	**1.49**	**1.70**

Figure C8 Crane Structural Geometry- Photos by B.Hand

Appendix D - Design Optimisation Extended Versions

Desgn Criteria

Table D1 Design Requirements - B.Hand 2014

Problem Statement: Tie-down Design Optimisation		
#	Demand/Wish (D) / (W)	Requirements
Performance Requirements		
1	D	Must exert correct tensile force
2	D	Must resist deformation
3	D	Must have accurate tightening system
4	W	Must be light weight
5	W	Portable
6	W	Long service life (20 years)
7	D	Operate in all weather conditions
8	D	Must be corrosive resistant
9	D	Easily maintained (lubrication)
10	D	Must give indicated tension exerted
11	W	Easily operated
12	W	Low centre of gravity
13	D	Integrated system to allow equalizing of tensile forces
14	D	Easily adjusted for different situations
15	W	Interchangeable parts
16	D	Adequate safety features
Manufacturing Requirements		
17	D	High quality components & materials
18	D	Efficient production time
19	D	Relatively Inexpensive
20	W	Production using CNC
21	W	Minimise waste
22	W	Reduce complexity in manufacture

Table D2 Design Selection Matrix - B.Hand 2014

Criteria	**Weight**	**Rating**	**Rating**	**Rating**
	(1-5)	**Design 3**	**Design 2**	**Design1**
Safety	5	8	5	6
Adjusting	4	8	4	2
Operation	4	7	4	5
Mechanical Advantage	3	8	3	2
User Friendliness	3	8	4	2
Corrosion Protection	3	5	5	6
Complexity	2	5	7	7
Manufacture	2	6	5	5
Product Life	2	7	6	2
Effectiveness	4	8	4	3
Calculations	1	7	7	7
Total Score		**77/110**	**54/110**	**47/110**

Material Selection Process

Figures D2 and D3 illustrate in diagrammatic form the material selection process undertaken by the author For the redesign, mechanical factors for the material such as stiffness, tensile strength, yield strength, fatigue strength and impact strength are crucially important in selecting the most suitable material. Environmental factors are also important also as this component is placed in an exposed environment where salt laden air is present with moisture, which can cause significant amount of corrosion on certain materials if not properly treated or designed for. The material cost and availability is also an important consideration for this design.

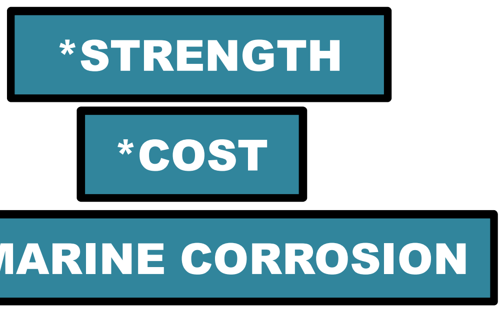

Figure D1 Core Material Requirements - B.Hand 2014

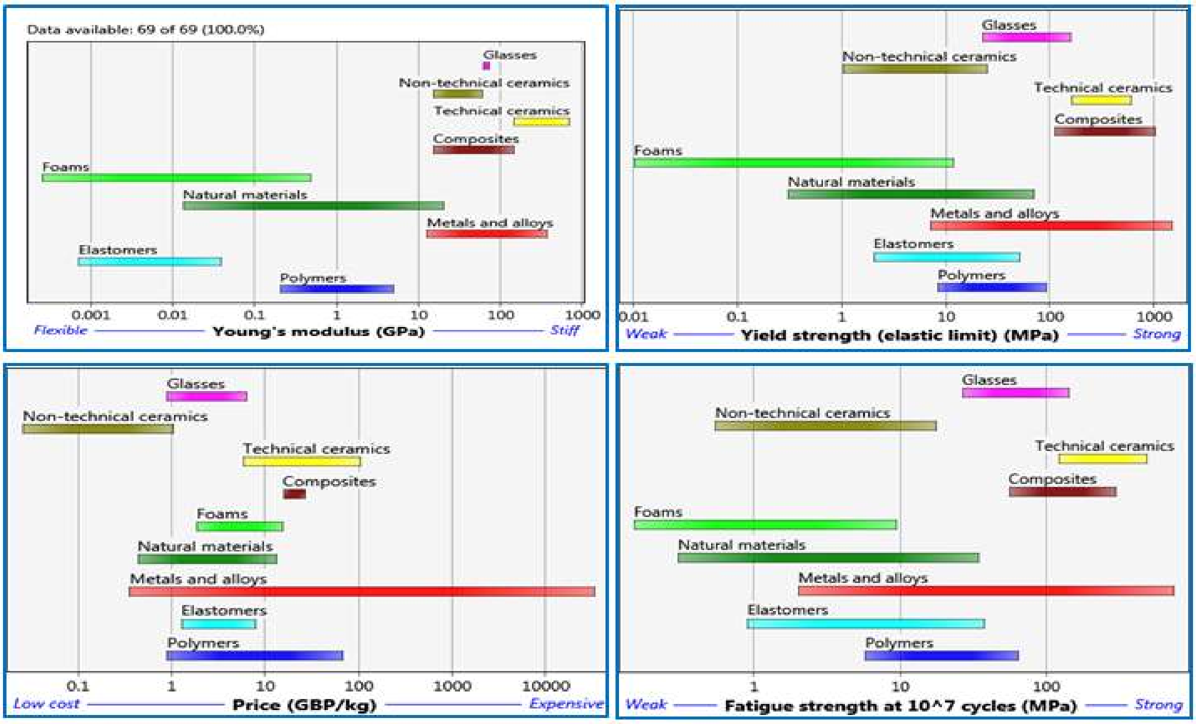

Figure D2 Diagrammatic image showing important material properties [29]

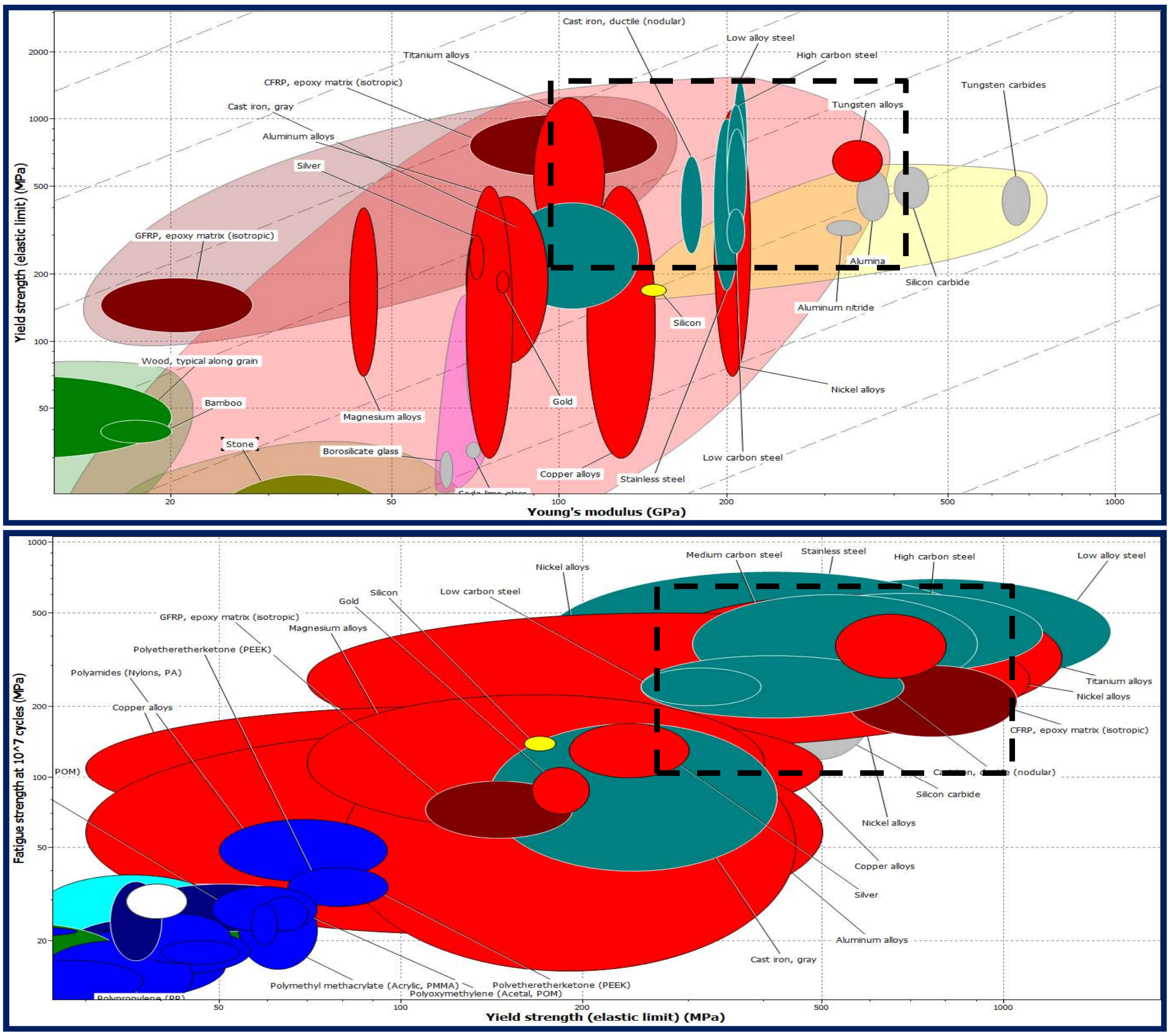

Figure D3 Material Selection and Elimination [29]

Photoelasticity Experimental Testing

2 Stress Fringes (138.3N Load)

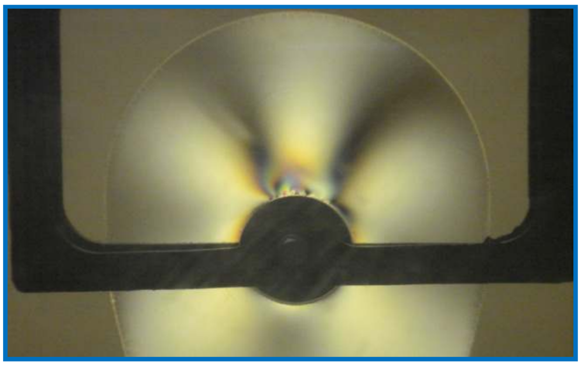

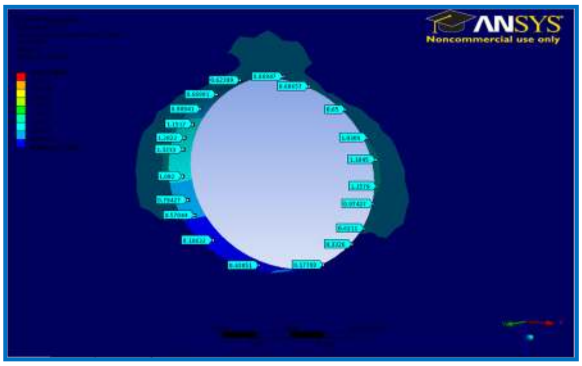

3 Stress Fringes (234N Load)

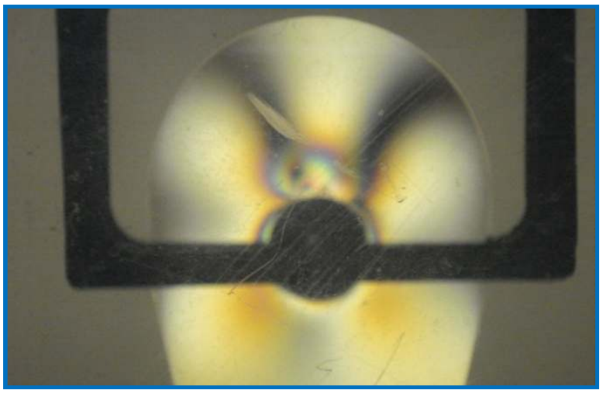

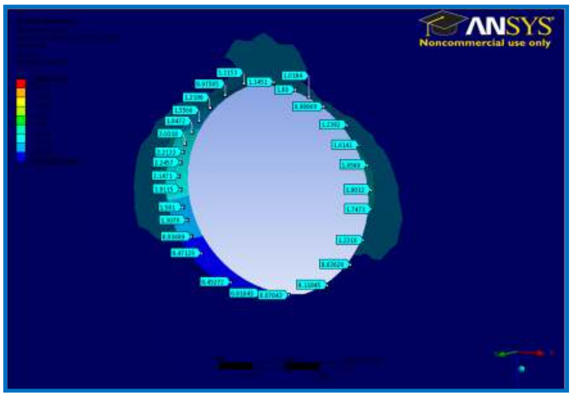

4 Stress Fringes (326.4N Load)

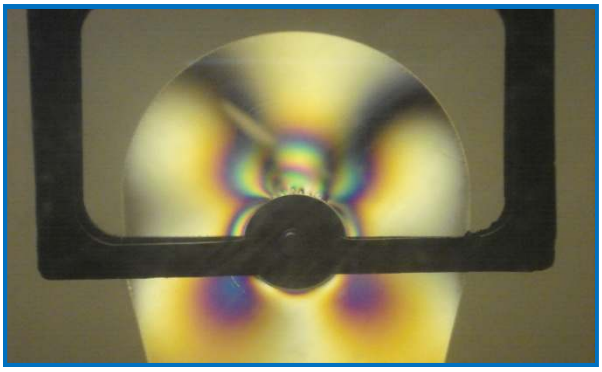

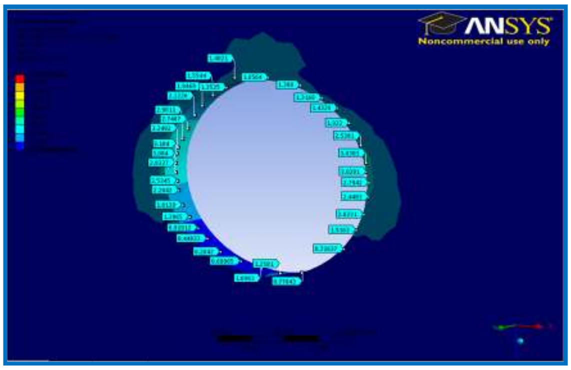

5 Stress Fringes (436N Load)

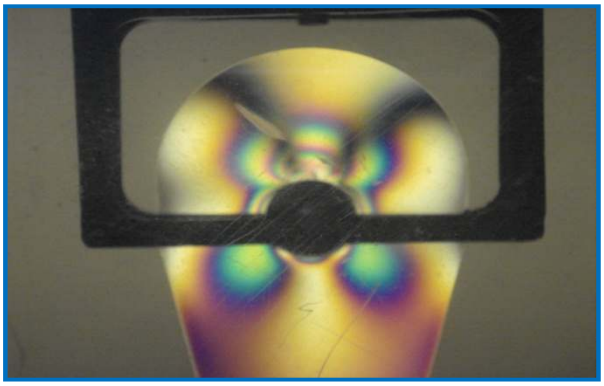

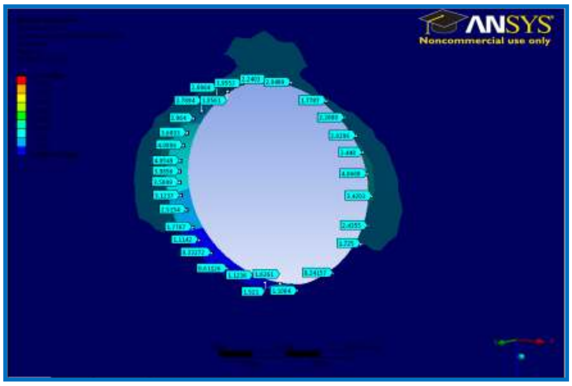

Prototype Development

Figure D4 Manufactured Prototype Top Link and Bearing Plates - B.Hand 2014

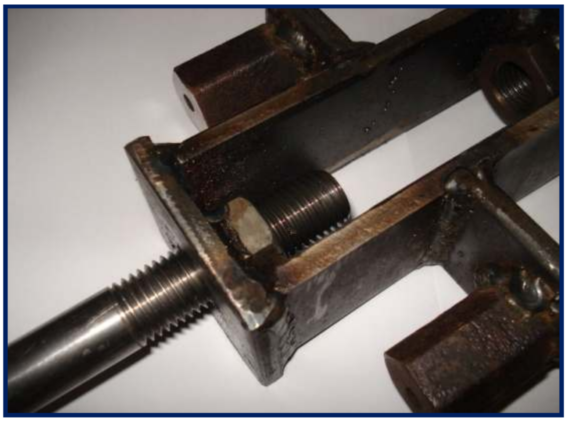

Figure D5 Manufactured Prototype Turnbuckle - B.Hand 2014

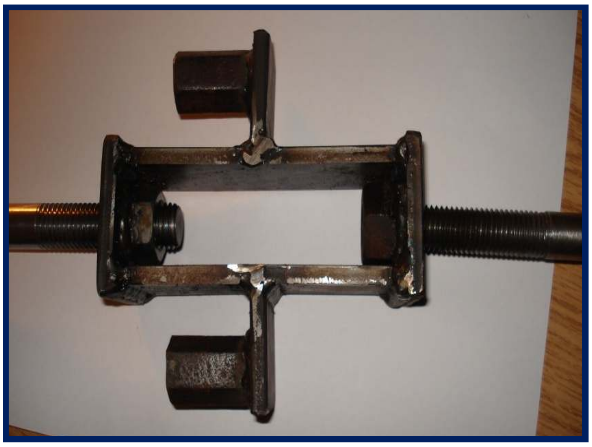

Figure D6 Prototype Assembly – insertion of Top link in Turnbuckle - B.Hand 2014

Figure D7 Orientation of Strain Gauges for prototype testing B.Hand 2014

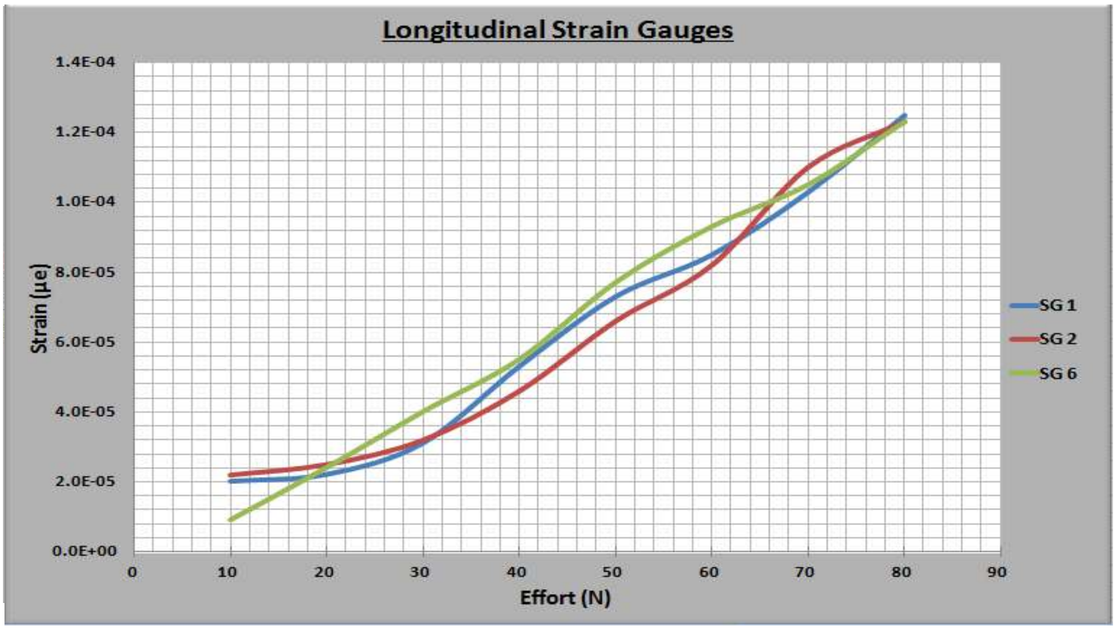

Figure D8 Axially loaded strain gauge results B.Hand 2014

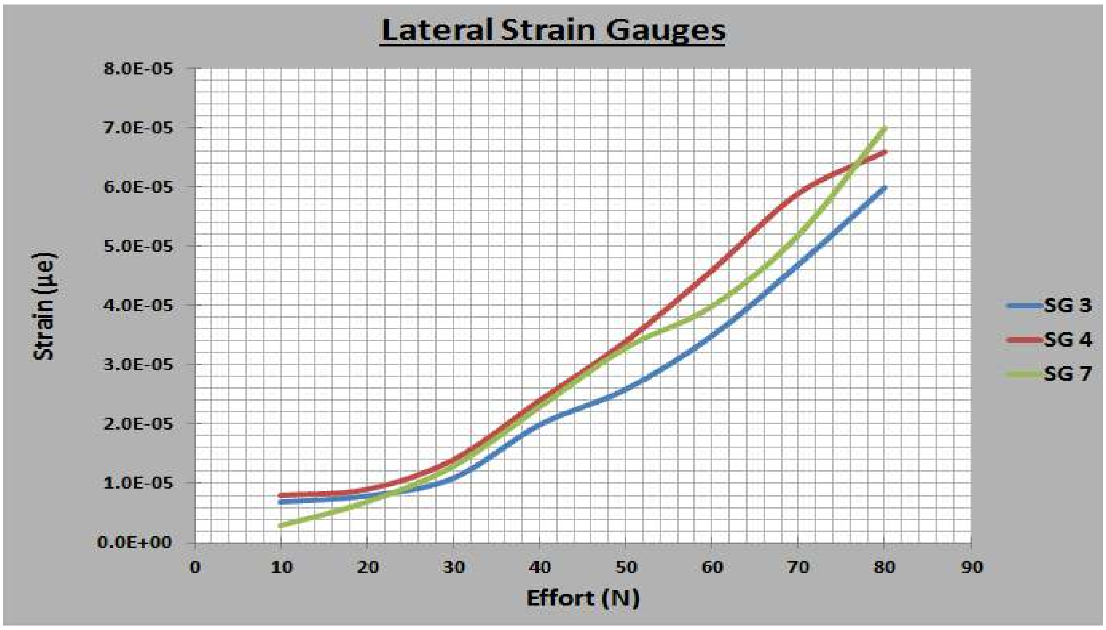

Figure D9 Transverse loaded strain gauge results B.Hand 2014

Research & Development

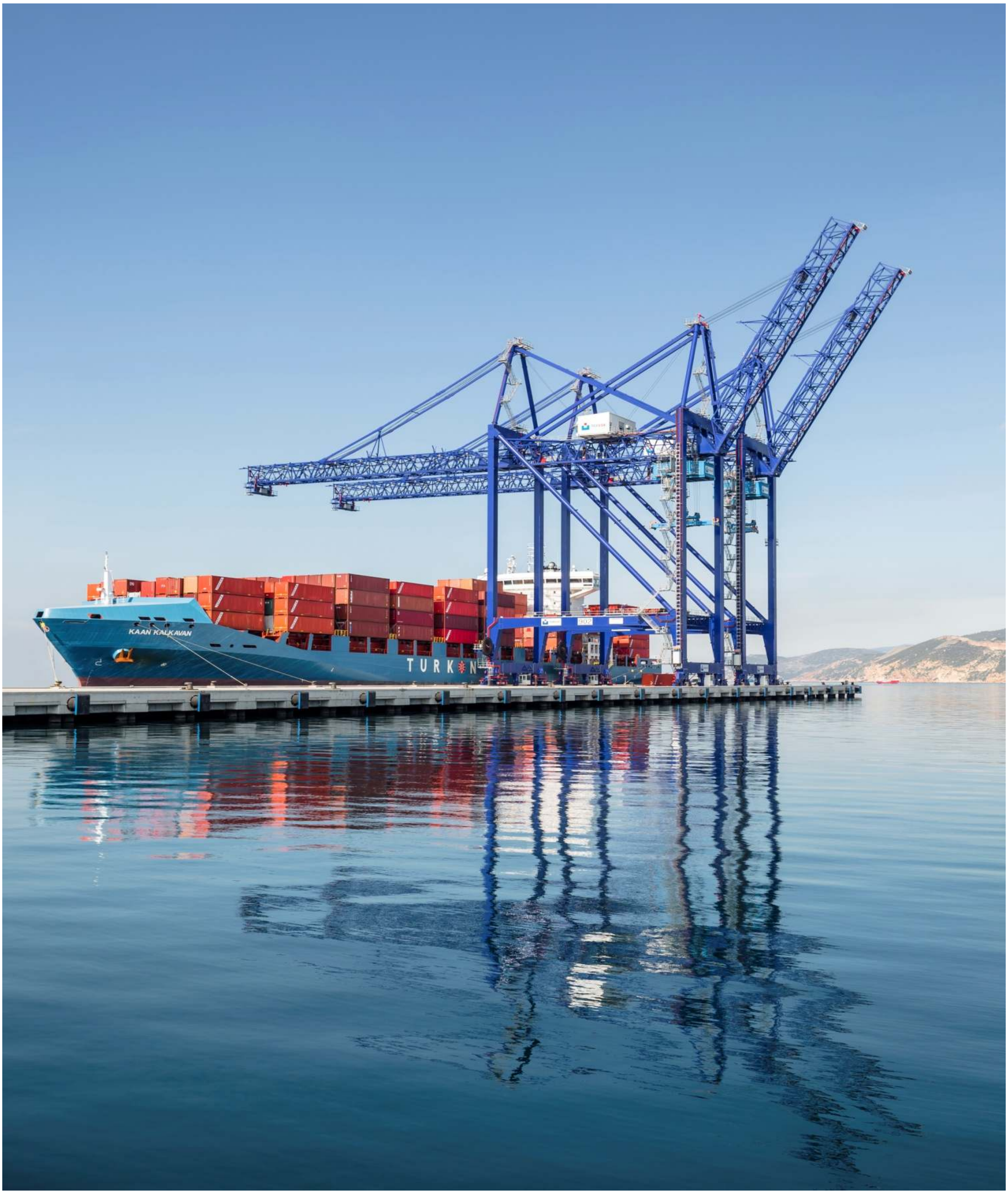

Figure D10 Emerging Liebherr Double Crane Boom Technology [1]

The research and analysis undertaken by the author contributes most positively to the current research and development activities and initiatives at Liebherr - including new crane designs encompassing double boom technology designed to dramatically improve productivity. (See Figure D10 - Photo taken of commissioned Double Boom STS Crane at Port of Nemrut Bay, Turkey 2013)

Dimensions

STS Model Designation

P 210 L (WS) / (GS)
- AC / DC Drive
- Lattice Structure for Main Beam
- Outreach Length in Feet
- Portal Type Structure

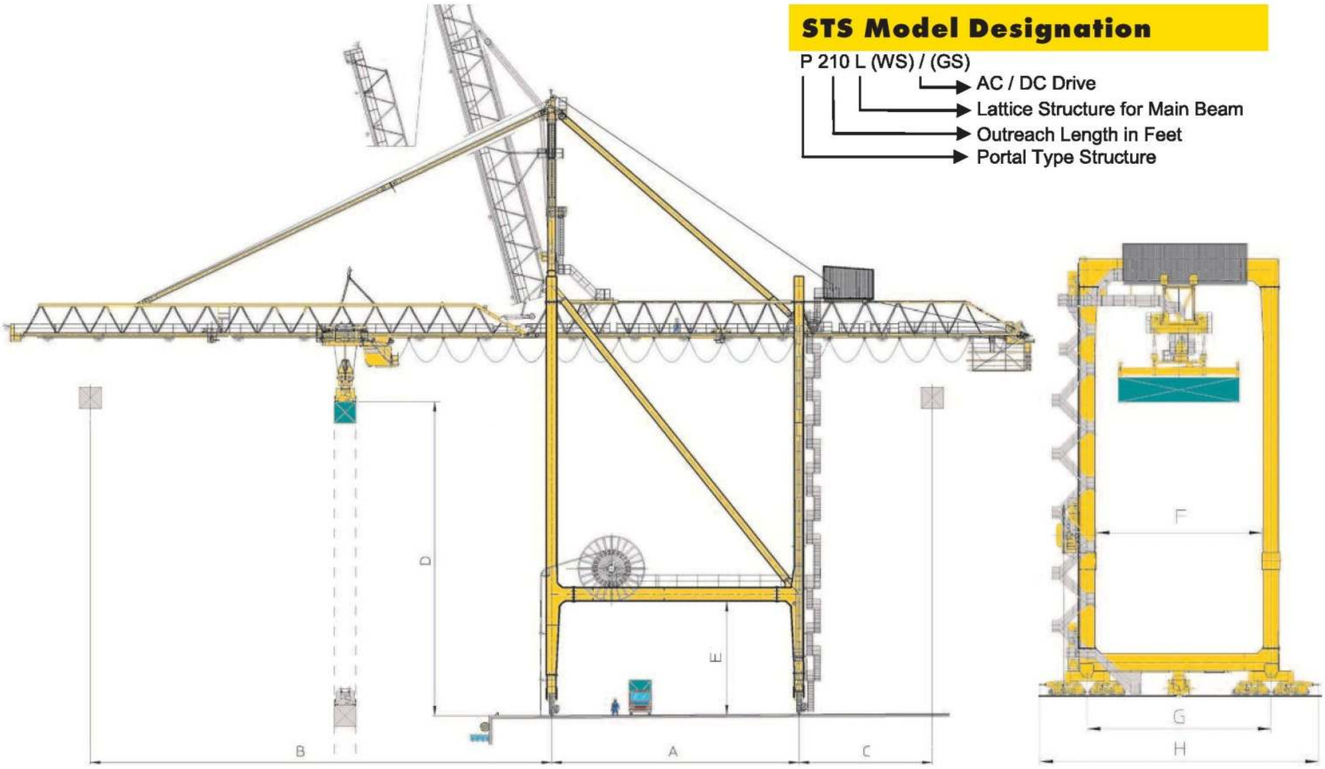

Typical Quayside Crane *

A Gantry Span	15.00 - 35.00m
C Backreach	0.00 - 25.00m
E Clearance Under Sill Beam	12.00 - 18.00m
G Travel Wheel Gauge **	18.20m
H Buffer to Buffer	27.00m
Wheel Spacing **	1.00 - 2.00m
Wheels per Corner **	6 / 12 - Seaside
Wheels per Corner **	6 / 12 - Landside
Max. Width Trolley & Main Beam/Boom	7.60m

** Dependant on Required Wheel Loads

Typical WideSpan Crane *

A Gantry Span	35.00 - 50.00m
B Outreach	30.00 - 40.00m
C Backreach	15.00 - 30.00m
D Lift Height	20.00 - 25.00m
SWL Capacity	40/50T Single - 65T Twin
Hoisting Speed	50 / 125 m/min
Trolley Speed	180 m/min
Travel Speed	100 - 140 m/min
Wheel Load per Meter **	40 - 50T Per Meter

** Based on 8 Wheels per Corner at 1.00m Spacing

Typical Design Parameters *

Classification according F.E.M._______U7-Q2-A7
In service wind Speed____________72km/h (20m/s)
Out of service wind Speed_________151.2km/h (42m/s)
Ambient Temperature Range_______- 40°C to +50°C
Frequency___________________50Hz to 60Hz
Voltage_____________________3.3kV to 20kV

Typical Feeder - Panamax Crane *

B Outreach	30.00 - 40.00m
D Lift Height	24.00 - 30.00m
SWL Capacity	40/50T Single - 65T Twin
Hoisting Speed	50 / 125 m/min
Trolley Speed	150 - 180 m/min
Travel Speed	45 m/min
Wheel Load **	30 - 45T Per Meter

** Based on 8 Wheels per Corner at 1.00m Spacing

Typical Post Panamax Crane *

B Outreach	40.00 - 45.00m
D Lift Height	30.00 - 35.00m
SWL Capacity	40/50T Single - 65T Twin
Hoisting Speed	60 / 150 m/min
Trolley Speed	180 - 210 m/min
Travel Speed	45 m/min
Wheel Load **	40 - 55T Per Meter

** Based on 8 Wheels per Corner at 1.00m Spacing

Typical Super Post Panamax / Megamax

B Outreach	46.00 - 70.00m +
D Lift Height	35.00 - 49.00m
SWL Capacity	65T Twin - 80T Tandem
Hoisting Speed	70 / 175 m/min
Trolley Speed	210 - 240 m/min
Travel Speed	45 m/min
Wheel Load **	60 - 80T Per Meter

** Based on 8 Wheels per Corner at 1.00m Spacing

* Other Features, Dimensions and Design Parameters Also Available